A quantumchemical study on photochemical sigmatropic shifts and cis-trans isomerizations

A QUANTUMCHEMICAL STUDY ON PHOTOCHEMICAL SIGMATROPIC SHIFTS AND CIS-TRANS ISOMERIZATIONS

G.J.M. DORMANS

A QUANTUMCHEMICAL STUDY ON PHOTOCHEMICAL SIGMATROPIC SHIFTS AND CIS-TRANS ISOMERIZATIONS

A QUANTUMCHEMICAL STUDY ON PHOTOCHEMICAL SIGMATROPIC SHIFTS AND CIS-TRANS ISOMERIZATIONS

PROEFSCHRIFT

TER VERKRIJGING VAN DE GRAAD VAN DOCTOR AAN DE TECHNISCHE UNIVERSITEIT EINDHOVEN, OP GEZAG VAN DE RECTOR MAGNIFICUS, PROF. DR. F.N. HOOGE, VOOR EEN COMMISSIE AANGEWEZEN DOOR HET COLLEGE VAN DEKANEN IN HET OPENBAAR TE VERDEDIGEN OP DINSDAG 16 JUNI 1987 TE 16.00 UUR

door

GUIDO JOZEF MARIA DORMANS

geboren te Geleen

Druk: Dissertatiedrukkerij Wibro, Helmond.

DIT PROEFSCHRIFT IS GOEDGEKEURD DOOR

DE PROMOTOREN

PROF. DR. H.M. BUCK

EN

PROF. DR. R.P.H. RETTSCHNICK

Voor Carla
en mijn Ouders

CONTENTS

CHAPTER 1

Introduction

1.1 Theoretical Organic Photochemistry

The detailed understanding of photochemical processes (such as absorption and emission of light, vibronic interactions, intersystem crossings, internal conversions and chemical reactions in excited states) is very important since such processes play an essential role in many fields varying from laser techniques and photophysics via organic photochemistry to the biochemistry of visual perception and photosynthesis.

A photochemical reaction differs from a thermal reaction in at least one fundamental way: the absorption of light by a molecule prepares it in a nonstationary state with a nonuniform distribution of the energy over several vibrational modes, whereas a ground state molecule is almost always in a state in which the distribution of energy is (nearly) uniform. Besides this vibrational distribution, the excitation of a molecule leads to an essentially different electronic distribution from that in the ground state. For instance, a nonpolar ground state may be associated with a highly polar excited state. Hence, photochemical reaction mechanisms are often strikingly different from those obtained when the molecule is thermally activated.

The dynamics of a thermal process are mainly described by the energy and geometry of the reactant, transition state and the product. However, for photodynamics the presence of avoided crossings and funnels through which an excited molecule may return to its ground state are as much of interest as barrier heights. Therefore, a thorough understanding of photodynamics asks for a detailed knowledge of potential energy surfaces from qualitative arguments or more sophisticated quantumchemical calculations.

Probably the first application of quantumchemistry to organic photoreactions originates from Mulliken[1], who was able to describe the *cis-trans* isomerization in alkenes from the potential energy curves of the four valence excited states of ethylene, which can be formed by distributing the two π-electrons over the bonding and antibonding π-molecular orbitals. Moreover, he noticed that the minimum on the excited state potential energy curve corresponds to a maximum on the ground state potential energy curve, thus creating a condition from which a radiationless transition is likely to occur.

The next step forward in the interpretation of organic photochemistry was the recognition of the importance of orbital symmetry. Thus it was Havinga[2] who mentioned that the complementary stereochemistry of the thermal and

photochemical octatriene - cyclohexadiene interconversion can be formalized in terms of the different symmetries of the highest occupied molecular orbitals for the ground and excited state processes. This theoretical prediction was based on a suggestion of Oosterhoff[2] (*vide infra*). The concept of conservation of symmetry has been generalized by Woodward and Hoffmann[3] for the description of pericyclic reactions. They predicted that reactions which proceed with conservation of orbital symmetry would have an activation energy much lower than reactions which occur without this conservation of orbital symmetry. These predictions have thereafter been confirmed by many experiments, especially for thermal reactions.

However, the application of this concept to photochemical reactions is less straightforward and it may be questioned why the course of such a reaction should be governed by the symmetry of a molecular orbital which is occupied by only one of the frontier electrons. The concept deals with strictly concerted reactions and, therefore, can not account for the fact that the absorption of a photon by a molecule causes an electronic redistribution which often results in the breaking of a former (double) bond leading to a diradicalar structure. It was found that many organic photoreactions can be interpreted assuming such diradicalar intermediates[4]. Another important feature in which this qualitative concept lacks, is the prediction of avoided crossings between excited states and the nonadiabatic interactions associated with them[5].

That the situation for photochemical reactions is more complicated, was demonstrated by van der Lugt and Oosterhoff[6] via a quantumchemical calculation of the intramolecular ring opening - ring closure of the cyclobutene - *cis*-butadiene system. They found that the mechanism of the photoreaction is not determined by the initially excited $(\pi-\pi)^*$-state but by a second excited state which has a potential energy well at a nuclear conformation for which the ground state has a potential energy barrier.

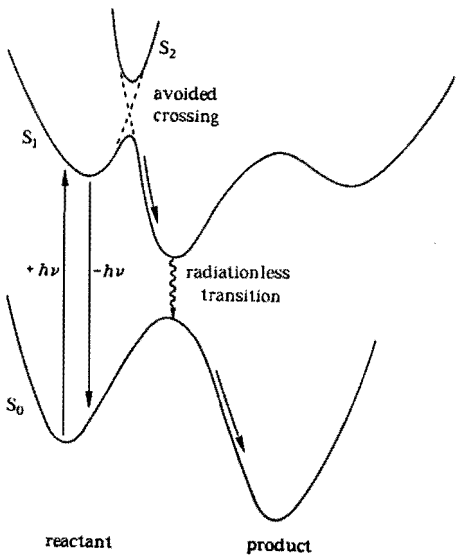

An overall photochemical reaction can be thought of as to be composed of photophysical and strictly photochemical processes. It starts with the interaction of light with a molecule leading to the absorption of a photon. The electronically excited molecule will relax its geometry to a minimum on the excited state surface from which there are two processes possible. The first one is the emission of a photon (fluorescence or phosphorescence) after which the molecule relaxes in the ground state to its equilibrium geometry, so that no net reaction has occured. Alternatively, a photochemical reaction may take place for which there is generally a potential energy barrier to be crossed. The driving force for this process is the excess kinetic energy of the excited molecule or a thermal activation in the excited state. Once the barrier has been crossed, the molecule will return to its ground state via a radiationless transition (internal conversion or intersystem crossing) at a point on the reaction coordinate for which the surfaces come close and the nonadiabatic interactions are strong.

In many organic photoreactions there is a continous competition between the photochemical and photophysical processes. In this thesis examples will be given of both cases. For the *cis-trans* isomerization in biochemically relevant molecules an efficient radiationless transition is a requisite to prevent photochemical reactions and to account for the high quantumyields. On the contrary, a small nonadiabatic interaction is a necessity for the occurence of photochemical sigmatropic shifts.

1.2 Quantumchemical Methods in Organic Photochemistry

The calculation of potential energy surfaces is of great importance for the understanding of photochemical reactions. Quantumchemical methods are widely used to calculate these surfaces for the study of organic reaction mechanisms. However, the application of these methods to reactions in the excited state is very limited. This is mainly due to the fact that excited states are more difficult to describe quantumchemically since electron correlation plays a more important role. Whereas the molecular ground state is usually well represented by a single closed shell SCF configuration, there are normally several configurations which are close in energy and interact strongly to produce a particular excited state.

An additional problem in dealing with photochemical reactions is the calculation of interstate properties for the description of interactions between the ground and excited states (radiative and nonradiative transitions). The best description of an electronic state can be achieved from a seperate SCF calculation. However, if a different one-electron basis is used for each state, a significant complication arises from the fact that the one-electron bases are mutually nonorthogonal. This practical problem can be avoided by employing a single one-electron basis to calculate all electronic states. Thus starting from a SCF calculation for (in most cases) the ground state, a set of molecular

orbitals is obtained of which the occupied ones describe this particular state.

In a zeroth order approximation, the excited states can now be described by constructing a number of configurations obtained from a promotion of one or several electrons from an occupied to a virtual MO and mixing these configurations variationally with the ground state. The lowest energy root (eigenvalue) and corresponding wavefunction (eigenvector) of the CI matrix then give an improved description of the ground state, whereas the next eigenvalue and eigenvector represent the energy and wavefunction of the lowest excited state. However, when the electronic states have quite different characteristics, the SCF MOs give a relatively poor description of the excited states. In the limiting case of a full CI treatment, this imperfection disappears. However, such an approach is both extremely time consuming and, in most cases, impractable with the present techniques for molecules of sizes which are of interest in organic chemistry.

One of the promising techniques that might be capable of handling this problem is the complete active-space SCF method (CASSCF[7]). In this method a selection is made of a set of orbitals which are optimized self-consistently and which are employed in a full CI treatment simultaneously. As the full CI results are invariant to a unitary transformation, a different CASSCF basis may be used for each electronic state while avoiding the nonorthogonality problem. However, it is always necessary to restrict the number of active orbitals to keep the computation feasible. Besides, this technique shows a slow convergence and it may encounter problems when a calculation is performed for an excited state for which there is a lower state with the same symmetry.

As stated before, the full CI limit is not realizable for organic molecules, so that the CI calculation should be restricted to a limited number of configurations. The choice of this set is one of the most difficult and challenging steps in the calculation of electronic wavefunctions. The methods most frequently used are the closely related multi-reference CI treatment (MRD CI[8]) and the CIPSI[9] method (Configuration Interaction by Perturbation of a multiconfigurational wavefunction Selected Iteratively) of which the latter has been used for the CI calculations in the work described in this thesis.

The method starts with the choice of a zeroth order configuration space $\{S^{(0)}(\Phi)\}$ including a number of configurations ($|\Phi_i>$) which are expected to dominate the CI expansion of the electronic states of interest. These configurations are treated variationally by a diagonalization of the CI matrix. This yields the zeroth order wavefunctions ($|\Psi_K^{(0)}>$) of these electronic states.

$$|\Psi_K^{(0)}> = \sum_{i \in \{S^{(0)}(\Phi)\}} c_{Ki}^{(0)} |\Phi_i> \qquad K = 0,1,2,.. \qquad 1$$

In a next stage, a second order perturbation is performed with all configurations single or double excited with respect to the states of interest and which have not been selected previously. This yields an improved energy ($E_K^{(pert)}$) of these states.

$$E_K^{(pert)} = \sum_{i \in \{S^{(0)}(\Phi)\}} \frac{|<\Psi_K^{(0)}|H|\Phi_i>|^2}{E_K^{(0)} - E_i} \qquad 2$$

From all generated configurations ($|\Phi_i>$) those are selected which have an interaction with the zeroth order wavefunctions larger than a certain treshold η:

$$\left|\frac{<\Psi_K^{(0)}|H|\Phi_i>}{E_K^{(0)} - E_i}\right| > \eta \qquad 3$$

These selected configurations, together with the previously selected configurations, now span the first order configuration space $\{S^{(1)}(\Phi)\}$. A diagonalization of the new CI matrix then gives the improved wavefunctions.

$$|\Psi_K^{(1)}> = \sum_{i \in \{S^{(1)}(\Phi)\}} c_{Ki}^{(1)} |\Phi_i> \qquad K = 0,1,2,.. \qquad 4$$

This procedure may then be repeated iteratively by decreasing the value of η and consequently increasing the dimension of $\{S^{(n)}(\Phi)\}$.

The advantages of this approach are obvious. There is no a priori selection of configurations and by performing this treatment for a number of electronic states simultaneously this yields a balanced description of these states. The program is able to deal with up to six unpaired electrons which makes it possible to include configurations which are triple excited from the ground state. This is important because in a first order approximation, a certain wavefunction is improved by adding doubly excited configurations (i.e. the π^2-ground state of ethylene interacts with the π^{*2}-configuration). However, as the excited states are often represented by a singly excited configuration (i.e. the ($\pi-\pi^*$)-state of ethylene) their wavefunctions must be improved by triply excited configurations with repect to the ground state.

A well-known drawback of ab initio calculations on excited states is that reasonable estimates of energies and properties are obtained only when fairly large basis sets and correspondingly large CI is included. Therefore, such studies have so far been confined to rather small systems. To study larger systems, the use of semi-empirical methods is inevitable. Various semi-empirical procedures (CNDO/S[10], HAM[11]) have proved to be effective in calculating excitation energies of molecules. However, non of these methods seems to be particularly suited to calculate excited state surfaces as they are not parametrized to reproduce geometries or relative stabilities of different molecules.

The MNDO-method[12] has proved to be satisfactoraly parametrized to describe ground state properties of organic molecules including radicals, cations and anions[13] and calculations for some photochemical reactions gave encouraging results[14]. The main drawback of this method is to underestimate transition energies. Both ab initio and MNDO calculations have been used in the work described in this thesis. It was found that for the purpose of the description of organic photoreactions, both methods yield (at least qualitatively) comparable results.

1.3 Nonadiabatic Interactions

The standard quantumchemical procedures used to calculate potential energy surfaces start from the Born-Oppenheimer approximation. Due to the large difference in the masses of the electrons and the nuclei in a molecule, their motions can be treated seperately. For each nuclear conformation, the Schrödinger equation may then be solved thus generating the so called adiabatic potential energy surfaces. However, in regions where two or more electronic states come close in energy, the Born-Oppenheimer approximation breaks down. In such cases, an interconversion of electronic and nuclear kinetic energy can take place. In fact, for photochemical reactions such nonadiabatic interactions describe the radiationless transitions by which an electronically excited molecule may return to its ground state.

To study photodynamics there are two methods which can be classified as pure quantummechanical[15] and semi-classical[16,17]. In the first method, the nuclear motion is explicitely incorporated in the model Hamiltonian. This method is used in chapter 2 to describe the dynamics of the photochemical *cis-trans* isomerization process. In the latter method, the electronic wavefunction is described quantumchemically whereas the nuclear motion is assumed to be classical, leading to the semi-classical trajectory equations. This method is used in chapter 3.

In both methods, it is necessary to evaluate the coupling functions $g_{KL}(Q)$ describing the perturbation which determines the nonadiabatic interaction between the potential energy surfaces:

$$g_{KL}(Q) = \langle \Psi_K \mid \partial/\partial Q \mid \Psi_L \rangle \qquad 5$$

These elements can be calculated numerically[17,18] by performing a SCF calculation followed by a CI calculation for two values of the nuclear coordinate Q. The method can be employed for both semi-empirical and ab initio wavefunctions and is described in detail in the appendix.

1.4 Scope of this Thesis

The purpose of the work described in this thesis is the elucidation of two types of organic photochemical reactions (*cis-trans* isomerizations and sigmatropic shifts) by means of quantumchemical calculations. The *cis-trans* isomerization of double bonds in the excited state has been chosen because it is a prototype of an organic photochemical reaction observed in unsaturated hydrocarbons. Moreover, it is found to play a decisive role in several important biological processes including the chemistry of vision. In these processes, the *cis-trans* isomerization is the primary step in which the absorbed light energy is converted into thermal energy used to initiate a variety of chemical reactions. The

striking efficiency and selectivity of this primary photochemical step is a feature which is still not well understood. From a theoretical point of view, the *cis-trans* isomerization is of particular interest because this reaction can be described properly by a well defined one-dimensional reaction path (the rotation around the double bond). The sigmatropic shifts have been chosen because they play a central role in the study of the photochemistry of the cyclic 1,5-diene system germacrol in our laboratory, for which Fransen[19] found a unique [1,3]-OH shift. The mechanism of this photochemical reaction is assumed not to be controlled by orbital symmetry but to be initiated by an energetically favourable *cis-trans* isomerization of the excited double bond.

In chapter 2 a pure quantummechanical treatment is presented for the calculation of the photodynamics of *cis-trans* isomerization in small polyenes. The nuclear motion associated with the twist of the double bond is explicitely incorporated in the model Hamiltonian. Potential energy curves, (transition) dipole moments and nonadiabatic couplings have been calculated from ab initio CI calculations. It is shown that this one-dimensional approach gives an adequate description of the photochemical process. There is a direct relation between the shape of the potential energy curve of the excited state, the appearance of the UV absorption spectra and the photodynamics of these molecules. Upon increasing the number of conjugated double bonds, the molecules show an increasing tendency to be planar in the excited state so that the driving force for a photochemical *cis-trans* isomerization decreases. This observation seems to contradict with the remarkably rapid and efficient *cis-trans* isomerization in the protonated Schiff base of retinal. This molecule is the common chromophore in the light active protein systems rhodopsin and bacteriorhodopsin and consists of five carbon - carbon double bonds of which particularly one is found to exhibit a photoisomerization.

In chapter 3, MNDO CI calculations on the model compound 1-imino-2,4-pentadiene provide the potential energy surfaces and nonadiabatic couplings from which the dynamics of the *cis-trans* isomerization are studied using the semi-classical trajectory method. The remarkable difference between protonated Schiff bases and the common polyenes is shown to originate from the presence of the electron deficient nitrogen atom which strongly stabilizes the 90° twisted structure of the molecule in the excited state. This stabilization is found to depend on the distance from the twisted bond to the nitrogen atom and can be influenced by external point-charges in the neighbourhood of the molecule. This latter feature demonstrates how the surrounding protein can steer the photoisomerization by providing such external point-charges.

Chapters 4 and 5 are concerned with the description of photochemical sigmatropic reactions. A mechanism is elaborated which is not governed by the symmetry of the highest (singly) occupied molecular orbital but by the energetically favourable *cis-trans* isomerization of a double bond. From the 90° twisted conformation of the molecule, an atom (or group) may now shift in the plane of the carbon skeleton (planar shift) via a transition state of C_{2v}-symmetry. Both MNDO calculations with a minimal CI (chapter 4) and extensive ab initio CI calculations (chapter 5) strongly support this mechanism in the excited state. In contrast to the retinal-like systems, the *cis-trans*

isomerization which initiates the reaction, should be associated with a relatively small nonadiabatic coupling so that a photochemical shift can take place. Recent experiments[20] on the mechanism of photochemical sigmatropic shifts in our laboratory have confirmed the model of the planar shift in acyclic unsaturated hydrocarbons.

Finally, chapter 6 deals with the reaction kinetics of the thermal [1,5]-H shift in *cis*-1,3-pentadiene. It is found that, beside the (suprafacial) transition state as expected from orbital symmetry considerations, the planar transition state is close in energy. However, the calculated activation energy and kinetic isotope effect for both reactions are found to disagree with the experiment. Therefore, a mechanism is proposed by which the hydrogen atom shifts between two thermally activated twisted geometries via quantumchemical tunneling. The overall reaction rates for this mechanism are found to be in better agreement with the experiment. This is best accentuated for the reaction via the planar transition state.

1.5 References

1 R.S. Mulliken, Phys. Rev., **41**, 751 (1932)

2 E. Havinga, J.L.M.A. Schlattmann, Tetrahedron, **16**, 146 (1961)

3 R.B. Woodward, R. Hoffmann, J. Am. Chem. Soc., **87**, 395, 2046 (1965)
R.B. Woodward, R. Hoffmann, Angew. Chem., Int. Ed. Engl., **8**, 781 (1969)

4 L. Salem, Science, **191**, 822 (1976)
W.G. Dauben, L. Salem, N.J. Turro, Acc. Chem. Res., **8**, 41 (1975)

5 L. Salem, C. Leforestier, G. Segal, R. Wettmore, J. Am. Chem. Soc., **479** (1975)
N.J. Turro, J. McVey, V. Ramamurthy, P. Letchken, Angew. Chem., **91**, 597 (1979)

6 W.Th.A.M. van der Lugt, L.J. Oosterhof, J. Am. Chem. Soc., **91**, 6042 (1969)
W.Th.A.M. van der Lugt, Thesis, Leiden (1968)

7 M. Larsson, P.F.M. Siegbahn, J. Chem. Phys., **79**, 2270 (1983)

8 R.J. Buenker, S.D. Peyerimhoff, Theoret. Chim. Acta, **35**, 33 (1974)
R.J. Buenker, S.D. Peyerimhoff, W. Butscher, Mol. Phys., **35**, 771 (1978)

9 B. Huron, J.-P. Malrieu, P. Rancurel, J. Chem. Phys., **58**, 5745 (1973)

10 J. Del Bene, H.H. Jaffe, J.Chem. Phys., **48**, 1807, 4050 (1968)
J. Del Bene, H.H. Jaffe, J.Chem. Phys., **49**, 1221 (1969)

11 L. Asbrink, C. Fridh, E. Lindholm, Chem. Phys. Lett., **52**, 69 (1977)
L. Asbrink, C. Fridh, E. Lindholm, S. de Bruijn, D.P. Chong, Phys. Scrip., **22**, 475 (1980)

12 M.J.S. Dewar, W. Thiel, J.Am. Chem. Soc., **99**, 4899, 4970 (1977)

13 M.J.S. Dewar, H.S. Rzepa, J. Am. Chem. Soc., **100**, 784 (1978)

14 M.J.S. Dewar, M.A. Fox, K.A. Campbell, C.-C. Chen, J.A. Friedheim, M.K. Holloway, S.C. Kim, P.B. Liescheski, A.M. Pakiari, T.-P. Tien, E.G. Zoebisch, J. Compt.

Chem., **5**, 480 (1984)

15 See e.g.:

J.C. Tully in "Dynamics of Molecular Collisions", Part B, W.H. Miller Ed., Plenum Press, New York (1976)

R. Cimiraglia, M. Persico, J. Tomasi, Chem. Phys., **34**, 103 (1978)

16 See e.g.:

E.E. Nikitin in "Chemische Elementarprozesse", H.Hartmann Ed., Springer, Berlin (1968)

M. Desouter-Lecomte, J.C. Leclerc, J.C. Lorquet, Chem. Phys., **9**, 147 (1975)

17 C. Galloy, J.C. Lorquet, J. Chem. Phys., **67**, 4672 (1977)

18 G. Hirsch, P.J. Bruna, R.J. Buenker, S.D. Peyerimhoff, Chem. Phys., **45**, 335 (1980)

R. Cimiraglia, M. Persico, J. Tomasi, Chem. Phys., **53**, 357 (1980)

19 H.R. Fransen, H.M. Buck, J. Chem. Soc., Chem. Commun., 786 (1982)

H.R. Fransen, Thesis, Eindoven (1983)

20 W.J.G.M. Peijnenburg, G.J.M. Dormans, H.M. Buck, to be published

W.J.G.M. Peijnenburg, forthcoming thesis, Eindhoven (1988)

CHAPTER 2

Dynamical Calculations on the Photoisomerization of Small Polyenes in a Nonadiabatic Formalism

2.1 Introduction

The *cis-trans* isomerization in photoexcited unsaturated hydrocarbons is one of the most studied photoreactions[1] because it plays an important role in many organic systems including the visual pigment[2]. Despite a considerable amount of experimental and theoretical work on this subject, there still remain many questions about the fundamental photophysical and photochemical processes taking place.

Upon initial light absorption, an electron is promoted from a bonding π-MO to an antibonding π^*-MO. This excitation causes an electron redistribution which may lead to a geometrical relaxation of the double bond towards a 90° twisted structure. For ethylene there are two valence excited states which are needed to describe this process. In the case of a nonsymmetrical ethylene (such as monopyramidalized ethylene or propylene), the twisting motion leads to the development of an opposite dipole moment for the two states. This "sudden polarization" has first been described theoretically by Salem and coworkers[3] and has thereafter been found to persist by many theoretical calculations at different levels of sophistication[4].

In the 90° region the two excited states, which are commonly described as Z_1 and Z_2 due to their zwitterionic character, come very close in energy and their wavefunctions may change very rapidly. This causes a strong nonadiabatic coupling and the Born-Oppenheimer approximation may no longer be valid. In the extreme case, this may even lead to a cancellation of the opposite dipole moments[5]. Moreover, it is particularly this nonadiabatic coupling which is commonly regarded as the perturbation by which a molecule returns from its excited state to its ground state via a radiationless transition[6–8]. For this reason the *cis-trans* isomerization was investigated within a nonadiabatic treatment which incorporates explicitly the coupling through the twisting motion.

First it is shortly demonstrated how the time evolution of an excited molecule can be described within this model. Then, this is applied to three model systems, 10° monopyramidalized ethylene, butadiene and *trans*-hexatriene twisted around its terminal double bond, in order to investigate how the shape of the potential energy curves influences the dynamics of the photochemical *cis-trans* isomerization.

The results of the calculations will be discussed in relation to the appearance of the UV-spectra of small polyenes which show an increase in band width upon decreasing chain length[1,9]. Possible explanations for this intriuging feature are the tendency of the molecules to be nonplanar in the excited state[10], the presence of efficient radiationless processes[11] and the overlap between the absorbing excited state and the so called "hidden state", which might gain oscillatorstrength via a vibrational coupling[12]. Besides, these calculations may give some insight in the influence of this latter nonabsorbing excited state on the photodynamics of the polyenes, a feature which is still not well understood[11–14].

2.2 Methodology

In order to describe the dynamical behaviour of an excited molecule, not only the electron coordinates (r), but also the nuclear coordinates have to be included in the model Hamiltonian. For the description of the *cis-trans* isomerization it is convenient to restrict the calculation to only one motion: the twist around the double bond (θ). For a discussion of the influence of other nuclear motions on this reaction see references 14 to 16.

The solution of the time dependent Schrödinger equation generally starts with the calculation of the matrix elements of the total time independent Hamiltonian in a Born-Oppenheimer basis set[17]:

$$H^{tot}_{KiLj} = \langle \psi_{Ki}(r,\theta) \mid H^{tot}(r,\theta) \mid \psi_{Lj}(r,\theta) \rangle_{r,\theta} \qquad 1$$

$$H^{tot}(r,\theta) = H^{el}(r,\theta) + T(\theta) \qquad 2$$

$$\mid \psi_{Ki}(r,\theta) \rangle = \mid \psi^{el}_{K}(r,\theta) \chi_{Ki}(\theta) \rangle \qquad 3$$

$T(\theta)$ is the kinetic energy operator of the molecule for the twist around the double bond:

$$T(\theta) = -\frac{1}{2I}\frac{\partial^2}{\partial\theta^2}$$

The moment of inertia (I) equals $I_1 \times I_2/(I_1 + I_2)$, where I_1 and I_2 are the moments of inertia of the two groups on each side of the twisted double bond. The integration over θ is performed from $\theta = 0°$ to $\theta = 360°$. The index K runs over the electronic states $\psi^{el}_K(r,\theta)$ and i over the vibrational functions $\chi_{Ki}(\theta)$ (with energy E_{Ki}) of state K, which are defined by:

$$T(\theta) + E^{el}_K(\theta) \mid \chi_{Ki}(\theta) \rangle = E_{Ki} \mid \chi_{Ki}(\theta) \rangle \qquad 4$$

where $E^{el}_K(\theta)$ is the energy of the K^{th} electronic state:

$$H^{el}(r,\theta) \mid \psi^{el}_K(r,\theta) \rangle = E^{el}_K(\theta) \mid \psi^{el}_K(r,\theta) \rangle \qquad 5$$

$E^{el}_K(\theta)$ depends parametrically on θ and represents the potential energy curve

of the electronic state K for the twist around the double bond, as calculated from a standard quantumchemical calculation. Using these definitions, the matrix elements of eq. 1 now become[18]:

$$H^{tot}_{KiLj} = E_{Ki}\delta_{KL}\delta_{ij} - \frac{1}{2I}<\chi_{Ki}(\theta)\,|\,2g_{KL}(\theta)\frac{\partial}{\partial\theta} + t_{KL}(\theta)\,|\,\chi_{Lj}(\theta)>_{\theta} \quad 6$$

The functions $g_{KL}(\theta)$ and $t_{KL}(\theta)$ are known as the nonadiabatic coupling elements:

$$g_{KL}(\theta) = <\psi^{el}_{K}(r,\theta)\,|\,\partial/\partial\theta\,|\,\psi^{el}_{L}(r,\theta)>_{r} \quad 7$$

$$t_{KL}(\theta) = <\psi^{el}_{K}(r,\theta)\,|\,\partial^2/\partial\theta^2\,|\,\psi^{el}_{L}(r,\theta)>_{r} \quad 8$$

Finally, the energies E_n and wavefunctions $\psi_n(r,\theta)$ are obtained as eigenvalues and eigenfunctions of the total Hamiltonian matrix (eq. 6):

$$H^{tot}(r,\theta)\,|\,\psi_n(r,\theta)> = E_n\,|\,\psi_n(r,\theta)> \quad 9$$

$$|\,\psi_n(r,\theta)> = \sum_{Ki} c_{Ki}(n)\,|\,\psi^{el}_{K}(r,\theta)\chi_{Ki}(\theta)> \quad 10$$

To calculate the time evolution of the molecule, an initial state after excitation (t = 0) is obtained from:

$$\Psi(r,\theta,0) = \sum_{n}\alpha_n\psi_n(r,\theta) \quad 11$$

where the coefficients α_n are proportional to the transition dipole moments between the lowest vibrational level (i=1) of the ground state and the n^{th} vibrational level of the excited state (electronic dipole transition):

$$\alpha_n \propto <\psi_0(r,\theta)\,|\,\vec{r}\,|\,\psi_n(r,\theta)>_{r,\theta} = \mu_{1n} \quad 12$$

The total wavefunction at a time t is now given by:

$$\Psi(r,\theta,t) = \sum_{n}\alpha_n\psi_n(r,\theta)e^{-iE_n t} \quad 13$$

The time evolution of the wavefunction can be followed by calculating the overlap between the initial wavefunction and the wavefunction at a time t:

$$P(t) = |\,<\Psi(r,\theta,0)\,|\,\Psi(r,\theta,t)>_{r,\theta}\,|^2 \quad 14$$

This property is generally known as the radiationless decay of the initial state[19].

To study the sudden polarization effect, the time development was calculated of the total dipole moment $\mu_z(t)$ of the excited molecule in the direction parallel to the twisted double bond (which is chosen as the z-axis in the coordinate system):

$$\mu_z(t) = <\Psi(r,\theta,t)\,|\,z\,|\,\Psi(r,\theta,t)>_{r,\theta} \quad 15$$

$$= \sum_{n}\alpha_n^2\mu_{z,nn} + 2\sum_{n<m}\alpha_n\alpha_m\mu_{z,nm}\cos(E_n - E_m)t \quad 16$$

where $\mu_{z,nn}$ is the dipole moment of the wavefunction $\psi_n(r,\theta)$. The (transition) dipole moments $\mu_{z,nm}$ are obtained from the (transition) dipole moments

in the Born-Oppenheimer basis ($\mu_{z,KiLj}$) and the eigenvectors ($c_{Ki}(n)$, eq. 10):

$$\mu_{z,nm} = \sum_{Ki}\sum_{Lj} c_{Ki}(n)\, c_{Lj}(m)\, \mu_{z,KiLj} \qquad 17$$

$$\mu_{z,KiLj} = \langle \psi_K^{el}(r,\theta)\chi_{Ki}(\theta) \mid z \mid \psi_L^{el}(r,\theta)\chi_{Lj}(\theta)\rangle_{r,\theta} \qquad 18$$

$$= \langle \chi_{Ki}(\theta) \mid \langle \psi_K^{el}(r,\theta) \mid z \mid \psi_L^{el}(r,\theta)\rangle_r \mid \chi_{Lj}(\theta)\rangle_\theta$$

$$= \langle \chi_{Ki}(\theta) \mid \mu_{z,KL}(\theta) \mid \chi_{Lj}(\theta)\rangle_\theta$$

In this equation $\mu_{z,KL}(\theta)$ is the electronic (transition) dipole moment between the states $\psi_K^{el}(r,\theta)$ and $\psi_L^{el}(r,\theta)$.

2.3 Calculational Method

All the electronic state calculations have been carried out for fixed standard geometries ($r_{C=C}$ = 1.33 Å, r_{C-C} = 1.50 Å, r_{C-H} = 1.09 Å and all angles 120°) except for the twisted double bond, which was taken to be 1.40 Å. This restriction will inevitably introduce some errors in the results, but these effects are thought to be of minor importance with respect to the overall description of the energy curves and related properties for the reaction coordinate. The molecules were oriented in such a way, that the twisted double bond was placed along the z-axis, with the rotated CH_2-fragment in the positive direction.

The SCF calculations were performed with the GAUSSIAN 80 program package[20], employing the standard split valence basis set 3-21G for all three molecules. The extended basis sets 6-31G* (butadiene) and 6-31G** (ethylene) have also been used, mainly to improve the description of the vertical excitation to the absorbing ($\pi-\pi^*$)-state. The results of the calculations were found to depend only slightly on the size of the basis set.

For a proper discussion of the spectroscopy of the planar molecules, the inclusion of Rydberg orbitals is needed, especially for ethylene[21,22] and to a minor extent for butadiene[23]. However, it is not the purpose of this work to give a detailed description of the absorption spectra of these molecules. Moreover, for larger values of the twist angle, electronic states containing large contributions from Rydberg orbitals become highly unfavourable and are, therefore, expected not to influence the dynamics of the process in this region.

The many electron wavefunctions were obtained from a CI calculation based on one orthogonal basis of MOs for all electronic states, which greatly facilitates the calculation of interstate properties[24]. The choice of the one electron basis influences the final results of the calculation, especially when the HOMO and LUMO are nearly degenerate, as is the case for highly symmetrical twisted molecules. For nonsymmetrical molecules, this choice becomes less critical when an appropriate CI calculation follows[15].

Closed shell MOs were used rather than triplet MOs, because this yields smoother coupling functions. The coupling matrix elements are calculated as a sum of a so called MO- and CI-term (see appendix). For closed shell MOs the CI-term is much larger than the MO-term, whereas for the triplet MOs both terms become very large with opposite sign in the 90° region due to the rapid change of the character of the triplet MOs from delocalized to localized. Therefore, in this latter case, the results for the coupling matrix elements are found to depend highly on the CI treatment[25].

In the CI calculations all MOs were used except for the core MOs and their virtual counterparts. A zeroth order wavefunction was constructed for the lowest singlet states by a CI among the leading configurations. In a second stage, those configurations were selected through a second order perturbation calculation among all singly and doubly excited configurations, with an interaction coefficient with the zeroth order wavefunction larger than 0.02[26]. This procedure was repeated for several values of θ and the final wavefunctions were constructed from all selected configurations. This procedure gives a balanced description of the wavefunctions all along the reaction path. The dimensions of the final CI subspaces ranged from 208 for ethylene (3-21G) to 425 for *trans*-hexatriene.

The nonadiabatic coupling elements $g_{KL}(\theta)$ can be expressed as[27]:

$$g_{KL}(\theta) = \langle \psi_K^{el}(r,\theta) \mid \partial/\partial\theta \mid \psi_L^{el}(r,\theta) \rangle_r = g_{KL}^{CI}(\theta) + g_{KL}^{MO}(\theta) \qquad 19$$

In this equation $g_{KL}^{CI}(\theta)$ involves the differentiation of the CI coefficients and $g_{KL}^{MO}(\theta)$ the differentiation of the molecular orbitals. Both terms were evaluated approximately by the method of finite differences[27], with $\Delta\theta$ = 0.02°. The numerical accuracy of the calculation can be estimated from the antisymmetry condition: $g_{KL}(\theta) = - g_{LK}(\theta)$. The second derivative nonadiabatic coupling elements $t_{KL}(\theta)$ were calculated from the $g_{KL}(\theta)$ terms using the expression:

$$t_{KL}(\theta) = \sum_j g_{KJ}(\theta) g_{JL}(\theta) + \frac{\partial}{\partial\theta} g_{KL}(\theta) \qquad 20$$

All functions of θ (E_K , g_{KL} , t_{KL} , $\mu_{z,KL}$) were expanded in a Fourier series after a cubic spline interpolation. This procedure makes it possible to calculate all matrix elements analytically. The number of terms included in the expansion (72) was taken equal to the number of data points between θ = 0° and θ = 360°. Because of the symmetry of the molecules at θ = 0° (C_s) and θ = 90° (C_s), the functions are series of either pure cos(2nθ), cos((2n+1)θ), sin(2nθ) or sin((2n+1)θ) (see Table 1).

In a subsequent step, the Born-Oppenheimer vibrational wavefunctions ($\chi_{Ki}(\theta)$) and corresponding energies (E_{Ki}) were calculated. The highest order terms in $\chi_{Ki}(\theta)$ were cos(90θ) and sin(90θ). The moments of inertia used were 5500 au (ethylene) and 11000 au (butadiene and *trans*-hexatriene). Finally, the vibrational states $\mid \psi_n(r,\theta) \rangle$ and energies E_n were obtained from a diagonalization of the total Hamiltonian matrix (eq. 1). The number of Born-Oppenheimer wavefunctions included in this calculation ranged from 40 to 80 per electronic state.

Table 1. Symmetry properties of the electronic states, (transition) dipole moments and nonadiabatic coupling functions.

Symmetry[a] at		Basis-function	Operator	Ethylene	Butadiene	Hexatriene
0°	90°					
S	S	$\cos(2n\theta)$	z	S_1 g_{02} $\mu_{z,i}$ t_{ii}	S_1 S_3 $\mu_{z,i}$ t_{ii} $\mu_{z,02}$ $\mu_{z,13}$ t_{02} t_{13}	S_2 S_3 S_4 $\mu_{z,i}$ t_{ii} $\mu_{z,01}$ $\mu_{z,23}$ $\mu_{z,24}$ $\mu_{z,34}$ t_{01} t_{23} t_{24} t_{34}
S	A	$\cos((2n+1)\theta)$		S_0 $\mu_{z,01}$ g_{12} t_{01}	S_0 S_2 $\mu_{z,01}$ $\mu_{z,12}$ $\mu_{z,03}$ $\mu_{z,23}$ t_{01} t_{12} t_{03} t_{23}	S_0 S_1 $\mu_{z,02}$ $\mu_{z,12}$ $\mu_{z,03}$ $\mu_{z,13}$ $\mu_{z,04}$ $\mu_{z,14}$ t_{02} t_{12} t_{03} t_{13} t_{04} t_{14}
A	S	$\sin((2n+1)\theta)$		S_2 $\mu_{z,12}$ g_{01} t_{12}	g_{01} g_{12} g_{03} g_{23}	g_{02} g_{12} g_{03} g_{13} g_{04} g_{14}
A	A	$\sin(2n\theta)$	$\partial/\partial\theta$	$\mu_{z,02}$ t_{02}	g_{02} g_{13}	g_{01} g_{23} g_{24} g_{34}

[a] S = Symmetric, A = Antisymmetric

2.4 Results

2.4.1 Ethylene

The *cis-trans* isomerization in 10° monopyramidalized ethylene has been calculated by both a split valence 3-21G basis (208 x 208 CI) and an extended 6-31G** basis (280 x 280 CI). Because the results are found to be qualitatively the same, only the extended basis set calculation will be presented here.

For ethylene, there are three valence singlet states relevant for the description of the *cis-trans* isomerization dynamics and the related sudden polarization. These are the ground state (S_0) and two excited states (S_1 and S_2), of which the former correlates with the $(\pi-\pi^*)$ and the latter with the $(\pi-\pi^*)^2$ excited state at $\theta = 0°$. The energy curves, coupling functions and most important (transition) dipole moments are given in Figure 1.

A detailed description of the characteristics of these curves is given in the literature[6,8a,15], so only the main features will be discussed here.

The ground state shows an energy barrier for a rotation around the double bond. The wavefunction is almost purely covalent (diradicalar) along the twist

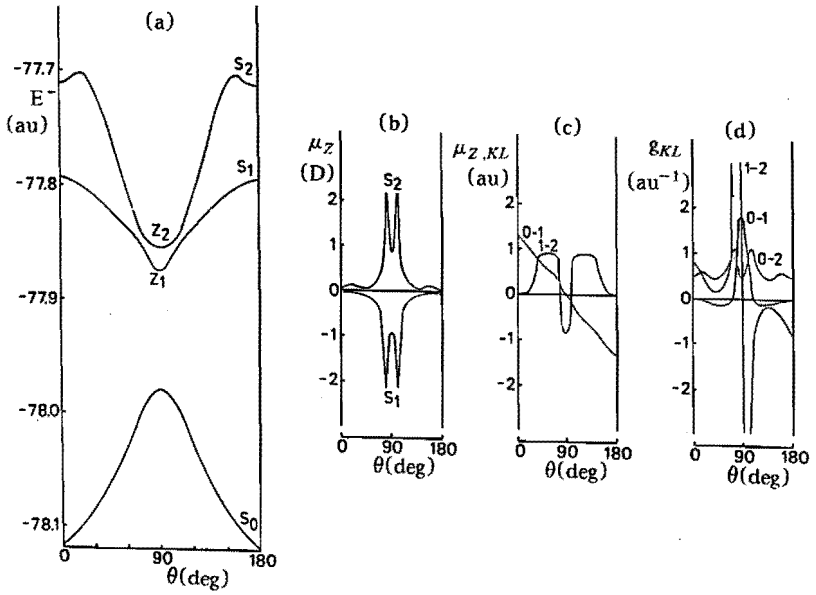

Figure 1. Potential energy curves (a), dipole moments (b), transition dipole moments (c) and nonadiabatic couplings (d) of 10° monopyramidalized ethylene as a function of the twist angle (θ). The dipole moment of the ground state is small and, therefore, not shown. Only the relevant transition dipole moments are presented.

coordinate and, consequently, the dipole moment of this state is very small (<-0.05 D). The light absorption for the planar molecule is located in S_1 (($\pi-\pi^*$) transition), for which an electronic oscillatorstrength (f_1^{el}) was calculated of 0.41.

$$f_K^{el} = \frac{2}{3}\Delta E_{0,K} \mid \mu_{z,0K} \mid^2 \qquad 21$$

This value is too high compared with the experimental value of 0.34[28], because the transition energy is overestimated (calculated 8.83 eV, observed 7.66 eV[29]).

Upon twisting, the potential energy of S_1 decreases monotonically going from $\theta = 0°$ to $\theta = 90°$, in accordance with the fact that ethylene is expected to relax to an orthogonal conformation in this singlet excited state. The nonadiabatic coupling function (Figure 1d) between S_1 and S_0 shows a symmetric curve with a maximum of $g_{01} = 1.86$ au^{-1} at $\theta = 90°$, where the energy difference between these two states is minimal (2.83 eV). Generally, this observation is interpreted as an indication that the probability for a radiationless transition to the ground state is maximal at this point on the reaction coordinate (*vide infra*).

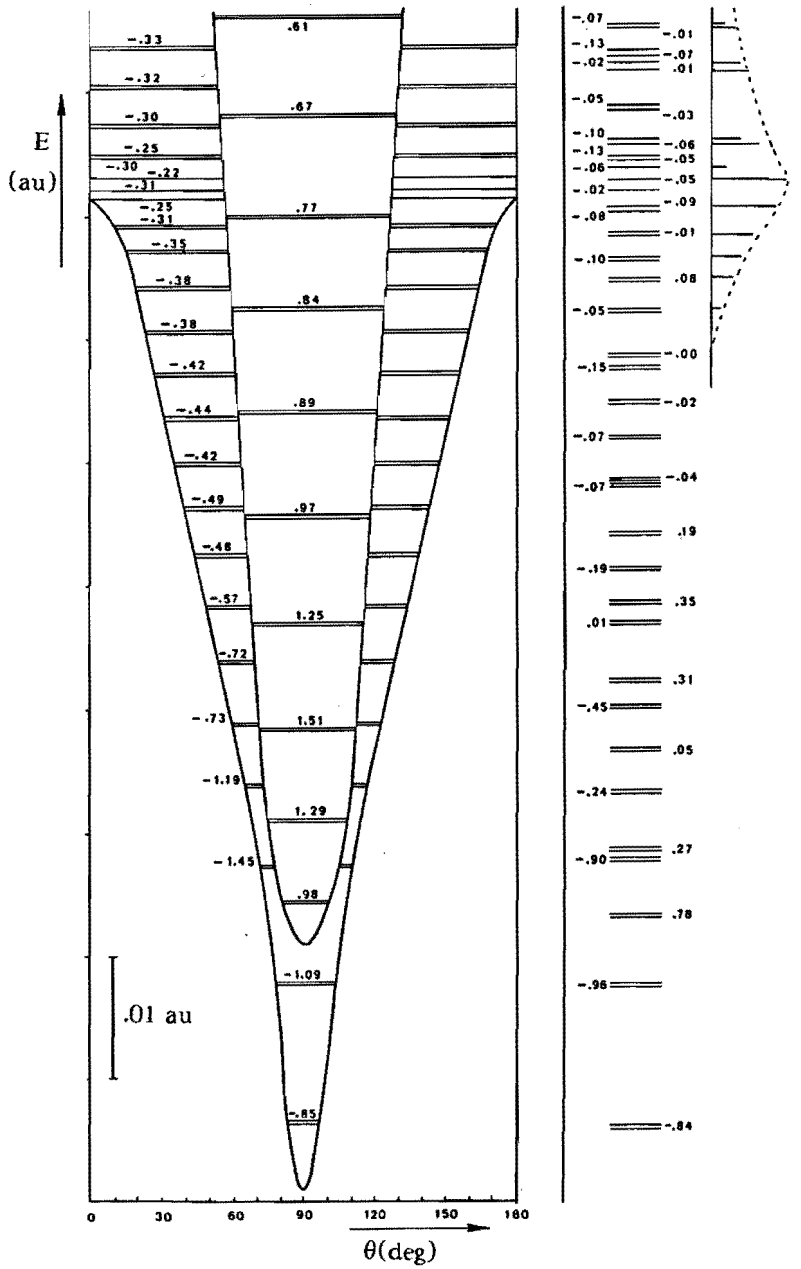

Figure 2. Potential energy curves, Born–Oppenheimer energy levels and dipole moments (in Debye) of the excited states of 10° monopyramidalized ethylene. Right: energy levels and dipole moments after nonadiabatic treatment, and the initially excited wavefunction ($|\alpha_n|$, see eq. 12).

The nonadiabatic coupling function g_{12} is antisymmetric with respect to θ = 90° (Table 1) and shows a sharp peak at θ = 75° ($g_{12}(75°)$ = 10.65 au^{-1}) as a result of an avoided crossing between S_1 and S_2. At this value of θ, the wavefunctions of these states change rapidly, which is also reflected in the change of the sign of the transition dipole moment $\mu_{z,12}(\theta)$ (see Figure 1c).

Both excited states are known to be ionic in character (see e.g. reference 8a). Upon twisting, the contribution to S_1 of the configuration which bears the two π-electrons at the pyramidalized CH_2-fragment constantly increases. This results in a developing negative dipole moment. For S_2, the contribution of the ionic configuration with a positive dipole moment becomes larger. For θ-values larger than 75° the two states have undergone an avoided crossing and the wavefunctions are mixed. This leads to a decrease of the absolute value of both dipole moments (see Figure 1b).

In Figure 2 the results of the vibrational treatment for the two excited states are presented in detail. First the "static" result will be discussed, i.e. the calculation of the Born-Oppenheimer wavefunctions ($\chi_{Ki}(\theta)$), energies (E_{Ki}) and dipole moments ($\mu_{z,Ki}$) without adding the nonadiabatic coupling (eqs. 4 and 18).

Due to the symmetry of the molecule, the vibrational states are (accidentally) twofold degenerate. Rotating θ over 180° implies an interchange of the two protons of the CH_2-fragment. As a consequence, the vibrational wavefunctions can be symmetric or antisymmetric with respect to this symmetry operation. For low vibrational quantumnumbers, the energies of the symmetric and antisymmetric wavefunctions are almost identical. For example, the energy difference between $|\chi_{0,1}(\theta)>$ and $|\chi_{0,2}(\theta)>$ is only 8×10^{-12} au = 0.0002 cm^{-1}. Because of this small energy difference, already a very small perturbation (which lies in the order of error in the calculation) causes the final wavefunctions to be a linear combination of the two symmetry adapted wavefunctions.

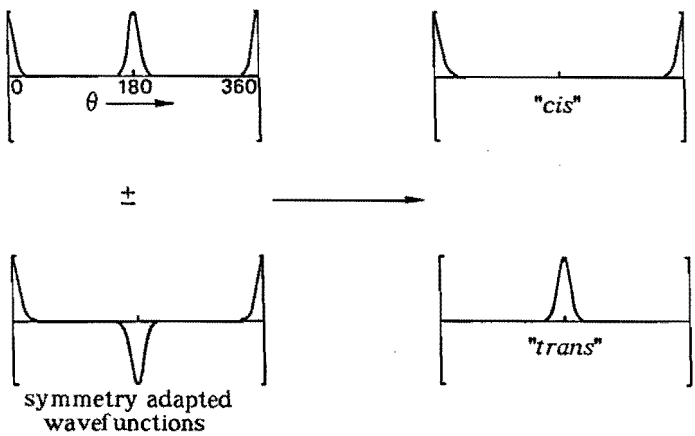

In this way, the lowest vibrational states of the ground state are located at θ = 0° or θ = 180° respectively, in this way creating an artificial difference between the "*cis*" and the "*trans*" isomers of ethylene. This feature will be employed in the description of the time evolution of the excited molecule.

For the higher vibrational quantumnumbers, the energy difference between the even and odd wavefunctions increases, and the perturbation no longer cancels the symmetry properties of the wavefunctions. In the neighbourhood of the top of the potential curves, the (accidental) degeneracy disappears. For yet higher quantumnumbers, the vibrational wavefunctions are (almost) pure rotational and the symmetric and antisymmetric wavefunctions are degenerate again.

Going to higher quantumnumbers, the energy difference between two successive even (or odd) vibrational levels in the ground state decreases to a value of about 1100 cm^{-1}. This value compares well with the experimental result of 1023 cm^{-1} [30]. The dipole moments are small (< -0.05 D) for all vibrational levels of the ground state.

The shapes of the potential energy curves of the two excited states are essentially nonharmonical in the 90° region due to the avoided crossing near θ = 75° (and θ = 105°). As a result, the spacing between the lowest vibrational levels of S_1 is enlarged while the opposite occurs for S_2. At higher quantumnumbers, the energy differences between the even (and odd) levels become equidistant again with ΔE = 840 cm^{-1} for S_1 and 1440 cm^{-1} for S_2.

The dipole moments of the Born-Oppenheimer wavefunctions of S_1 first increase to a maximum value of -1.45 D for i=5,6 and then decrease again. This behaviour is fully consistent with the shape of the electronic dipole moment curve (see Figure 1b). This curve has a maximum at θ = 75° (and θ = 105°) and, therefore, those vibrational wavefunctions which are located near these values of θ will exhibit the largest dipole moments. For the lower vibrational quantumnumbers, the wavefunctions have their maxima near θ = 90°, where the electronic dipole moment is smaller. For the higher levels, the wavefunctions are additionally more diffuse, causing an extra decrease in the dipole moment. The same behaviour can be seen for the vibrational levels of S_2. It is thus seen that just those Born-Oppenheimer vibrational wavefunctions with the largest dipole moments are located near the avoided crossing, where the nonadiabatic coupling function is maximal. Therefore, it is expected that particularly these large dipole moments will be most affected by the nonadiabatic perturbation.

The energy levels and dipole moments of the vibrational wavefunctions after the inclusion of the nonadiabatic coupling are shown on the right hand side of Figure 2. It is found that the vibrational states of S_0 are almost unaffected by the twisting motion. Not only the nonadiabatic coupling with the excited states is relatively small, but also the overlap between the Born-Oppenheimer wavefunctions of the ground state and the excited states. Therefore, the off-diagonal matrix elements of eq. 6 are small, even for the higher vibrational levels of the ground state.

On the other hand, the Born-Oppenheimer wavefunctions of the excited states are strongly mixed, and the dipole moments (partially) cancel. In Figure 3 the correlation diagram is given between the lowest Born-Oppenheimer vibrational states of S_1 and S_2 and the final eigenstates. Only in the lowest vibrational eigenstates the dipole moment persists.

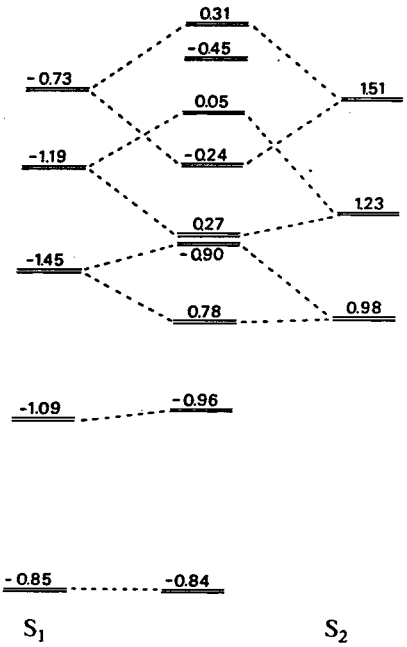

Figure 3. Correlation diagram between the lowest Born-Oppenheimer vibrational wavefunctions of S_1 and S_2 of 10° monopyramidalized ethylene and the eigenfunctions after nonadiabatic coupling. The dipole moments are given in Debye.

To calculate the time development of the excited molecule, an initial wavefunction is defined through the eqs. 11 and 12. The coefficients $|\alpha_n|$ are presented at the utmost right hand side of Figure 2. It can be seen that for ethylene several vibrational eigenfunctions are excited. This is a direct consequence of the shape of the potential energy curve of S_1 (*vide infra*).

As indicated in eq. 12, the coefficients α_n are proportional to the transition dipole moments μ_{1n}, from which the oscillatorstrength for a given vibrational eigenfunction can be calculated:

$$f_n = \frac{2}{3}\Delta E_{1,n} |\mu_{1n}|^2 \qquad 22$$

The total oscillatorstrength for the S_0 - S_1 absorption is then given by:

$$f^{tot} = \sum_n f_n \qquad 23$$

Comparing these parameters with the experimental $\pi - \pi^*$ absorption spectrum

gives a check of the initial wavefunction. For ethylene the value of f^{tot} is 0.39, which is somewhat smaller than the calculated electronic oscillatorstrength (f^{el} = 0.41). This is caused by the excitation which is found to be nonvertical, i.e. the center of the calculated absorption band is located near an energy of 8.75 eV, which is lower than the vertical transition energy (8.83 eV). More decisive is the fact that the total vibrational wavefunction is not exactly located at θ = 0° and that $\mu_{01}(\theta)$ decreases for values away from θ = 0° (Figure 1c).

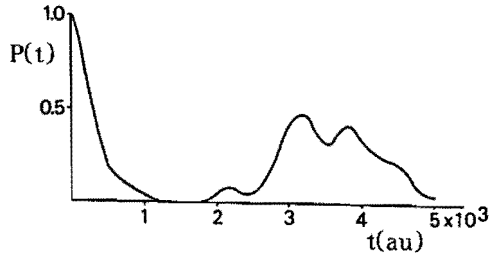

Figure 4. The radiationless decay P(t) of 10° monopyramidalized ethylene.

The radiationless decay P(t) of 10° monopyramidalized ethylene is shown in Figure 4. Until t = 1500 au (= 3.6×10^{-2} psec), the radiationless decay is almost exponential. This is a typical behaviour of a wavefunction built up from several eigenfunctions. The overlap between the initial wavefunction and the wavefunction at the time t is minimal at t = 1500 au (P(t) = 1×10^{-3}). This corresponds with a rotation angle of 180°. At t = 3100 au (7.5×10^{-2} psec), P(t) reaches a maximum again. The molecule has now performed one full rotation around the double bond. As the time proceeds, the wavefunction is spread out and this is the reason why P(t) not equals 1.0, but only 0.48 after one rotation. For even larger values of t, the wavefunction becomes so diffuse, that the rotation is no longer recognized.

Note, that the time for one rotation (7.5×10^{-2} psec) is very short compared to the estimated radiative lifetime of ethylene, which is in the order of 10^3 psec.

The rotation around the double bond can also be nicely demonstrated with the time evolution of the total dipole moment $\mu_z(t)$ of the molecule. To indicate the importance of the nonadiabatic coupling, this dipole moment was calculated with the unperturbed Born-Oppenheimer wavefunctions and with the final vibrational eigenfunctions (see Figure 5).

In the former formalism, only vibrational wavefunctions belonging to S_1 are excited. A developing dipole moment is observed (Figure 5a) which reaches a maximum of $\mu_z(t)$ = -0.55 D at t = 650 au (1.6×10^{-2} psec) and then decreases again. It can thus be said that there is indeed some polarization. The maximum corresponds to a twist angle of approximately 90°. A second (less pronounced) maximum occurs at t = 2300 au, corresponding to θ = 270°. For increasing times, the amplitude of the oscillating dipole decreases as a result of the wavefunction becoming more diffuse.

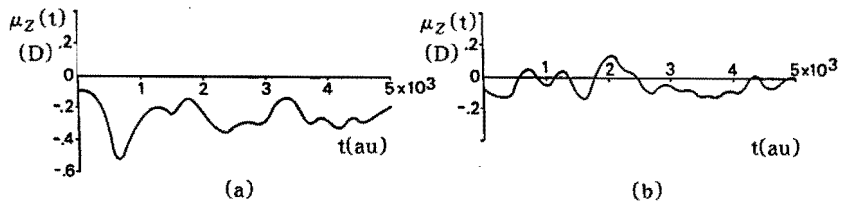

Figure 5. The dipole moments $\mu_z(t)$ of 10° monopyramidalized ethylene before (a) and after (b) the inclusion of the nonadiabatic coupling.

The influence of the nonadiabatic coupling can be seen in Figure 5b. The dipole moment is now much smaller and oscillates between -0.15 D < $\mu_z(t)$ < 0.15 D. No appreciable polarization is left. This is a direct consequence of the mixing of the two oppositely polarized excited states. To illustrate this, the contribution of the electronic states to the total wavefunction was calculated:

$$P_K(t) = \sum_i | \langle \psi_K^{el}(r,\theta)\chi_{Ki}(\theta) | \Psi(r,\theta,t) \rangle_{r,\theta} |^2 \qquad 24$$

The result of this calculation is shown in Figure 6.

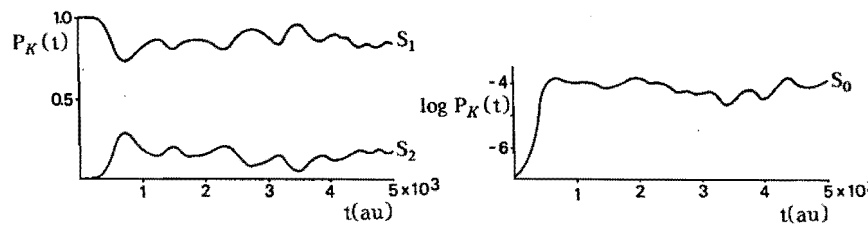

Figure 6. The contributions $P_K(t)$ of the electronic states to the total wavefunction (eq. 24) of 10° monopyramidalized ethylene.

At t = 0, the total wavefunction $|\Psi(r,\theta,t)\rangle$ is made up almost entirely from $|\psi_1^{el}(r,\theta)\rangle$. As the molecule reaches the 90° region, this contribution drops to a value of 0.7 at the cost of an increasing contribution of $|\psi_2^{el}(r,\theta)\rangle$, thus nicely demonstrating the avoided crossing between these two states. In the same figure the contribution of the electronic ground state is shown, which also reaches its maximum at $\theta = 90°$. However, the maximum value of $P_0(t)$ is very small ($< 2\times10^{-4}$). $P_0(t)$ is sometimes regarded as the probability for a radiationless transition to the ground state[6,18]. Such an interpretation would only be correct when the molecule stays on the ground state potential energy surface. However, this can only be achieved when the total energy of the twisting motion decreases, a feature which is not accounted for in the present model.

2.4.2 Butadiene

So far, theoretical investigations for butadiene have been concentrated mainly on the energy ordering and equilibrium geometry of the lowest excited states for the planar conformation and the 90° twisted structure[11–16,23,31–33]. From these calculations it seems plausible to consider four valence singlet states for the description of the dynamics of the one-bond *cis-trans* isomerization in butadiene. In the symmetry classification of all-*trans* polyenes (C_{2h}-symmetry) these are indicated as the $1^1A_g^-$ (ground state), $1^1B_u^+$ ($\pi-\pi^*$), $1^1A_g^+$ ($(\pi-\pi^*)^2$) and the $2^1A_g^-$ states. The former three are basically the same as those used for ethylene. The latter excited state is generally known as the "hidden state", due to the fact that the single-photon transition from the ground state is symmetry forbidden. Therefore, this state is not observed in the UV absorption spectrum.

To elucidate the dynamics of the isomerization, the potential energy curves, (transition) dipole moments and nonadiabatic coupling functions were calculated for the twist around one double bond using a 6-31G* basis set (415 x 415 CI). The calculated curves are depicted in Figure 7, and the symmetry properties of these functions in Table 1.

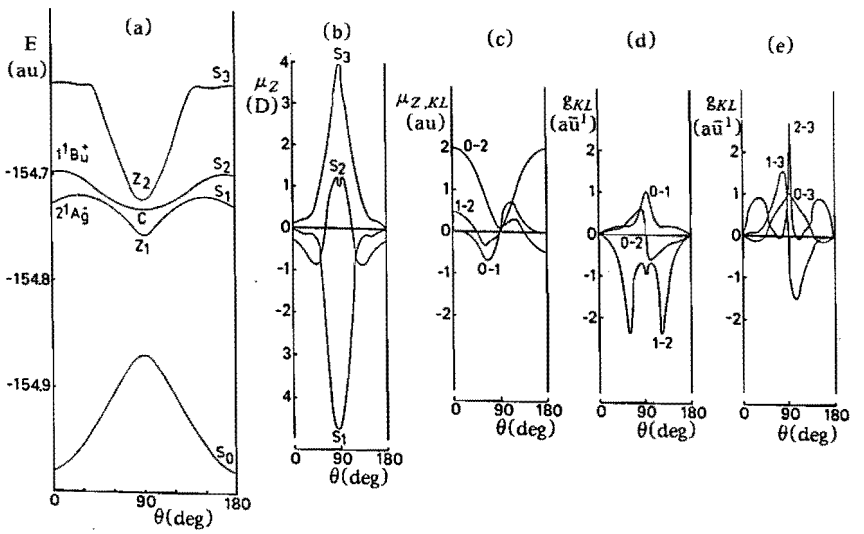

Figure 7. Potential energy curves (a), dipole moments (b), transition dipole moments (c) and nonadiabatic couplings (d,e) of butadiene as a function of the twist angle (θ). The dipole moment of the ground state is small and, therefore, not shown. Only the relevant transition dipole moments are presented.

Again, the results of a 3-21G calculation are found to be qualitatively the same (energy curves, avoided crossings, etc.) thus confirming the idea that for the purposes of this work the main features are independent of the quality of

the basis set.

For the planar molecule, the $^1A_g^-$ excited state (S_1) lies below the $^1B_u^+$-state (S_2): $\Delta E_{0,1}$ = 6.83 eV, $\Delta E_{0,2}$ = 7.67 eV. However, it is the latter state which is optically excited (f_2^{el} = 0.80) and the $^1A_g^-$- state can thus only be populated via an internal conversion from S_2[34]. Like the ground state, the $^1A_g^-$-state has a purely covalent (diradicalar) nature[14] in the 90° region and is, therefore, referred to as the C-state. Its dipole moment should be small all along the twist coordinate, in contrast to the other two excited states (Z_1 and Z_2) which are (zwitter)ionic in character.

At θ = 90° the electronic wavefunction which bears the two π-electrons on the methylene (M) group (Z_1 : A^+-M^-) is better stabilized than the configuration with the two electrons on the allyl (A) fragment (Z_2 : A^--M^+). In this terminology[13,14], the ground state at θ = 90° is described as $A^\bullet-M^\bullet$ and the C-state as $A^{\bullet *}-M^\bullet$ thus indicating that the allyl-fragment is in an excited configuration. For this orthogonal conformation C was calculated to lie 17.1 kcal/mol above Z_1 and 4.5 kcal/mol below Z_2. This sequence is in agreement with the results of a large scale MRD CI calculation for this geometry[14]. The fact that the energy ordening of C and Z_1 is reversed with respect to the situation at θ = 0°, implies that these states must have undergone an avoided crossing upon twisting. This is indeed the case as can be deduced from the coupling function $g_{12}(\theta)$, which shows a maximum (2.34 au^{-1}) at θ = 60°, and the transition dipole function $\mu_{z,12}(\theta)$ which changes sign at this angle.

Now the shapes of the dipole moment curves can also be understood (Figure 7b). For small twist angles, S_1 is predominantly built up from C and, therefore, exhibits a small dipole moment. In the neighbourhood of θ = 60° S_1 starts to gain a contribution from Z_1 and, consequently, the dipole moment sharply increases to a maximum value of $\mu_{z,1}(90°)$ = -4.81 D. In the same region the dipole moment of S_2 decreases and even becomes positive due to an admixture of Z_2. This is clear from the nonadiabatic coupling between S_2 and S_3 near θ = 90°. In its turn, S_3 is almost purely made up from Z_2 and shows a maximum of $\mu_{z,3}(90°)$ = 3.95 D which absolute value is somewhat smaller than that of S_1 due to the coupling with the covalent C-state.

Just as for ethylene, the transition dipole moment to the absorbing state (S_2) strongly decreases upon twisting. The nonadiabatic coupling (Figure 7d) between the ground state and the excited states is largest between S_0 and $S_1(Z_1)$: $g_{01}(90°)$ = 1.06 au^{-1}. On the other hand, the nonadiabatic coupling with C is zero at this angle for symmetry reasons (Table 1). It might be deduced from this, that a radiationless transition to the ground state must be rather ineffective from C. However, one must be very cautious in ascribing the calculated properties strictly to C($^1A_g^-$) or $Z_1(^1B_u^+)$ as the wavefunctions show characteristics of both configurations all along the twist coordinate. The nonadiabatic coupling function between the polarized states $Z_1(S_1)$ and $Z_2(S_3)$ shows a similar behaviour as for ethylene, the maximum (1.53 au^{-1}) being much smaller because of the absence of an avoided crossing between these two states.

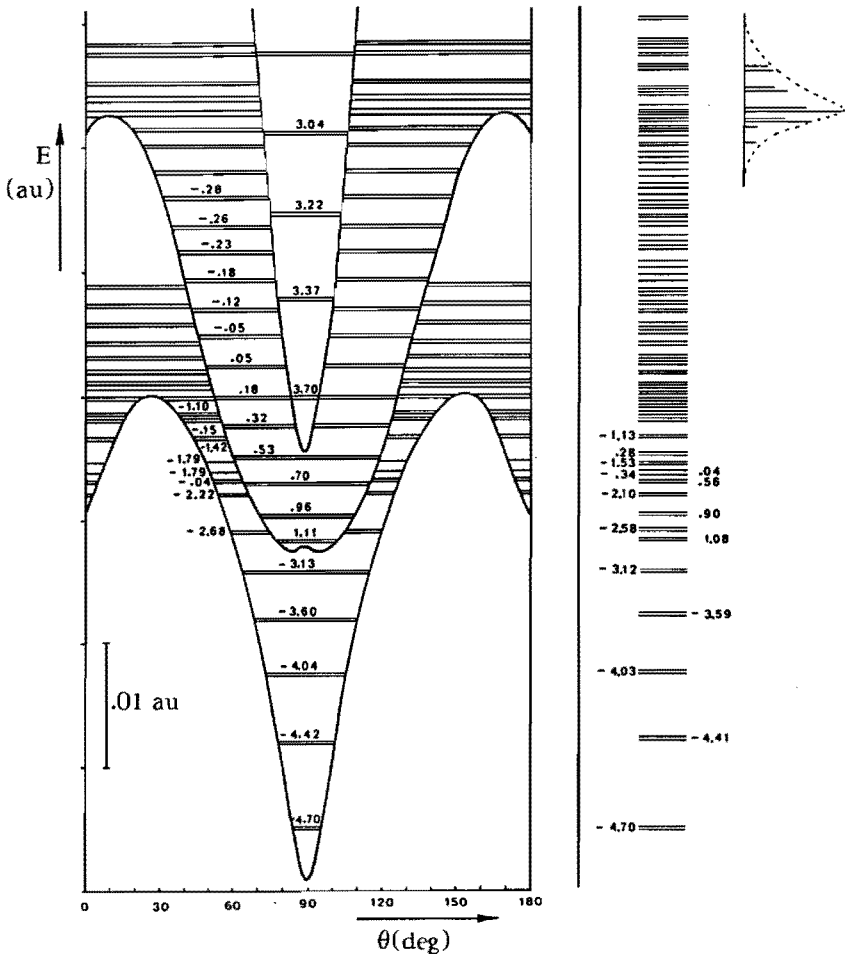

Figure 8. Potential energy curves, Born-Oppenheimer energy levels and dipole moments (in Debye) of the excited states of butadiene. Right: energy levels and dipole moments after the nonadiabatic treatment, and the initially excited wavefunction ($|\alpha_n|$, see eq. 12). The highest Born-Oppenheimer wavefunctions of each electronic state are not shown.

In Figure 8 the detailed energy curves, Born-Oppenheimer vibrational levels and corresponding dipole moments of the three excited states of butadiene are shown. Both S_1 and S_2 have a barrier for rotation around the double bond. In S_1 the top of the barrier at $\theta = 30°$ is 0.0096 au (= 6.0 kcal/mol) above the minimum at 0°. As a consequence, the vibrational wavefunctions of S_1 in the neighbourhood of this barrier are located at either small values of θ and correspondingly small dipole moments (e.g. for i=13,14 $\mu_{z,1} = -0.04$ D) or at larger values of θ with larger dipole moments (e.g. for i=11,12 $\mu_{z,1} = -2.22$ D). Because of the relatively large energy difference and small nonadiabatic coupling between Z_1 and the two higher excited states, there are several

vibrational levels of Z_1 with large negative dipole moments which remain unchanged upon inclusion of the twisting perturbation (see the right hand side of Figure 8).

The energy spacings between the successive even (and odd) vibrational energy levels of the excited states much smaller than in ethylene. On the one hand this is a consequence of the moment of inertia of butadiene being twice as large as the one of ethylene. On the other hand, the gradients of the energy curves are smaller. These two facts, together with the presence of vibrational levels belonging to the hidden state are the reason that the density of vibrational eigenfunctions near the vertical absorption is much larger than is the case for ethylene. Moreover, it is seen (from the coefficients α_n, utmost right hand side of Figure 8) that the number of eigenfunctions in the initially excited wavefunction is smaller. Due to the very small energy barrier (0.0014 au = 0.9 kcal/mol at θ = 10°) in S_2, several wavefunctions are more centered near θ = 0°. These wavefunctions have a relatively large overlap with the first vibrational wavefunction of the ground state. The integrated value of the oscillatorstrength for this absorption is f^{tot} = 0.72, again somewhat smaller than the calculated electronic oscillatorstrength (f^{el} = 0.80).

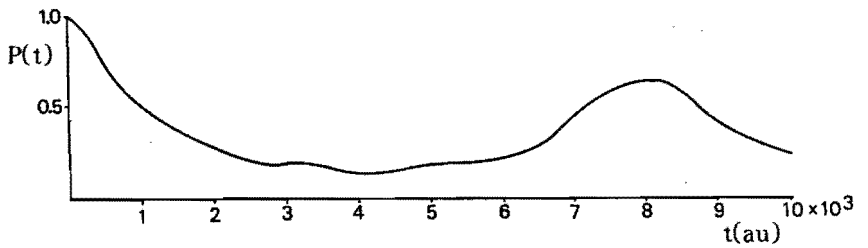

Figure 9. The radiationless decay P(t) of butadiene.

The shape of the radiationless decay curve (Figure 9) of butadiene lies in between the limiting cases of an exponential behaviour (large number of excited eigenfunctions, see ethylene) and a pure oscillatory behaviour as would be observed when exactly two eigenfunctions were excited. In this latter case, the oscillation time is inversely proportional to the energy difference between the two eigenfunctions : $\Delta t \approx \hbar \times \Delta E^{-1}$. Compared to ethylene, the density of excited vibrational levels is larger. Therefore, the times at which P(t) is minimal (t = 4200 au = 0.1 psec, θ = 180°) and reaches its maximum again (t = 8100 au = 0.2 psec, θ = 360°) are larger. Classically this can be interpreted as butadiene rotating slower than ethylene because of the larger moment of inertia.

In Figure 10 the time dependent dipole moment $\mu_z(t)$ and the contributions of the electronic states to the total wavefunction ($P_K(t)$) are shown. The time averaged dipole moment of butadiene is -0.4 D which is more negative than that of ethylene because of the larger asymmetry. The oscillatory behaviour of the dipole moment mimics the rotating double bond. The minimum at t = 1900 au and the maximum at t = 5900 au correspond with twist angles of θ = 90° and θ = 270° respectively, where the electronic dipole moments of the

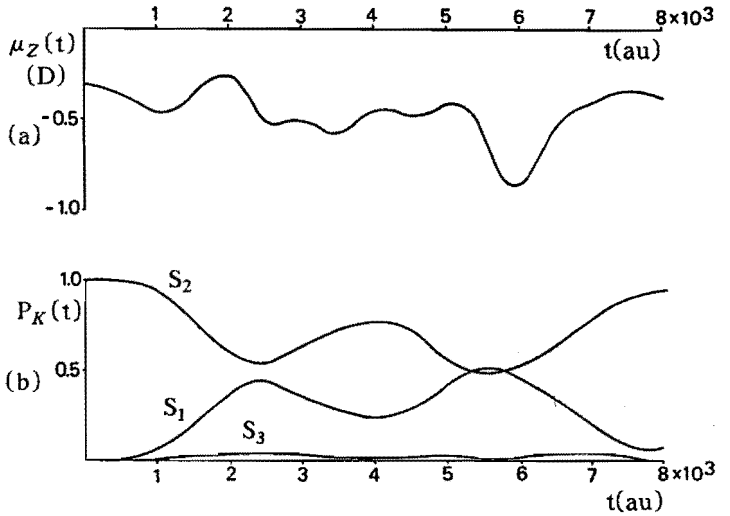

Figure 10. The dipole moment $\mu_z(t)$ (a) and contributions $P_K(t)$ of the electronic states to the total wavefunction (b) (eq. 24) of butadiene.

excited states have their maxima (Figure 7b). From Figure 10b it can be seen that at t = 1900 au the contribution of S_2 (positive dipole moment) is larger than the contribution of S_1 (strong negative dipole moment). This situation is reversed near t = 5900 au thus explaining the relative decrease and increase of $|\mu_z(t)|$ at 1900 au and 5900 au. The fact that the contribution of S_1 may become so large (> 50%), is a direct result of the avoided crossing between S_2 and S_1. It demonstrates that the nonabsorbing hidden state indeed becomes populated in a very short time (0.05 psec) and that this state may thus play a role in the photodynamics of *cis-trans* isomerization.

The contribution of the electronic ground state to the total wavefunction never exceeded a value of 5×10^{-7}. From this one may conclude that, within the present model, the probability of the excited molecule to return to its electronic ground state is neglectable.

2.4.3 *Trans*-Hexatriene

The results of the 3-21G calculation (425 X 425 CI) for the *cis-trans* isomerization of the external double bond in *trans*-hexatriene are shown in Figure 11.

The $^1A_g^-$(C)-state (vertical absorption 6.49 eV) lies below the $^1B_u^+(Z_1)$-state (vertical absorption 7.85 eV) all along the twist coordinate. An extension of the basis set with polarization functions would lower the energy of the $^1B_u^+$-

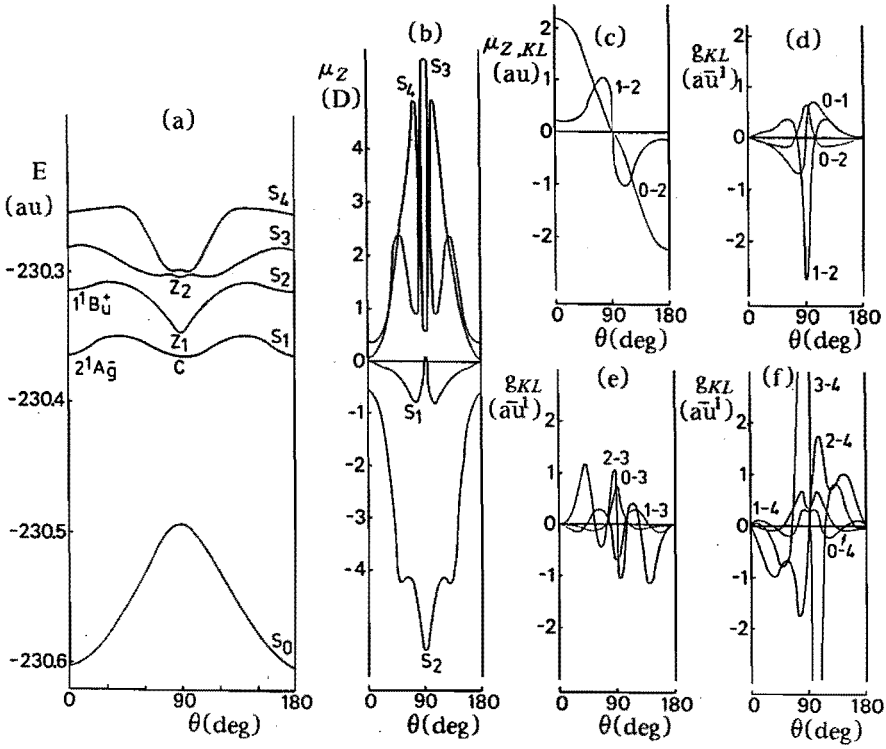

Figure 11. Potential energy curves (a), dipole moments (b), transition dipole moments (c) and nonadiabatic couplings (d,e,f) of *trans*-hexatriene as a function of the twist angle (θ). The dipole moment of the ground state is small and, therefore, not shown. Only the relevant transition dipole moments are presented.

state, but from the experience with ethylene and butadiene it is not expected that the energy ordening of the $^1A_g^-$- and $^1B_u^+$-state will reverse. Whereas for butadiene the exact location of the hidden state is unclear, for octatetraene and longer polyenes it is definitely found below the photoactive $^1B_u^+$-state[1,35]. An extrapolation of the $^1A_g^-$ and $^1B_u^+$ excitation energies from the higher polyenes to *trans*-hexatriene suggests the same ordening, fully in line with most theoretical investigations[13,32,33,36].

In the orthogonal conformation, C is the lowest excited state, in accordance with the calculations of Malrieu et al.[13]. The potential energy curve of this state has an energy barrier of 0.0164 au (= 10.3 kcal/mol) at θ = 40°. However, this barrier may be lowered or even disappear when the geometry of the molecule in this state is optimized. The energy barrier in Z_1 is 0.0066 au (= 4.1 kcal/mol) at θ = 40°. Again, the height of this barrier might be influenced by relaxing the geometry, but there are indications from both experimental[9] and theoretical[32,33] work that the planar geometry is a (local) minimum on this energy surface.

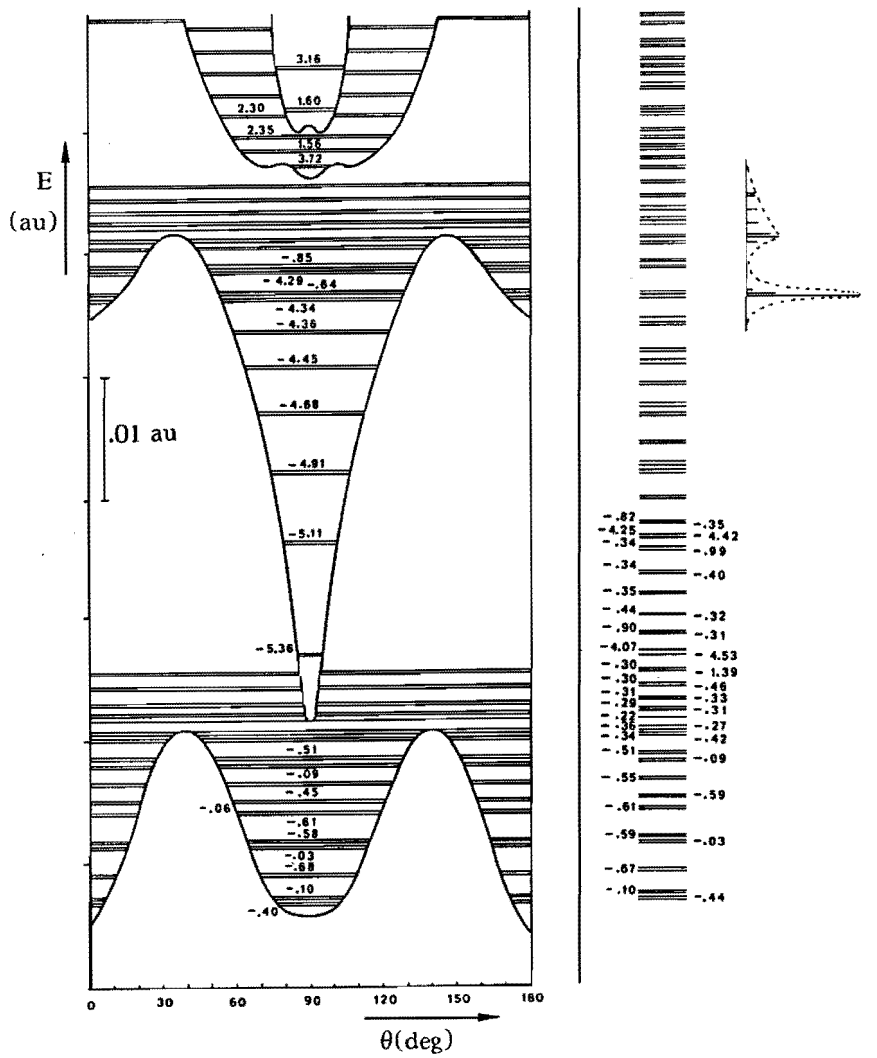

Figure 12. Potential energy curves, Born-Oppenheimer energy levels and dipole moments (in Debye) of the excited states of *trans*-hexatriene. Right: Energy levels and dipole moments after the nonadiabatic treatment, and the initially excited wavefunction($|\alpha_n|$, see eq. 12). The highest Born-Oppenheimer wavefunctions of each electronic state are not shown.

From the dipole moment curves (Figure 11b) it can be seen that $S_1(C)$ is predominantly covalent and $S_2(Z_1)$ almost exclusively ionic with a maximum of $\mu_{z,2}(90°)$ = -5.51 D. This value is larger than that of Z_1 in butadiene because of the larger asymmetry, which is also the reason that the energy splitting at θ = 90° between $Z_1(S_2)$ and $Z_2(S_3)$ has increased to 30 kcal/mol

(butadiene 21.6 kcal/mol). Z_2 is found to have an avoided crossing with a lower excited state which is obvious from the sharp peaks for the nonadiabatic coupling function $g_{34}(80°) = -g_{34}(100°) = 5.88$ au^{-1}, and the behaviour of the dipole moments of S_3 and S_4 in this region. However, the meaning of these high energy states is less important as they play a minor role in the *cis-trans* isomerization mechanism. They have merely been included to improve the calculation of the second derivative coupling functions $t_{KL}(\theta)$ of the lower states (see eq. 20).

In Figure 12 the results of the vibrational calculations with and without the nonadiabatic coupling are presented for the excited states of *trans*-hexatriene upon twisting. The vibrational levels of S_1 are no longer equidistant but show a pattern which is typical for a double well potential. The vibrational wavefunctions are located at either small or large twist angles as is obvious from the values of their dipole moments. As for the vibrational wavefunctions of $Z_1(S_2)$, there are always some vibrational levels of C close in energy, but these are rather ineffective in perturbing these functions. As an example, the dipole moment of the two lowest vibrational levels of Z_1 diminishes from -5.36 D to -4.53 D and -4.07 D due to the nonadiabatic coupling.

As a result of the energy barrier on the S_2 energy curve, some of the vibrational wavefunctions of the absorbing Z_1-state are located near $\theta = 0°$. In particular the Born-Oppenheimer wavefunction with quantumnumber i=16 has a very large overlap with the first vibrational level of the ground state: the calculated oscillatorstrength f_n for this vibrational level is 0.84, whereas the total oscillatorstrength f^{tot} for the $(\pi-\pi^*)$ transition is 0.92. The vibrational excitation is thus nearly completely localized in only one eigenfunction. In the extreme case where the initially excited wavefunction is made up of just one eigenfunction, the molecule would be in a stationary condition. As can be seen from Figure 13, this is almost the case for *trans*-hexatriene.

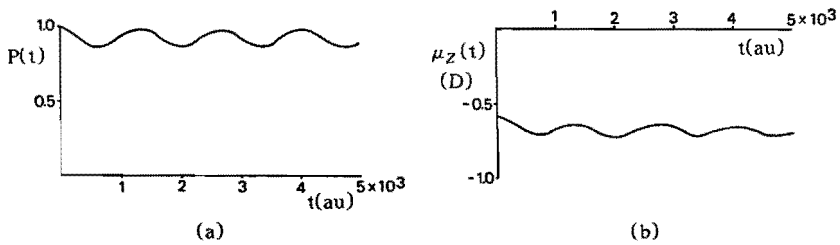

Figure 13. Radiationless decay P(t) (a) and dipole moment $\mu_z(t)$ (b) of *trans*-hexatriene.

The oscillations originate from a small contribution ($\alpha_n = 0.12$) of two higher vibrational levels to the initial wavefunction. The oscillating time (1400 au) can be directly derived from the energy difference between the main and minor absorptions (0.0046 au) as is indicated in the former section. The dipole moment oscillates with the same frequency. The average value of $\mu_z(t)$ is -0.65 D, almost identical with the dipole moment of the mainly excited vibrational wavefunction (-0.64 D).

Due to the absence of an avoided crossing between the $^1A_g^-$- and the $^1B_u^+$-state and the correspondingly small nonadiabatic coupling, the contribution of the hidden state to the total wavefunction is very small ($<5\times10^{-5}$). In contrast to butadiene, the hidden state in *trans*-hexatriene does not become rapidly populated. Evidently, the contribution of the electronic ground state is completely neglectable.

2.5 Discussion

Now the detailed results of the calculations for the *cis-trans* isomerization in ethylene, butadiene and *trans*-hexatriene have been presented, these three molecules will be compared to see how the shape and the ordening of the potential energy curves influence the dynamical behaviour. The time evolution was found to be directly related to the appearance of the initially excited wavefunction, so that this feature will be discussed first.

As indicated in 2.2, the prepared state is defined by the coefficients α_n, which are related to the oscillatorstrength of the vibrational levels via the transition dipole moments μ_{0n} (see 2.4.1). This means that the appearance of the initially excited wavefunction should be reflected in the shape of the UV absorption spectra of these molecules.

Ethylene is known to have an only partially resolved absorption spectrum whose most characteristic feature is a long torsional progression[37] as a result of the nonplanarity of the molecule in the $^1B_u^+$ excited state. Compared to octatetraene and the higher polyenes, butadiene and *trans*-hexatriene also show rather diffuse spectra from which it might be concluded that their equilibrium geometries are nonplanar as well[10]. On the other hand, the jet absorption spectra of butadiene, *trans*-hexatriene and octatetraene show basically the same primary vibrational progression resulting from the C=C stretch mode, thus indicating that all three molecules are planar in the $^1B_u^+$-state[9]. However, the vibrational bandwidths are markedly different: 1000 cm^{-1} for butadiene, 150 cm^{-1} for *trans*-hexatriene and 20 cm^{-1} for octatetraene. From the calculations presented here, a possible explanation raises from the shapes of the potential energy curves of the $^1B_u^+$ absorbing state in the 0° region. To demonstrate this, some of the relevant Born-Oppenheimer vibrational wavefunctions of this state are shown near the vertical absorption (Figure 14).

For ethylene, the energy curve of S_1 is monotonically decreasing from $\theta = 0°$ to $\theta = 90°$. Therefore, the vibrational wavefunctions near the vertical absorption are highly oscillatory and the overlap between these functions and the first vibrational wavefunction of the ground state is thus small. As a result, the initially excited wavefunction is diffuse (Figure 2) and consequently the UV absorption band broad. For butadiene, the energy curve is nearly flat between $\theta = 0°$ and $\theta = 30°$ causing the vibrational wavefunctions to be more located near $\theta = 0°$ and thus to have a larger overlap with $|\psi_{0,1}>$. This fact, together with

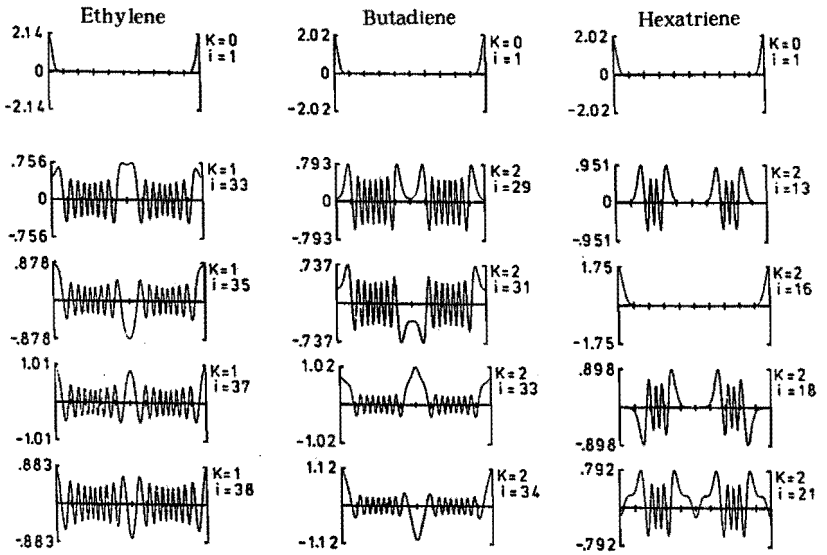

Figure 14. The lowest Born-Oppenheimer vibrational wavefunction of the ground state $|\psi_{0,1}>$ and some Born-Oppenheimer vibrational wavefunctions of the $1^1B_u^+$-state near the vertical absorption.

the larger moment of inertia for the rotation of a double bond in butadiene, causes a narrowing of the absorption band (Figure 8). From the calculated energies E_n and oscillatorstrengths f_n an approximated bandwidth of 700 cm^{-1} is obtained. In the case of *trans*-hexatriene, the planar conformation appears to be a real (local) minimum. Consequently, there is one vibrational wavefunction which has a very large overlap with $|\psi_{0,1}>$. This would lead to an almost fully resolved absorption band, though experimentally a bandwidth of 150 cm^{-1} is measured. As mentioned before, the height of the potential energy barrier may be diminished upon relaxing the excited state geometry of *trans*-hexatriene leading inevitably to a broadening of the absorption band. An additional explanation would be the twist around the central double bond in *trans*-hexatriene. A calculation of the energy barrier for this rotation yields a value of 0.0030 au (= 1.9 kcal/mol) thus also inducing a broadening of the absorption band.

In summary, it is found that the increasing bandwidth upon decreasing chain length of the polyenes may be directly explained from the increasing tendency of these molecules to be nonplanar in the $^1B_u^+$ excited state. In reverse, these bandwidths form an indication of the reliability of the calculated potential energy curves.

Concluding that the initially excited wavefunction is reliable, there is good reason to believe that, at least during the first rotation, the radiationless decay is well described. For ethylene, many eigenfunctions with a relatively large energy difference are excited, leading to an exponential decay and a rotation time of 3100 au (0.075 psec). For butadiene the number of excited eigenfunctions and their mutual spacing is smaller, resulting in a slower rotation (8100

au $\approx$ 0.2 psec). At the end of this series *trans*-hexatriene is found, which excited wavefunction is nearly stationary.

It is obvious that the dynamical behaviour is predestined by the shape of the potential energy curve which is consistent with common chemical intuition. For butadiene the moment of inertia for the twist is larger and the molecule rotates slower. The slope of the potential energy curve for ethylene is largest and this molecules thus rotates fastest. For *trans*-hexatriene the energy barrier is so large that the molecule does not rotate unless it is thermally activated.

It was also seen how for butadiene the hidden state becomes rapidly populated (within 0.05 psec), which is an important observation because this state is supposed to play a characteristic role in the *cis-trans* isomerization dynamics. An example of this is found in the recent work of Becker and Freedman on the photoisomerization of the Shiff bases of retinal[38] (see also chapter 3). They explained the variation in quantumyields as a function of protonation-state and solvent polarity in terms of the changing contributions of the $^1A_g^-$ and $^1B_u^+$ states. The fact that the hidden state may play such a role is a direct result of the avoided crossing and the consequently strong nonadiabatic coupling with the absorbing excited state upon twisting the double bond.

An additional point of interest concerns the extent to which the sudden polarization is affected by the nonadiabatic coupling. In the case of ethylene, the energy difference between the two electronic states with opposite dipole moments (Z_1 and Z_2) is relatively small. Besides, they show an avoided crossing and thus a large nonadiabatic coupling. As a result, only the lowest vibrational wavefunctions of Z_1 maintain their negative dipole moment after the nonadiabatic mixing. For butadiene the asymmetry is larger and, therefore, the dipole moments of Z_1 and Z_2 are larger. Moreover, their mutual coupling is small and consequently there are more vibrational eigenfunctions with large negative dipole moments. This trend goes on for *trans*-hexatriene, but here a complication raises from the fact that the hidden state now lies below Z_1. However, the nonadiabatic coupling with this state is small and the dipole moments of the vibrational wavefunctions of Z_1 remain almost unaffected.

However, the final wavefunction does not constitute of these low vibrational states but is fully defined by the characteristics of the initially excited eigenfunctions. Therefore, no substantial polarization will be found within the present model. In the absence of the nonadiabatic perturbation ethylene did show some polarization because the wavefunction was purely Z_1. Upon including the coupling the contribution of Z_2 is found to increase as the molecule reaches the 90° region and the dipole moments cancel. A similar behaviour is found for butadiene, whereas *trans*-hexatriene does not show any polarization because this molecule never reaches the orthogonal conformation.

From this, it might be concluded that the sudden polarization does not take place upon inclusion of the nonadiabatic coupling. In fact, this is an intrinsic characteristic of the present model. Without any further perturbation, the system will remain in the initially excited eigenfunctions and exhibit their features. The same arguments hold for the contribution $P_0(t)$ of the electronic ground state. The small values obtained for ethylene ($<2\times10^{-4}$) and butadiene ($<5\times10^{-7}$) imply that the molecule will oscillate back and forth several

times on the potential energy surface and cannot predict a product distribution between *cis* and *trans* isomers other than 1:1[7]. On the other hand, these small values of $P_0(t)$ are a requisite for the occurence of other photochemical reactions from these twisted minima on the excited state potential energy surface[39] (see chapters 4 and 5).

A more realistic model to describe the sudden polarization would include a perturbation by which the extra energy available for the torsional motion can be dissipated so that the molecule will follow the potential energy curve and in this way reaches the lower vibrational levels. Such a semi-empirical approach based on classical trajectory calculations has been used to account for the rapid *cis-trans* isomerization in rhodopsin[40]. A straightforward extension of the present model would include a second (nonreactive) vibrational mode, to which the torsional energy can be (temporarily) partitioned. This second vibrational mode should be electronically coupled to the first and have a frequency of the same size of order. Future work will be aimed at finding such vibrations and extending the present model to more dimensions.

In this chapter a first attempt was made at studying in an elementary way the details of photochemical *cis-trans* isomerization. Although an extension of the one-dimensional model is certainly needed to obtain a more realistic picture of the sudden polarization and radiationless transition to the ground state, the present approach yields important insights into the spectroscopics and photodynamics of small alkenes.

2.6 References

1 B.S. Hudson, B.E. Kohler, K. Schulten in "Excited States", Volume 6, E.C. Lim, Ed., Academic, New York (1982)

2 See e.g.: R.S.H. Liu, A.E. Asato, Proc. Natl. Acad. Sci. USA, **82**, 259 (1985)

3 V. Bonačić-Koutecký, P. Bruckmann, P. Hiberty, J. Koutecký, C. Leforestier, L. Salem, Angew. Chem., Int. Ed. Engl., **14**, 575 (1975)

L. Salem, Acc. Chem. Res., **12**, 87 (1979)

4 See e.g.:

P. Bruckmann, L. Salem, J. Am. Chem. Soc., **98**, 5037 (1976)

I. Baraldi, M.C. Bruni, F. Momicchioli, G. Ponterini, Chem. Phys., **52**, 415 (1980)

G.J.M. Dormans, H.R. Fransen, H.M. Buck, J. Am. Chem. Soc., **106**, 1213 (1984)

L. Pogliani, N. Niccolai, C. Rossi, Chem. Phys. Lett., **108**, 597 (1984)

O. Kikuchi, H. Yoshida, Bull. Chem. Soc. Jpn., **58**, 131 (1985)

B.R. Brooks, H.F. Schaefer III, J. Am. Chem. Soc., **101**, 307 (1979)

I. Nebot-Gil, J.-P. Malrieu, J. Am. Chem. Soc., **104**, 3320 (1982)

P. Karafiloglou, P.C. Hiberty, Chem. Phys. Lett., **70**, 180 (1980)

I.D. Petsalakis, G. Theodorakopoulos, C.A. Nicolaides, R.J. Buenker, S.D. Peyerimhoff, J. Chem. Phys., **81**, 3161 (1984)

5 G. Orlandi, P. Palmieri, G. Poggi, Chem. Phys. Lett., **68**, 251 (1979)

6 M. Persico, J. Am. Chem Soc., **102**, 7839 (1980)

7 R.M. Weiss, A. Warshel, J. Am. Chem. Soc., **101**, 6131 (1979)

8a M. Persico, V. Bonačić-Koutecký, J. Chem. Phys., **76**, 6018 (1982)

8b K. Morihashi, O. Kikuchi, Theor. Chim. Acta, **67**, 293 (1985)

9 D.G. Leopold, R.D. Pendley, J.L. Roebber, R.J. Hemley, V. Vaida, J. Chem. Phys., **81**, 4218 (1984)

10 M.F. Granville, B.E. Kohler, J.B. Snow, J. Chem. Phys., **75**, 3765 (1981)

11 U. Dinur, R.J. Hemley, M. Karplus, J. Phys. Chem., **87**, 924 (1983)

12 U. Dinur, B. Honig, J. Am. Chem. Soc., **101**, 4453 (1979)

13 M. Said, D. Maynau, J.-P. Malrieu, J. Am. Chem. Soc., **106**, 580 (1984)

J.-P. Malrieu, I. Nebot-Gil, J. Sánchez-Marín, Pure & Appl. Chem., **56**, 1241 (1984)

14 V. Bonačić-Koutecký, M. Persico, D. Döhnert, A. Sevin, J. Am. Chem. Soc., **104**, 6900 (1982)

15 R. J. Buenker, V. Bonačić-Koutecký, L. Pogliani, J. Chem. Phys., **73**, 1836 (1980)

16 I. Ohmine, J. Chem. Phys., **83**, 2348 (1985)

17 J.C. Tully in "Dynamics of Molecular Collisions", Part B, W.H. Miller, Ed., Plenum Press, New York (1976)

18 R. Cimiraglia, M. Persico, J. Tomasi, Chem. Phys., **34**, 103 (1978)

19 J.M.F. van Dijk, M.J.H. Kemper, J.H.M. Kerp, H.M. Buck, J. Chem. Phys., **69**, 2462 (1978)

20 J.S. Binkley, R.A. Whiteside, R. Krishnan, R. Seeger, D.J. DeFrees, H.B. Schlegel, S. Topiol, L.R. Kahn, J.A. Pople, GAUSSIAN 80, Department of Chemistry, Carnegie-Mellon University, Pittsburgh, PA (1980)

21 E.M. Evleth, A. Sevin, J. Am. Chem. Soc., **103**, 7414 (1981)

22 C. Petrongolo, R.J. Buenker, S.D. Peyerimhoff, J. Chem. Phys., **76**, 3655 (1982)

23 R.J. Buenker, S. Shih, S.D. Peyerimhoff, Chem. Phys. Lett., **44**, 385 (1976)

24 M.J.H. Kemper, L.Lemmens, H.M. Buck, Chem. Phys., **57**, 245 (1981)

25 V. Bonačić-Koutecký, L. Pogliani, M. Persico, J. Koutecký, Tetrahedron, **38**, 741 (1982)

26 B. Huron, J.-P. Malrieu, P. Rancurel, J. Chem. Phys., **58**, 5745 (1973)

See also chapter 1.

27 C. Galloy, J.C. Lorquet, J. Chem. Phys., **67**, 4672 (1977)

G. Hirsh, P.J. Bruna, R.J. Buenker, S.D. Peyerimhoff, Chem. Phys., **45**, 335 (1980)

R. Cimiraglia, M. Persico, J. Tomasi, Chem. Phys., **53**, 357 (1980)

See also the appendix

28 A.J. Merer, R.S. Mulliken, Chem. Rev., **69**, 639 (1969)

29 P.G. Wilkinson, R.S. Mulliken, J. Chem. Phys., **23**, 1895 (1955)

30 T. Shimanouchi, "Tables of Molecular Vibrational Frequencies", Consolidated Volume, National Bureau of Standards, Washington, D.C., p. 74 (1972), NSRDS-NBS 39.

31 V. Bonačić-Koutecký, Pure & Appl. Chem., **55**, 213 (1983)

32 A.C. Lasaga, R.J. Aerni, M. Karplus, J. Chem. Phys., **73**, 5230 (1980)

33 M. Aoyagi, Y. Osamura, S. Iwata, J. Chem. Phys., **83**, 1140 (1985)

34 W.Th.A.M. van der Lugt, L.J. Oosterhoff, J. Am. Chem. Soc., **91**, 6042 (1969)

35 J.R. Andrews, B.S. Hudson, Chem. Phys. Lett., **57**, 600 (1978)
R.M. Gavin Jr., C. Weisman, J.K. McVey, S.A. Rice, J. Chem. Phys., **68**, 522 (1978)

36 M.A.C. Nascimento, W.A. Goddard III, Chem. Phys., **53**, 265 (1980)

37 P.D. Foo, K.K. Innes, J. Chem. Phys., **60**, 4582 (1974)

38 R.S. Becker, K.A. Freedman, J. Am. Chem. Soc., **107**, 1477 (1985)
K.A. Freedman, R.S. Becker, J. Am. Chem. Soc., **108**, 1245 (1986)

39 G.J.M. Dormans, H.M. Buck, J. Mol. Struct. (Theochem), **136**, 121 (1986)

40 A. Warshel, Nature, **260**, 679 (1976)
A. Warshel, N. Barboy, J. Am. Chem. Soc., **104**, 1469 (1982)
R.R. Birge, L.M. Hubbard, Biophys. J., **34**, 517 (1981)

CHAPTER 3

A Quantumchemical Study on the Mechanism of *cis-trans* Isomerization in Retinal-like Protonated Schiff Bases

3.1 Introduction

The first step of the vision process involves the absorption of light by rhodopsin which transduces the light information into a nerve signal[1]. Bacteriorhodopsin acts as a light-driven proton pump in the purple membrane of the halophilic microorganism *Halobacterium Halobium*. It converts the light energy into an electrochemical gradient across the cell membrane[1].

Whereas the function and the conformation of rhodopsin and bacteriorhodopsin are different, they have in common that they are constructed from a covalent linkage between a protonated Schiff base of retinal and the ϵ-amino group of a lysine residue of the apoprotein opsin. In both systems, the primary step after light absorption involves a photochemical *cis−trans* isomerization of the retinylidene chromophore[1]. This process is known to proceed on a (sub)picosecond time scale with a high quantumyield for *cis−trans* isomerization (e.g. $\Phi = 0.7$ for rhodopsin[2]).

In rhodopsin, the conformation of the retinylidene chromophore is 11-*cis* and upon light absorption it is isomerized to the all-*trans* form (bathorhodopsin). This conversion is characterized by a red shift of the UV absorption maximum from 498 nm to 548 nm. Bathorhodopsin is stable below -140 °C and its ground state energy is 35 kcal/mol higher than that of rhodopsin[3] so that ca. 60% of the light energy is stored in this way.

Whereas it is well established that the conformation of the light adapted form of bacteriorhodopsin (BR_{568}) is all-*trans*, the exact conformation of the primary photoproduct[4] K_{610} is still a matter of dispute[5]. Anyway, the conversion from BR_{568} to K_{610} involves the photoisomerization of the $C_{13}-C_{14}$ double bond from all-*trans* to 13-*cis*[6]. K_{610} is stable below -120 °C and its ground state energy is 16 kcal/mol higher than that of BR_{568}[7].

Some questions that rise are how opsin directs the regioselectivity of the *cis−trans* isomerization and which conditions are necessary to account for the unusually rapid and efficient reaction. This is especially intruiging when it is born in mind that the retynilidene chromophore only has a very limited space within the pocket of the surrounding protein. A thorough understanding of these features asks for a detailed knowledge of the intrinsic characteristics of

the retinylidene chromophore. Once these are known, it may be deduced how the protein can direct the regioselectivity and increase the efficiency of the photoisomerization.

Freedman and Becker[8] studied the photoisomerization of various isomers of the n-butylamine Schiff base of retinal in detail. They found that the quantumyields for the 9-*cis*, 11-*cis*, 13-*cis* and all-*trans* isomers are less than 0.01 in hexane. Going from the nonpolar solvent hexane to the polar solvent methanol, the quantumyields drastically increase with a maximum of 0.24 for the 11-*cis* isomer. Whereas the photoproducts of the *cis* isomers are always the all-*trans* isomer, irradiation of the all-*trans* isomer gave a mixture of the *cis* isomers ($\Phi_{t \rightarrow c} = 0.12$) of which the 11-*cis* is predominantly formed. Upon protonating the Schiff base, only the 11-*cis* isomer shows an efficient isomerization to the all-*trans* isomer ($\Phi_{c \rightarrow t} = 0.24$, independent of solvent polarity[9]). The quantumyield for isomerization of the protonated all-*trans* isomer was 0.14 in all solvents, being only slightly higher than the quantumyield for the unprotonated species in a polar solvent. Again, the 11-*cis* isomer was predominantly formed.

Freedman and Becker explained these differences from the characteristics of the two lowest excited singlet states of the retynilidene Schiff base. These excited states are related to the two lowest singlet states of the set of *trans* linear polyenes which have C_{2h}-symmetry. One excited state is constructed from the promotion of an electron from the highest occupied π-MO to the lowest unoccupied π^*-MO. The symmetry of this singlet ($\pi-\pi^*$) excited state is $^1B_u^+$ (the + sign refers to the symmetry of the configurations in the CI expansion of a PPP wavefunction[10]). The transition to this state is symmetry allowed and is responsible for the strong absorptionband in the UV-spectra of these polyenes. Additionally, there is an excited state with the same symmetry as the ground state ($^1A_g^-$) to which a single photon transition is symmetry forbidden in C_{2h}-symmetry so that it is not observed in the UV-spectrum. Its presence was first indicated by quantumchemical calculations[11]. In a CI expansion, this state is described by the doubly excited $(\pi-\pi^*)^2$ configuration and two singly excited configurations ($\pi_{-1}-\pi^*$) and ($\pi-\pi^*_{+1}$) (π_{-1} and π^*_{+1} refer to the π-MOs just below the HOMO and just above the LUMO, respectively).

With the advent of two-photon spectroscopy the location of this $^1A_g^-$-state became possible and it has been shown to be the lowest excited singlet state in long chain linear polyenes. The same level ordening is found for the retynilidene Schiff bases[12]. In the valence bond formalism, the wavefunction of the $^1B_u^+$-state is dominated by ionic configurations whereas the $^1A_g^-$-state is mainly built up from covalent configurations[13]. This indicates that the polarity of the solvent and the protonation-state of the Schiff base may have a different impact on these two states. This prompted Freedman and Becker[8,9] to explain the observed photochemistry of the isomers of the n-butylamine Schiff base of retinal as a function of solvent polarity and protonation-state in terms of the mixing of the $^1B_u^+$ and $^1A_g^-$ states.

By means of INDO-CISD (configuration interaction with single and double excitations) calculations, Birge and Hubbard[14] indicated that particularly the $^1A_g^-$-state is photochemically labile for *cis*–*trans* isomerization and that its

interaction with the $^1B_u^+$-state might be responsible for the formation of a barrierless potential energy surface for *cis−trans* isomerization in this latter state. However, only this interaction cannot account for the fact that the photoisomerization of the isomers of the (protonated) Schiff bases is confined to one particular double bond.

Therefore, in this chapter MNDO/CI calculations are presented for the model compound protonated 1-imino-2,4-pentadiene (pentanimine-H^+) which has all relevant elements necessary to demonstrate the most important features that govern the *cis−trans* isomerization in protonated Schiff bases.

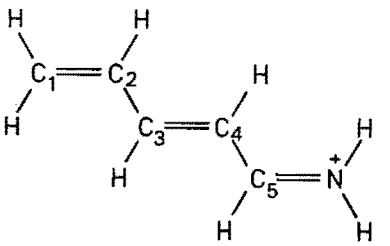

Pentanimine-H^+

Scheme 1

Potential energy curves of the ground and lower singlet excited states were calculated for the isomerization of the various double bonds in this molecule. The qualitative shape of these curves can be explained from the stability of the resonance structures which describe the ground and lowest excited state for the 90° twisted conformations. It is shown that the relative stability of these resonance structures may explain the rate (barrierless potential energy curve) and the quantumyield for isomerization (energy gap and nonadiabatic coupling between the ground and excited state in the 90° twisted region). The nonadiabatic interactions between the various singlet states were calculated explicitely from the multiconfigurational wavefunctions, which enables the evaluation of the probability for a radiationless transition to the ground state by means of semi-classical trajectory calculations. Finally, some preliminary results are presented which show how the protein can direct the photoisomerization process by supplying external point-charges in the neighbourhood of the retinylidene chromophore.

3.2 Quantumchemical Method

The semi-empirical MNDO method[15] was used to perform the SCF calculations. Subsequent configuration interaction calculations were performed with

the CIPSI algorithm[16]. Starting from a zeroth order wavefunction including 6 leading configurations (see Scheme 2) for the three lowest singlet states, the most important configurations were selected from a second order perturbation after generating all possible configurations single or double excited with respect to the reference space.

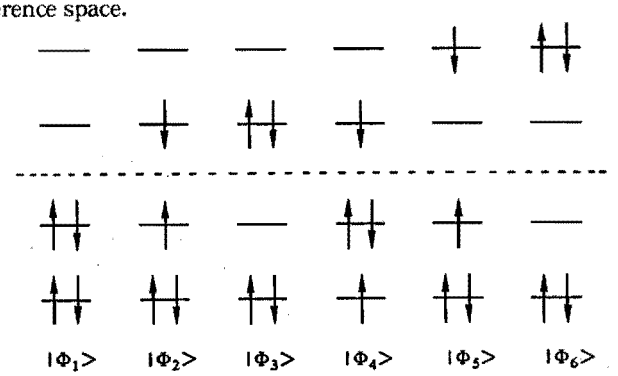

Scheme 2

The final CI space was constructed from a collection of the selected configurations at various nuclear conformations. No essential changes (level ordening of states, shapes of the potential energy curves etc.) were found upon increasing the active MO space from 6 MOs (selection treshold[16] $\eta = 0.0$; 170 configurations) to 20 MOs ($\eta = 0.02$; 450 configurations). A program was written to calculate natural orbitals, charge- and bond-densities, transition dipole moments, oscillatorstrenghts and nonadiabatic couplings from multiconfigurational wavefunctions. The nonadiabatic couplings were evaluated via a two-point numerical procedure[17] with a stepsize of $\Delta\theta = 0.02°$. The MNDO results were compared[18] with ab initio calculations[19] for the *cis–trans* isomerization of small polyenes. Both methods are found to compare qualitatively well, the main difference being that ab initio calculations tend to overestimate transition energies (especially for the $(\pi-\pi^*)$ excited state) whereas the MNDO calculations underestimate excitation energies.

3.3 Electronic Calculations

3.3.1 Double Bond Rotations in Pentanimine-H^+

The aim of this work is to demonstrate some essential characteristics of the *cis–trans* isomerization in protonated Schiff bases. Special attention has been drawn to the possibility of simultaneous double bond rotations for which

two-dimensional potential energy surfaces of the lowest singlet states and nonadiabatic couplings among them had to be calculated. Considering the large amount of calculations, pentanimine-H^+ was chosen as the smallest molecule which incorporates all essential elements of a protonated Schiff base.

The relatively small dimensions of this molecule made it possible to optimize all geometrical parameters for each electronic state individually with a reasonably large multiconfigurational wavefunction. It is known that especially the bond lengths of the carbon-carbon bonds may change drastically upon twisting such bond[20]. This is demonstrated in Figure 1 for the twist around the C_1-C_2 bond of pentanimine-H^+.

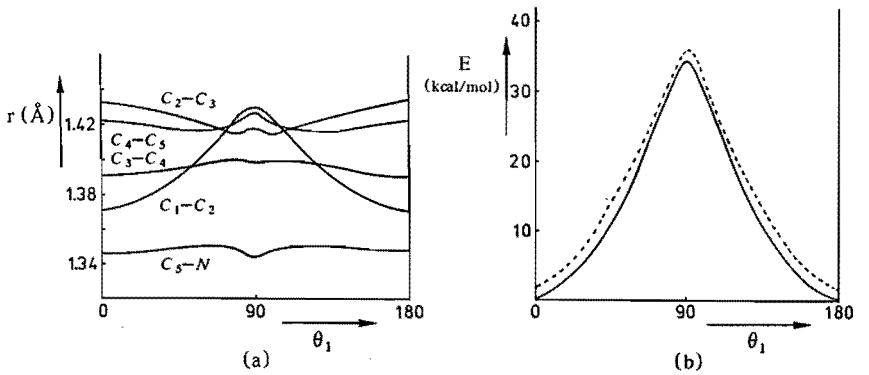

Figure 1. Optimal bond lengths (a) for a rotation around the C_1-C_2 bond in pentanimine-H^+ (optimized in S_0). Energy curve (b) of the ground state for a rotation around the C_1-C_2 bond when optimized in S_0 (solid line) or S_1 (broken line).

Due to the electron withdrawing capacity of the protonated nitrogen atom, already in the planar conformation the picture of alternating single and double bonds has almost vanished. The former double bonds are elongated whereas the single bonds have become shorter. This effect is more accentuated near the nitrogen atom. When the C_1-C_2 bond is twisted, the conjugation of this bond is broken and, consequently, the optimal bond length increases. The effect of this twist on the optimal bond lengths of the other bonds is much smaller.

In the same figure, the effect of a separate optimization in the ground and first excited state on the energy of the ground state is shown. Despite the fact that the geometrical parameters are markedly different in both states, the effect on the energy of the ground state is minimal. The energy barrier for a rotation around the C_1-C_2 bond is 34.5 kcal/mol when optimized in S_0 and 34.1 kcal/mol when optimized in S_1.

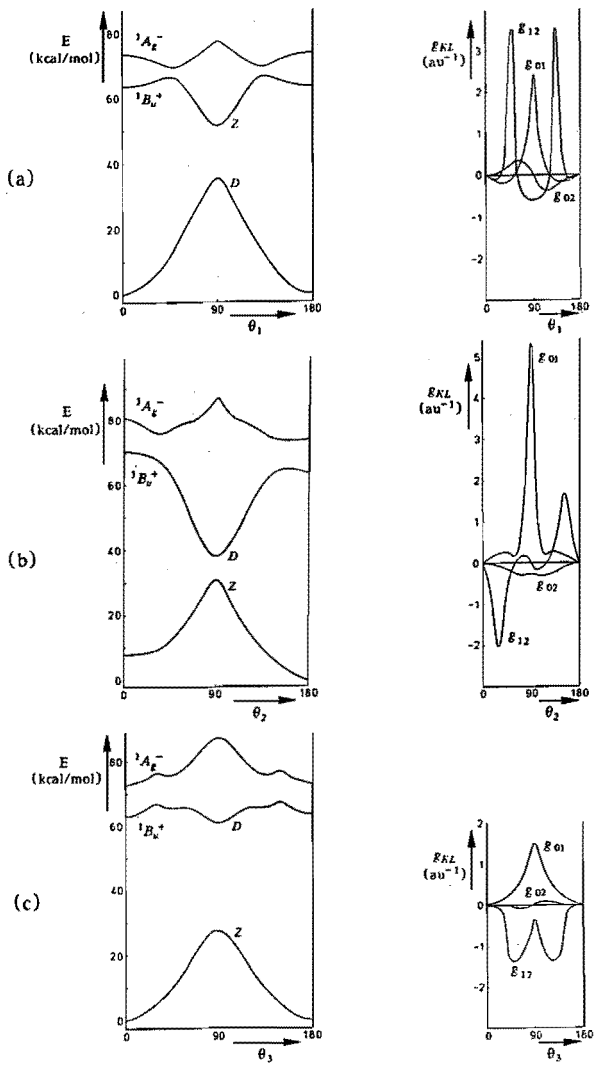

Figure 2. Energy curves and nonadiabatic couplings for a rotation around the C_1—C_2 (a), the C_3—C_4 (b) and the C_5—N (c) bonds in pentanimine-H^+.

The same effect is found for the excited states and for rotations around other bonds. It is obvious that the influence of geometry optimization on the general appearance of the potential energy curves is minimal. Therefore, one idealised geometry was chosen for all calculations ($r_{C_1-C_2}=r_{C_3-C_4}=$ 1.40 Å, $r_{C_2-C_3}=r_{C_4-C_5}=$ 1.42 Å, $r_{C_5-N}=$ 1.35 Å, $r_{C-H}=$ 1.10 Å, $r_{N-H}=$ 1.00 Å, all bond angles 120°).

The potential energy curves and nonadiabatic couplings for the rotations around the C_1-C_2, C_3-C_4 and C_5-N bonds are shown in Figure 2. For the C_1-C_2 and C_5-N bonds, the curves are symmetric (or antisymmetric for certain couplings) with respect to $\theta = 90°$. The rotation around the central C_3-C_4 bond represents an isomerization from the *cis* isomer ($\theta_2 = 0°$) to the *trans* isomer ($\theta_2 = 180°$). The ground state energy of the *cis* isomer is 7.3 kcal/mol higher than that of the *trans* isomer. This difference is obviously too high because the steric repulsion is overestimated for the idealised geometry (with all bond angles 120°).

The isomerization rate is determined by the moment of inertia associated with the rotation and, more important, the slope of the potential energy curve of the excited state near the vertical absorption maximum[19] ($\theta = 0°$ or $\theta = 180°$). This slope is markedly different for the three rotations considered, already indicating that there is a large difference to be expected for the dynamics of photochemical *cis*–*trans* isomerization around these bonds.

The quantumyield for *cis*–*trans* isomerization is related to the nonadiabatic coupling in the region where the potential energy curves of the ground and excited states come close. The extent of the nonadiabatic coupling determines the probability for a radiationless transition (see next section) and in its turn, this probability determines the quantumyield[21]. Qualitatively, it can be said that the probability increases when the energy gap between two potential energy curves decreases.

So there are two important features which are necessary to account for a rapid and efficient *cis*–*trans* isomerization: a barrierless potential energy curve of the excited state and a minimal energy gap with the ground state for the twisted geometry. These two conditions are best fulfilled for the rotation around the central C_3-C_4 bond.

Both the shape of the excited state potential energy curve and the energy gap with the ground state can be explained from the bond-densities of the planar geometry and resonance structures of the twisted geometries.

In Figure 3, the charge- and bond-densities of the carbon skeleton of pentanimine-H^+ are shown as calculated from the natural orbitals for each individual electronic state[22]. As indicated in the introduction, the lowest excited states of (protonated) Schiff bases are related to the low lying $^1B_u^+$- and $^1A_g^-$-states of *trans* linear polyenes. For these molecules in C_{2h}-symmetry the dipole transition to the former state is strongly allowed whereas the dipole transition to the latter state is forbidden. Though these symmetry restrictions do not strictly hold for pentanimine-H^+, the $^1B_u^+$-state has a large (0.61) and the $^1A_g^-$-state a relatively small (0.11) oscillatorstrength.

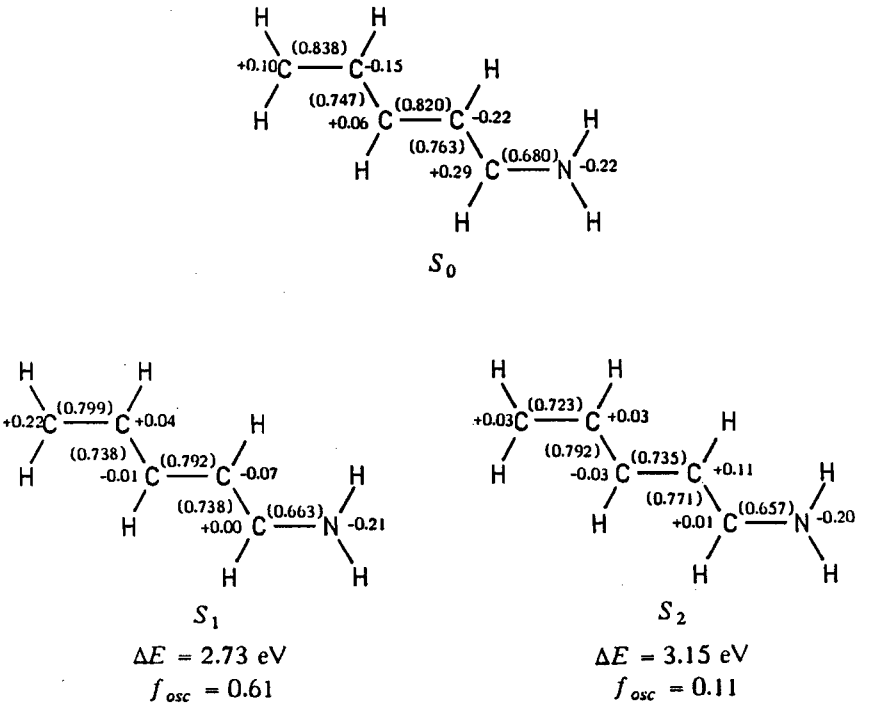

Figure 3. Calculated charge- and bond-densities (in brackets) of the three lowest singlet states of planar pentanimine-H^+.

The lowest excited state is found to be the $^1B_u^+$-state, in agreement with other calculations[14,23], and experimental data[24] for protonated Schiff bases. The energy splitting between the two states is calculated to be 0.42 eV (9.7 kcal/mol) and their wavefunctions are slightly mixed:

$|\Psi_{^1B_u^+}\rangle = 0.89\ |\Phi_2\rangle + 0.19\ |\Phi_3\rangle + 0.12\ |\Phi_4\rangle$; $|\Psi_{^1A_g^-}\rangle = 0.16\ |\Phi_1\rangle - 0.20\ |\Phi_2\rangle + 0.55\ |\Phi_3\rangle + 0.41\ |\Phi_4\rangle + 0.39\ |\Phi_5\rangle + 0.18\ |\Phi_6\rangle$

(the configurations in these CI expansions are those of Scheme 2). This mixing explains the relatively large oscillatorstrength of the $^1A_g^-$-state. The $^1A_g^-$-state has important contributions from the doubly excited configurations $|\Phi_3\rangle$ and $|\Phi_6\rangle$ and, therefore, has a more antibonding character than the $^1B_u^+$-state. This is reflected in the larger decrease in bond-densities of the double bonds going from the ground state to the $^1A_g^-$-state compared to the $^1B_u^+$-state (Figure 3). This effect is more accentuated for the C_1–C_2 and C_3–C_4 bonds than for the C_5–N bond, which implicates that a rotation around the former two bonds is energetically favoured in the $^1A_g^-$-state. As the $^1A_g^-$-state is located above the $^1B_u^+$-state for the planar geometry, the energy difference between the two states will decrease upon twisting. Because there is no symmetry in the molecule, the potential energy curves will exhibit an avoided crossing. This is indeed the case as can be seen from the peaks in the g_{12} coupling functions of Figure 2.

The effect of this avoided crossing is that the slope of the potential energy curve of the absorbing state ($^1B_u^+$) is bent downwards. Though the $^1A_g^-$-state is not directly involved in the absorption of protonated Schiff bases, it plays an important role in lowering (or even removing) the energy barrier in the $^1B_u^+$-state.

The description of the electronic structures of the 90° twisted molecule is intimately related to the description of twisted alkenes. For symmetric alkenes, the HOMO and LUMO become degenerate for $\theta = 90°$. Three singlet configurations can be generated from a distribution of the frontier two π-electrons over the two centra on each side of the twisted bond.

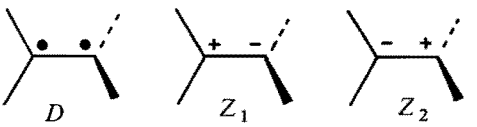

Scheme 3

In the first configuration, one electron is located on each side. Therefore, this configuration is a diradical (D) and has no net dipole moment. In the latter two configurations, the two electrons are located on one side of the twisted bond. These configurations are zwitterionic (Z) and have a strong dipole moment. The first time this polarization of charge upon twisting an excited double bond was theoretically described[25], it was found to occur in a small region around $\theta = 90°$. Therefore, this effect was called "sudden polarization". Many calculations[19,26] at various levels of theory have confirmed this effect, but showed that the polarization already develops in an earlier stage so that the term "sudden" is somewhat confusing.

In the limiting case of a twisted symmetric alkene (like ethylene or *trans*-hexatriene twisted around the central double bond), there is no difference between Z_1 and Z_2 and the electronic wavefunctions of S_1 and S_2 are essentially linear combinations of these two resonance structures. Therefore, the excited states of these symmetric molecules do not have a dipole moment. When this symmetry is broken by introducing a substituent on one side of the twisted bond, the former degeneracy is lifted and one of the resonance structures is energetically stabilized whereas the other is destabilized. As a result, the energy gap between S_1 and S_2 increases and their wavefunctions now resemble Z_1 and Z_2.

Such a situation is fulfilled for (protonated) Schiff bases. The resonance structure with the two electrons at the side of the electron deficient nitrogen atom (the N-end) is strongly stabilized. This stabilization may even become so large that the Z-state drops below the D-state so that the ground state now has the characteristics of the zwitterionic configuration[27].

For pentanimine-H^+ 90° twisted around the $C_1{-}C_2$, $C_3{-}C_4$ and $C_5{-}N$ bonds, the resonance structures are given in Figure 4. The relative energy sequence of the D- and Z-states can be derived from the stability of the two fragments on each side of the twisted bond:

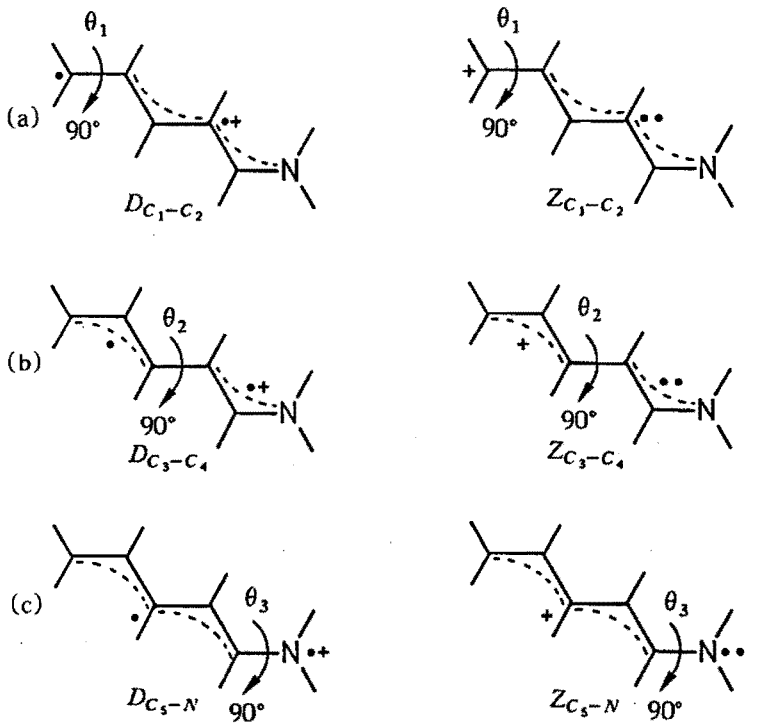

Figure 4. Resonance structures for pentanimine-H^+ 90° twisted around the C_1-C_2 (a), the C_3-C_4 (b) and the C_5-N (c) bonds. Because of the positive charge of the molecule, it is difficult to identify a particular resonance structure as a diradical or a zwitterion. For convenience, they are identified as D or Z merely indicating that the two former π-electrons are located at different sides or at the same side of the twisted bond, respectively. The subscripts indicate the bond which is 90° twisted.

$$D_{C_1-C_2} > D_{C_3-C_4} > D_{C_5-N}$$
$$Z_{C_1-C_2} < Z_{C_3-C_4} < Z_{C_5-N}$$

The fact that the direction of these energy sequences is opposite for the D- and Z-states indicates that there might be a bond for which the D- and Z-states come close in energy. For this bond, the energy gap between S_0 and S_1 is minimal. Twisting a bond which is closer to the N-end of the molecule increases this energy gap because Z is too strongly stabilized. Twisting a bond which is closer to the C-end of the molecule increases the energy gap because Z is not stabilized enough.

The present calculations show that the optimal condition for stabilization and destablization occurs for the twist (θ_2) around the central C_3-C_4 bond. Figure

5 gives the charge-densities on each side of this twisted bond for S_0 and S_1 as a function of the twist angle (θ_2). It clearly shows the polarization of charge and it follows that at $\theta_2 = 90°$ the ground state ("Z") bears the positive charge at the C-end of the molecule. From the situation for twisting in ethylene, it is known that Z correlates with the doubly excited configuration $|\Phi_3>$ of the planar molecule. Because the $^1A_g^-$-state has a large contribution from this configuration, it is obvious that the Z-structure at $\theta = 90°$ correlates diabatically with the $^1A_g^-$-state at $\theta = 0°$. Therefore, the energy curve of the $^1A_g^-$-state shows a negative slope for a twist around a double bond for which the Z-structure is strongly stabilized. The size of the slope depends on the extent of this stabilization.

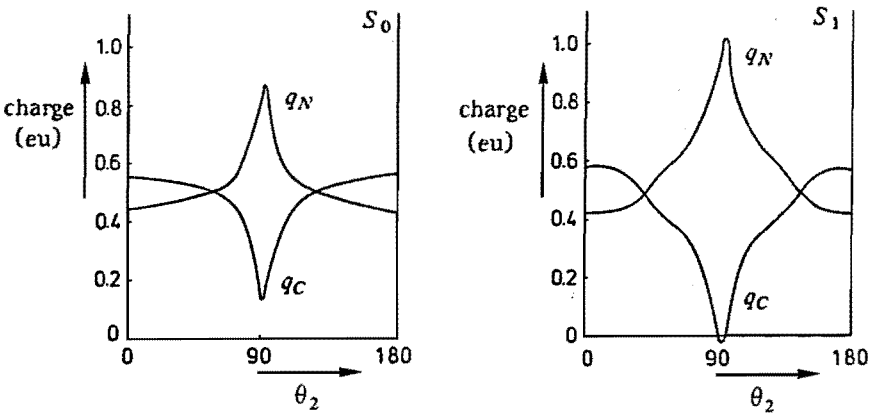

Figure 5. Calculated charge-densities of the ground state (S_0) and first excited state (S_1) for a rotation around the C_3–C_4 bond (θ_2) in pentanimine-H^+. The charge-densities are summed for all atoms at the C-end (q_C) and the N-end (q_N) of the molecule.

It follows from these considerations that there is a relation between the distance from the twisted bond to the N-end of the protonated Schiff base, the energy gap between S_0 and S_1 and the slope of the diabatic energy curve of the $^1A_g^-$-state. In its turn, the shape of this curve determines the shape of the energy curve of the absorbing $^1B_u^+$-state (*vide supra*) so that there is a direct relation between the distance from the twisted bond to the N-end and the rate and efficiency for *cis–trans* isomerization. In this way, the protonated Schiff base has introduced an intrinsic property which directs the regioselectivity of the photochemistry. Such a regioselectivity is found indeed for the photoisomerization of protonated allylimine[28], and it gives a possible explanation for the photochemical behaviour of the protonated Schiff bases of retinal[8,9] (see also next sections).

3.3.2 Multiple Double Bond Rotations in Pentanimine-H^+

It has been argued by several research groups[29,30] that the isomerization around one double bond cannot occur for the retynilidene chromophore in the confined pocket of the surrounding protein. Therefore, mechanisms have been proposed which involve the simultaneous isomerization of two double bonds (the "bicycle pedal" model[29]) or the simultaneous isomerization of a double bond and an adjacent single bond (the "hula twist" model[30]). From an inspection of the bond-densities of the excited states of pentanimine-H^+ (Figure 3) it follows that particularly a simultaneous rotation around the two carbon-carbon double bonds should be energetically favourable[31]. Therefore, MNDO/CI calculations were performed for the two-dimensional reaction surfaces for the twist around these bonds (θ_1 and θ_2). The results are shown in Figures 6 and 7.

The energy curves for the twist around the C_1–C_2 and C_3–C_4 bonds as shown in Figure 2 are essentially the sections of the two-dimensional surfaces which correspond to $\theta_2 = 180°$ and $\theta_1 = 180°$, respectively. From an inspection of Figure 6 it is seen that there is a region near $\theta_1 = \theta_2 = 90°$ where the energy of S_1 increases whereas the top of the energy surface of the ground state levels of. This is a result of a crossing of the wavefunctions describing S_0 and S_1 going from $\theta_1 = \theta_2 = 0°$ (180°) to $\theta_1 = \theta_2 = 90°$. To demonstrate this, the potential energy curves representing a simultaneous isomerization for the two bonds out of phase ($\theta_1 = -\theta_2$) are given in Figure 8.

This latter isomerization is especially interesting to describe the *cis–trans* isomerization of the retynilidene chromophore, where the N-end is anchored to the protein via a covalent linkage, because the motion of the N-end in this concerted isomerization is minimal. The relevant resonance structures for the doubly twisted structure can be deduced from the occupation of the MOs for this geometry (Figure 9).

For S_0 and S_1 the bond between C_1–C_2 and C_3–C_4 has become a real double bond. The resonance structures for these states differ mainly by the location of the positive charge in the molecule. This already indicates that these states will be differently influenced by a charged environment (*vide infra*). The potential energy curve for the out of phase rotation of the two double bonds (Figure 8) shows that this is unfavourable in both the ground and the excited state. The potential energy barrier in the excited state is 11.2 kcal/mol. Besides, there is a very strong nonadiabatic coupling between the two states for a twist angle less than 90°. The molecule will cross over to the ground state before it reaches 90° and, therefore, will isomerize back to its initial conformation (see also next section). This motion represents a trajectory which will lower the quantum-yield for *cis–trans* isomerization.

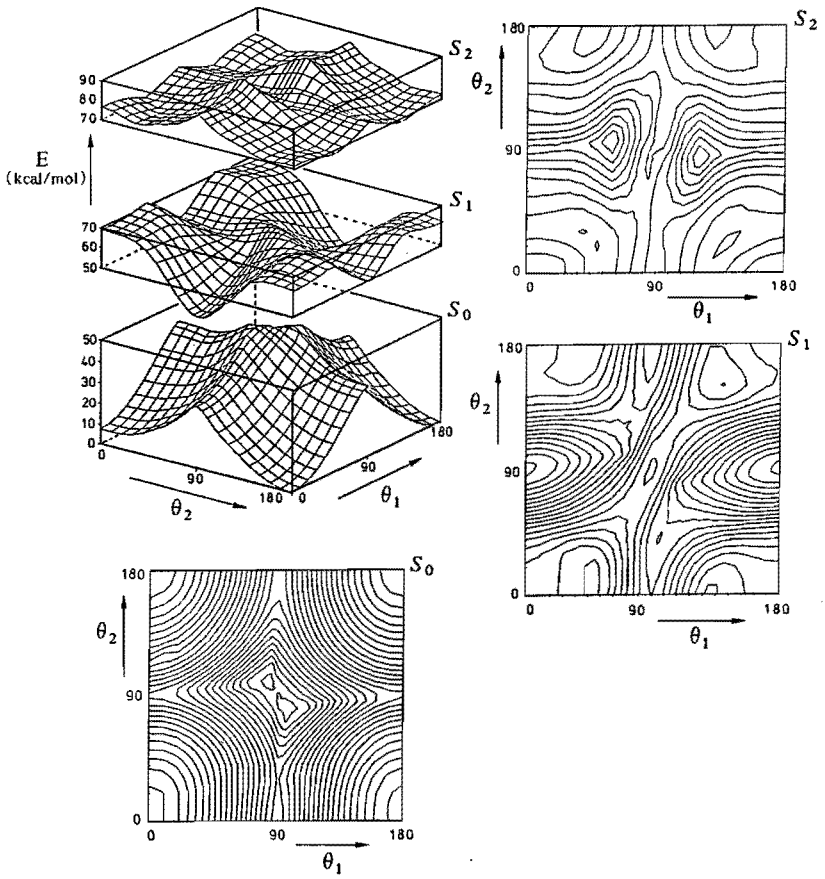

Figure 6. Potential energy surfaces and corresponding contour maps of S_0, S_1 and S_2 for a simultaneous rotation around the C_1–C_2 (θ_1) and C_3–C_4 (θ_2) bonds. The energy difference between two contour lines in the contour maps is 2 kcal/mol.

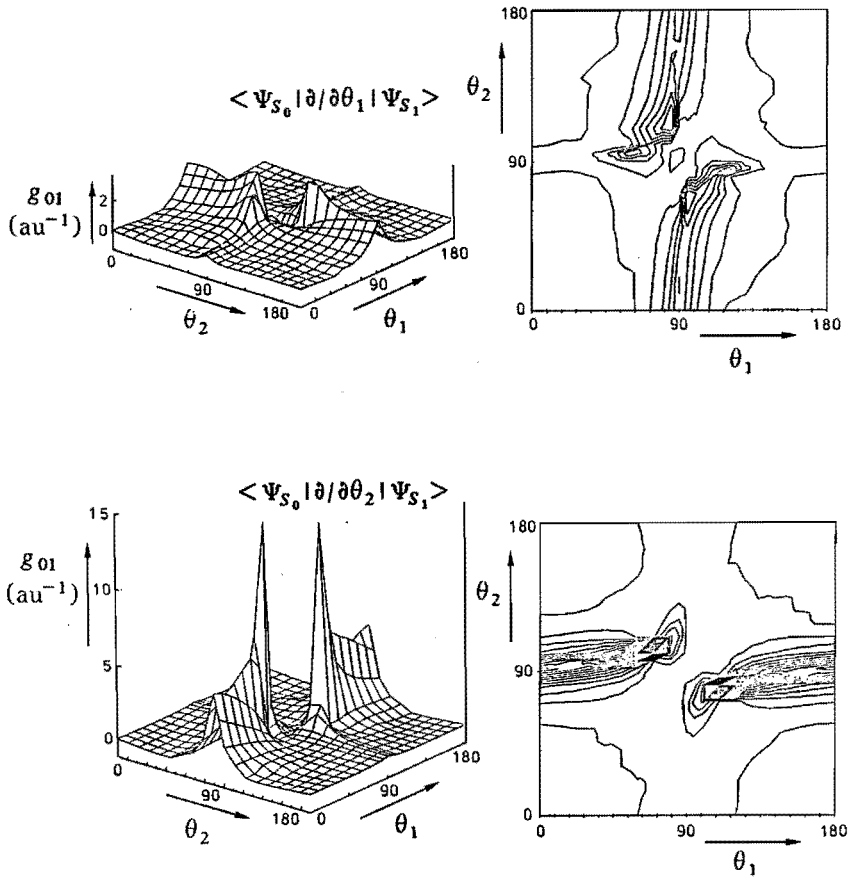

Figure 7. Two-dimensional plot of the nonadiabatic couplings $g_{01}(\theta_1)$ and $g_{01}(\theta_2)$ and corresponding contour maps for a simultaneous rotation around the C_1–C_2 (θ_1) and C_3–C_4 (θ_2) bonds. The difference between two contour lines in the contour maps is 0.5 au^{-1}.

In Figure 7 the nonadiabatic couplings $g_{01}(\theta_1) = <\Psi_0|\partial/\partial\theta_1|\Psi_1>$ and $g_{01}(\theta_2) = <\Psi_0|\partial/\partial\theta_2|\Psi_1>$ between the ground and first singlet excited state are shown for the two-dimensional reaction surface. It is seen that the nonadiabatic coupling for a certain twist is strongest in the direction of that twist (θ_1 for $g_{01}(\theta_1)$ and θ_2 for $g_{01}(\theta_2)$). In regions where the nonadiabatic coupling is large, the probability for a radiationless transition is relatively large (provided that the nuclear velocity is large as well, see next section). Therefore, any combined rotation bringing the molecule in such a region, may represent a trajectory which is favourable for a radiationless transition.

A trajectory is imaginable in which the C_3–C_4 bond isomerizes from $\theta_2 = 0°$ via $\theta_2 = 90°$ to $\theta_2 = 180°$ while at the meantime the C_1–C_2 bond rotates

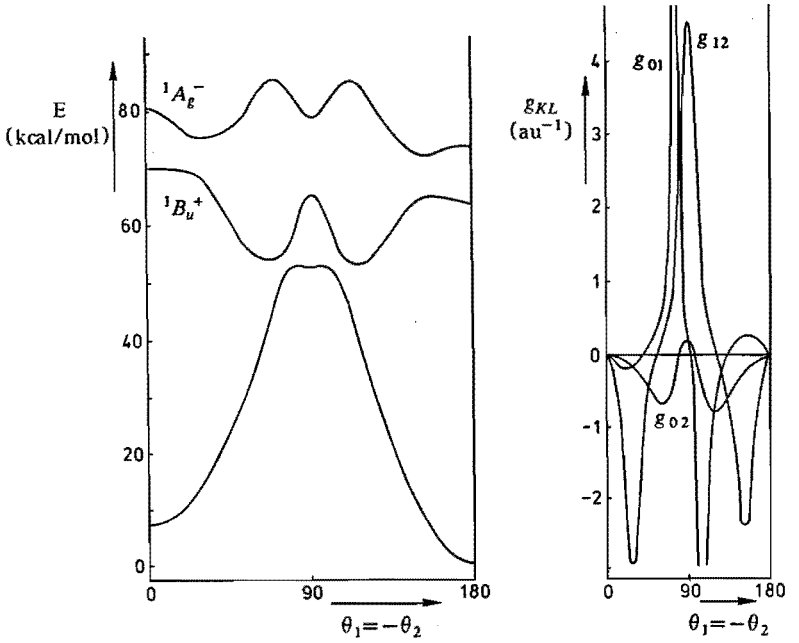

Figure 8. Potential energy curves and nonadiabatic couplings for a simultaneous out of phase rotation ($\theta_1 = -\theta_2$) around the C_1–C_2 and C_3–C_4 bonds in pentanimine-H$^+$.

partly to a twist angle of approximately 60° and then rotates back[32]. Such a mechanism would generate a route with a large transition probability. It has the advantage that the overall reaction only involves the isomerization of one double bond, as is observed for rhodopsine. The other bond only assists the reaction in that it brings the molecule in a region of large coupling whereas the volume needed for the isomerization is smaller. A more complete treatment of this concerted mechanism asks for the solution of trajectory equations in two dimensions. Present work is aimed at performing such calculations.

A similar concerted bicycle pedal motion has been proposed for the thermal isomerization of light adapted BR_{568} to dark adapted BR_{548}[33]. Resonance Raman spectra[5a] show that this transformation involves the isomerization from all-*trans* retinal to 13,15-di*cis* retinal. From the bond densities given in Figure 3 it follows that a simultaneous rotation around the C_3–C_4 and C_5–N bonds is unfavourable for pentanimine-H$^+$ in the excited state. Because of the complementarity of the thermal and photochemical processes, this mechanism might provide a route for the thermal process[5b].

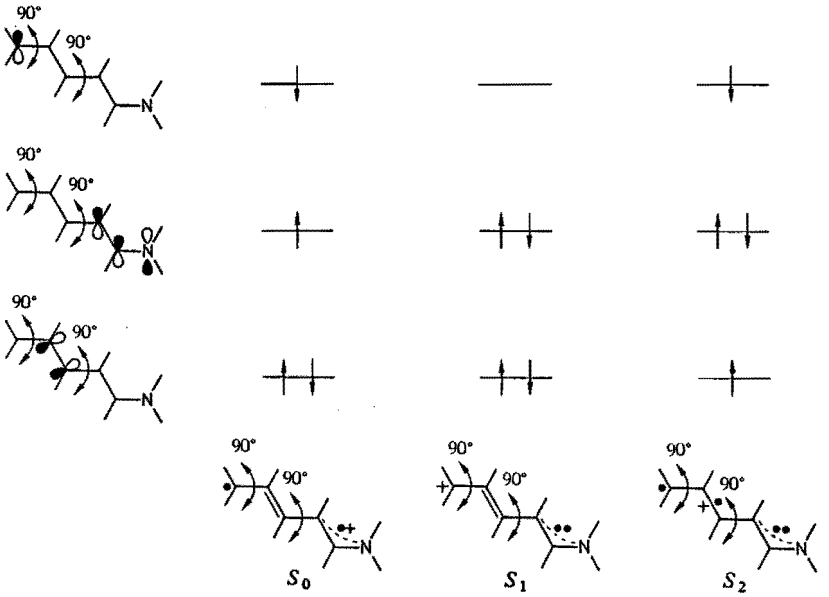

Figure 9. Frontier molecular orbitals, occupation of these molecular orbitals and derived resonance structures for the S_0, S_1 and S_2 states of pentanimine-H^+ 90° rotated around the C_1-C_2 and the C_3-C_4 bond.

3.4 Dynamical Calculations

In the preceding section it was pointed out that the efficiency and quantumyield for *cis—trans* isomerization is determined by the extent of the transition probability in a region of strong nonadiabatic coupling. In this section, the transition probability is calculated from the potential energy curves and nonadiabatic coupling functions. Such a calculation is possible with a pure quantumchemical treatment as described in chapter 2. However, this method can only be applied for one-dimensional isomerizations with a moment of inertia which is independent of the twist angle. In the present case, this restriction does not hold. Especially for the rotation around the central C_3-C_4 bond in pentanimine-H^+ and most of the combined rotations, the moment of inertia strongly depends on the twist angle. Therefore, the semi-classical trajectory method[34] has been used to study the dynamics of *cis—trans* isomerization in pentanimine-H^+. Similar calculations have been performed by Warshel[21,29] and Birge[14] in the study on the photoisomerization of the retinylidene chromophore. However, their calculations were based on a more or less semi-empirical

expression for the nonadiabatic coupling. The present calculations made explicitely use of the calculated nonadiabatic couplings.

In the semi-classical trajectory method[34], the time dependent wavefunction is written as an expansion of the wavefunctions of the electronic states:

$$|\psi^{el}(r,\theta(t))> = \sum_K a_K(t)\,|\psi_K^{el}(r,\theta)>\, e^{-\frac{i}{\hbar}\int_0^t E_K(\theta)d\tau} \qquad 1$$

In this equation, $|\psi_K^{el}(r,\theta)>$ represents the wavefunction of state K which depends on the electron coordinates (r) and parametrically on the twist angle θ. $E_K(\theta)$ stands for the potential energy curve of this state. The time dependent contribution of the electronic state K to the total wavefunction $|\psi^{el}(r,\theta(t))>$ equals $|a_K(t)|^2$. The contribution of the electronic ground state $|a_0(t)|^2$ can be interpreted as the transition probability of the molecule from the excited state to the ground state. The (complex) coefficients $a_K(t)$ are found by substituting eq. 1 in the time dependent Schrödinger equation:

$$i\hbar\frac{\partial}{\partial t}|\psi^{el}(r,\theta(t))> = H^{el}(r,\theta(t))\,|\psi^{el}(r,\theta(t))>\,, \qquad 2$$

resulting in a set of differential equations:

$$\dot{a}_L(t) = -\dot{\theta}(t)\sum_{K\neq L} a_K(t)\,g_{KL}(\theta)\,e^{-\frac{i}{\hbar}\int_0^t (E_K(\theta)-E_L(\theta))d\tau} \qquad 3$$

In this equation, $g_{KL}(\theta)$ represents the nonadiabatic coupling function as calculated from the multiconfigurational wavefunctions of the electronic states:

$$g_{KL}(\theta) = <\psi_K^{el}(r,\theta)\,|\,\partial/\partial\theta\,|\,\psi_L^{el}(r,\theta)>_r \qquad 4$$

The nuclear velocity $\dot{\theta}(t)$ was obtained from the classical equations of motion. The angular dependent moment of inertia $I(\theta)$ needed in these equations was evaluated by a calculation of the kinetic energy at a constant $\dot{\theta}$ of the molecule moving on the potential energy curve of the initially excited state. In practice, several trajectories were run with various initial conditions corresponding to a different excess kinetic energy of the excited molecule. This approach mimics the situation in which an ensemble of vibrational levels is excited, each with its own excess vibrational energy.

The calculations were performed for the rotations around the $C_1{-}C_2$ bond (Figure 2a), the $C_3{-}C_4$ bond (Figure 2b) and the simultaneous out of phase rotation around the $C_1{-}C_2$ and $C_3{-}C_4$ bonds (Figure 8) in order to demonstrate the influence of the shape of the potential energy curves and the nonadiabatic couplings on the dynamics of *cis–trans* isomerization. For all rotations, three singlet states were included in the calculations. It was assumed that all trajectories started on the potential energy curve of the first excited state ($|a_1(0)|^2 = 1$) because this state has the largest oscillatorstrength.

For the rotation around the $C_1{-}C_2$ bond in pentanimine-H^+ (Figure 2a), there is a strong nonadiabatic interaction between the two excited states at $\theta_1 = 50°$ and $\theta_1 = 130°$, as can be seen from the peaks in the nonadiabatic coupling

function $g_{12}(\theta_1)$ at these angles. As a result, it was found that the contribution of the second excited state to the total wavefunction $|a_2(t)|^2$ increased to a value of 0.60. On the other hand, the contribution of the electronic ground state $|a_0(t)|^2$ did not exceed a value of 0.06. When it is assumed that molecules cross over to the ground state with conservation of the direction of rotation, it follows that only a small fraction of the molecules will reach the isomerized structure after the first passage of the 90° region. The rest of the molecules will start to oscillate back and forth in the energy minimum with an equal probability to cross over to the ground state in either direction of the isomerization (provided the energy of the system does not decrease via intramolecular energy dissipation or collisions with the environment). The result is an almost 1:1 distribution of the *cis* and *trans* isomers in the ground state.

Another important feature is the energy barrier on the potential energy curve of the first excited state. Due to this barrier a number of trajectories corresponding to vibrational levels with low energies will not cross this barrier. Therefore, molecules with such low vibrational energies will not isomerize but exhibit other processes (such as fluorescence and other photochemical processes). This will reduce the quantumyield for *cis*—*trans* isomerization.

In contrast to the isomerization around the C_1—C_2 bond, a calculation of the contributions of the electronic states for a rotation around the central C_3—C_4 bond showed that in this case the transition probability to the ground state is much larger ($|a_0(t)|^2 = 0.30$). This is a direct result of the small energy gap and correspondingly large nonadiabatic coupling at $\theta_2 = 90°$ (see Figure 2b). From this value of 0.30, a quantumyield for isomerization is calculated[35] of 0.59 (assuming that no other processes occur). This transition probability is almost identical for the *cis* → *trans* isomerization and the *trans* → *cis* isomerization. However, for this latter isomerization the energy barrier on the potential energy curve of the first excited state will decrease the number of trajectories which reach the crossing region. Consequently, the quantumyield for *trans* → *cis* isomerization will be correspondingly small.

Finally, trajectory calculations were performed for the simultaneous out of phase rotation around the C_1—C_2 and C_3—C_4 bonds (Figure 8). The angle dependent moment of inertia for this motion is almost identical to that for the single bond rotation around the C_3—C_4 bond. Evidently, the orientation of the terminal CH_2-fragment does not influence this moment of inertia significantly. However, the effect of a combined rotation will be much larger in a situation where one end of the molecule is linked to a heavy fragment or to a protein (as is the case for rhodopsin and bacteriorhodopsin).

The contribution of the ground state ($|a_0(t)|^2$) was found to reach a value of 0.60 for a twist angle less than 90°. When the molecules cross over to the ground state at this angle, the potential energy curve of this state will direct them back to the initial conformation. The number of trajectories which will cross the energy barrier on the potential energy curve of S_1 and enter the second region of strong coupling is smaller. A crossing to the ground state in this region will lead to the isomerized product. From these considerations, it may be concluded that the quantumyield for *cis*—*trans* isomerization via this

coupled motion will be relatively small.

In summary, it is found that the transition probability to the ground state and the related quantumyield strongly depend on the energy gap between S_0 and S_1. In the preceding section it was shown that this energy gap is a function of the distance from the twisted bond to the nitrogen atom in the protonated Schiff base. An energy barrier on the potential energy surface of the excited state will cause a number of trajectories not to reach the region of strong nonadiabatic coupling. Therefore, such an energy barrier will also have a negative effect on the quantumyield for *cis—trans* isomerization.

3.5 Influence of External Point-charges

From the calculations for pentanimine-H^+ it follows that the regioselectivity and efficiency for photoisomerization in protonated Schiff bases is directed by the intrinsic properties of these molecules. The dynamics of the *cis—trans* isomerization can be understood from the bond-densities of the reactant in the excited state and the relative stability of the resonance structures describing the ground and excited state of the 90° twisted molecule. This stability was shown to depend on the distance from the nitrogen atom to the twisted bond. For a bond which is too close to the nitrogen atom the ground state, which is described by a Z-structure (the two former π-electrons at the N-end of the molecule, the C-fragment positively charged), is too strongly stabilized. The excited state, now described by a D-structure (one of the former π-electrons at each side of the twisted bond, the N-fragment positively charged) is so strongly destabilized that the energy minimum on the excited state potential energy surface becomes less deep. In this situation, the energy gap between S_0 and S_1 is relatively large. On the other hand, twisting a bond which is too far from the nitrogen atom results in an opposite stabilization of the Z- and D-structures (now describing S_1 and S_0, respectively). However, the effect is the same because the minimum on the excited state potential energy surface is less deep and the energy gap with the ground state relatively large.

The determining factor in this description is the stabilization of the positive charge in either of the two fragments on each side of the twisted bond. This feature indicates that the various twisted structures will be differently influenced by a polarizable (solvent) or charged (surrounding protein) environment. Freedman and Becker[8,9] argued that the variety in quantumyields of isomerized products upon irradiation of the n-butylamine Schiff base of retinal as a function of protonation-state and solvent polarity could be explained from the mixing of the $^1B_u^+$-state into the $^1A_g^-$-state. The charge stabilization in the excited state of the twisted molecule now introduces an additional property which will strongly influence the shape of the potential energy surface and, therefore, the dynamics and quantumyields for the various

photoisomerizations. Moreover, it offers an explanation for the regioselectivity of isomerization in the irradiated reactant.

For the free (protonated) Schiff base, the optimal condition will be fulfilled for the isomerization around one particular double bond. For the protonated n-butylamine Schiff base of retinal this seems to be the $C_{11}-C_{12}$ double bond[8] ($\Phi_{c \rightarrow t} = 0.24$, $\Phi_{t \rightarrow c} = 0.14$). When the chromophore is embedded in opsin, the quantumyield for isomerization in rhodopsin is strongly increased[36] ($\Phi_{c \rightarrow t} = 0.67$, $\Phi_{t \rightarrow c} = 0.50$) whereas for bacteriorhodopsin it is found that, instead of the $C_{11}-C_{12}$ double bond, the $C_{13}-C_{14}$ double bond isomerizes. These differences can now be understood by assuming that the surrounding protein provides external charges at different locations relative to the chromophore. Such external point-charge models[1,37–39] have been put forward by several research groups to explain the shift of the UV absorption maximum (opsin shift[37]) for the various intermediates in the photocycles of rhodopsin and bacteriorhodopsin, their vibrational spectra[5b] and the isomerization barriers in the ground state[20,40].

To demonstrate the influence of a charged environment on the relative stabilities of the *D* and *Z* resonance structures, calculations were performed for a model compound (RET-H$^+$) representing the protonated Schiff base of retinal.

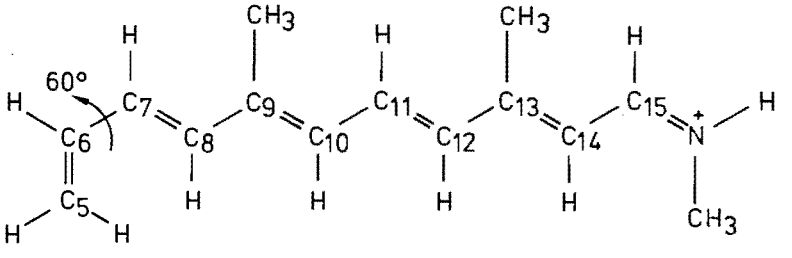

RET-H$^+$

Scheme 4

In this model compound, the cyclohexene-ring of retinal is replaced by a vinyl-group which is arbitrary twisted by 60° out of the plane of the polyene-chain[41]. This restricted molecule is found to be a suitable model for the study of the properties of the protonated Schiff base of retinal[20].

Figure 10 shows the charge- and bond-densities of the lowest singlet states of RET-H$^+$. It is found that the $^1B_u^+$-state is the lowest excited state. The calculated vertical excitation energy to this state is 1.97 eV (630 nm) which is too low compared with the experimental value of about 500 nm, but in agreement with the INDO-CISD calculations of Birge et al.[42] for a similar compound. The difference between the theoretical (gas phase) and experimental (solvent) values can be explained from the interactions of the molecule with the solvent which will (partly) shield the positive charge of the protonated nitrogen atom thereby inducing a red shift of the UV absorption maximum. The energy gap between the $^1B_u^+$- and the $^1A_g^-$-state is calculated to be 0.56 eV which is

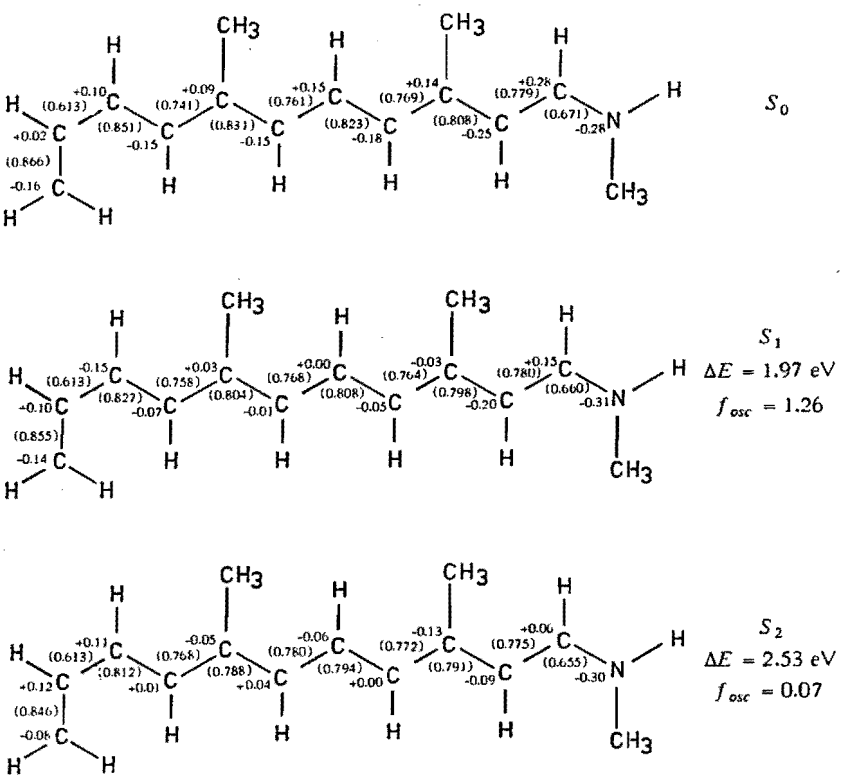

Figure 10. Calculated charge- and bond-densities (in brackets) for the three lowest singlet states of RET-H$^+$.

considerably smaller than the energy gap calculated by Birge et al.[42] (1.54 eV) but agrees much better with the observed value of ca. 0.25 eV for 11-*cis* rhodopsin[42]. The calculated oscillatorstrengths show that the one-photon absorption will take place almost entirely to the $^1B_u^+$-state.

An inspection of the changes in bond-densities going from the ground state to the $^1B_u^+$ (S_1) and $^1A_g^-$ (S_2) states shows that it is the latter state which has the most antibonding character. Therefore, the $^1A_g^-$-state is expected to be especially photochemical labile. The antibonding character of the double bonds in this state is found to increase going from the N-end of the molecule to the vinyl-group. This implies that a photoisomerization is expected for those double bonds close to the vinyl-group (*vide supra*). The bond-densities of the single bonds are found to increase upon excitation. From this observation it is suspected that rotations around these single bonds do not contribute to a decrease in energy of the excited states in the protonated Schiff bases of retinal. Therefore, it seems that the hula-twist model of Liu et al.[30] does not apply for photochemical isomerizations in these molecules[31]. On the other hand, a simultaneous twist around two double bonds[29] seems plausible from these calculations.

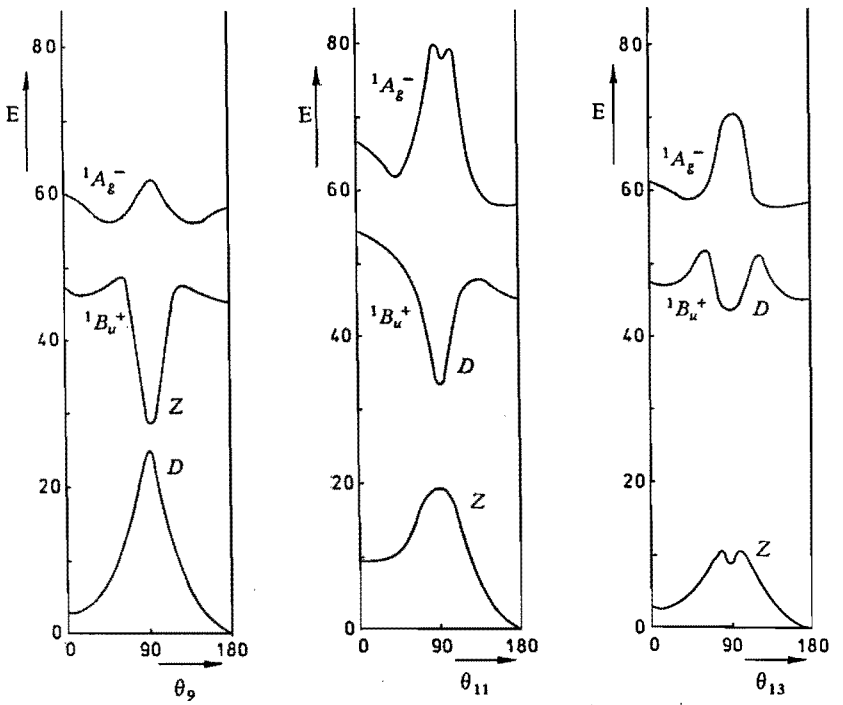

Figure 11. Potential energy curves for the rotation around the C_9–C_{10} (a), the C_{11}–C_{12} (b) and the C_{13}–C_{14} (c) bonds in RET-H$^+$. Energies are in kcal/mol.

The calculated potential energy curves for a rotation around the C_9–C_{10}, the C_{11}–C_{12} and the C_{13}–C_{14} double bonds in RET-H$^+$ are shown in Figure 11. They clearly show the characteristics of a protonated Schiff base as demonstrated for pentanimine-H$^+$. Both the energy barrier on the potential energy curve of the first excited state and the energy gap between S_0 and S_1 for the 90° twisted molecule strongly depend on the distance from the twisted bond to the nitrogen atom.

The energy barriers for the *trans* (θ = 180°) to *cis* (θ = 0°) isomerizations are 3.2 (C_9–C_{10}), 2.2 (C_{11}–C_{12}) and 5.9 (C_{13}–C_{14}) kcal/mol, respectively. These values lie in the order of the value of 2 kcal/mol obtained by Huppert and Rentzepis[43] from luminiscence measurements for the isomerization of the protonated Schiff base of retinal.

The calculated energy gaps at θ = 90° are 3.1 (C_9–C_{10}), 13.5 (C_{11}–C_{12}) and 34.8 (C_{13}–C_{14}) kcal/mol, respectively. For RET-H$^+$ 90° twisted around the C_9–C_{10} bond, the ground state is found to be a *D*-structure (the N-end positively charged) and the first excited state a *Z*-structure (the C-end positively charged). For RET-H$^+$ 90° twisted around the C_{11}–C_{12} and C_{13}–C_{14} bonds, the *Z*-structure is so strongly stabilized that it has become the ground state.

It follows from the energy curves that both the energy barrier in S_1 and the energy gap with S_0 favour an isomerization around the C_9-C_{10} double bond for RET-H$^+$. However, experiments[8] for this compound show a preferred isomerization of the $C_{11}-C_{12}$ double bond. This discrepancy probably raises from the fact that the influence of the solvent is not included in this calculation (*vide supra*). A solvent will increase the transition energy to the $^1B_u^+$-state and, consequently, increase the energy gap for RET-H$^+$ 90° twisted around the C_9-C_{10} double bond and decrease this value for RET-H$^+$ 90° twisted around the $C_{11}-C_{12}$ and $C_{13}-C_{14}$ double bonds.

A comparison of the energy curves for the *cis* isomers ($\theta = 0°$) shows an additional element which directs the photoisomerization. Due to the steric hindrance between the methyl-group at C_{13} and the hydrogen atom at C_{10}, the energy curve for the isomerization from 11-*cis* ($\theta_{11} = 0°$) to all-*trans* ($\theta_{11} = 180°$) is barrierless in the excited state. The calculated effect is overestimated (as is obvious from the energy difference of 9.3 kcal/mol between the 11-*cis* and the all-*trans* isomers[44]) because the molecule was not optimized for the 11-*cis* isomer. No such steric hindrance is present for the 9-*cis* and 13-*cis* isomers so that this feature offers an additional reason for the efficient *cis*–*trans* isomerization in the 11-*cis* isomer of the protonated Schiff base of retinal[8].

It is generally accepted that the proton at the Schiff base of the retinylidene chromophore interacts with a negatively charged counterion[1]. The presence of this negative charge is of great importance for the stability of the resonance structures of the twisted molecule. To demonstrate this, the energy curves were calculated[45] for a rotation around the C_9-C_{10}, the $C_{11}-C_{12}$ and the $C_{13}-C_{14}$ double bonds of RET-H$^+$ with a negative charge at a distance of 3 Å from the proton at the nitrogen atom in the all-*trans* conformation (see Scheme 5). These calculations mimic the situation for bacteriorhodopsin. During the rotation of the double bonds, the negative point-charge was fixed at its initial position. The calculated energy gaps between S_0 and S_1 in the various orthogonal conformations are given in Table 1.

The effect of the negative point-charge is to stabilize the *D*-structures (with the N-end positively charged) and to destabilize the *Z*-structures (with the C-end positively charged). As a matter of course, this stabilization is more effectuated for smaller distances between the twisted molecule and the negative charge. This distance decreases going from the molecule 90° twisted around the C_9-C_{10} double bond to the molecule 90° twisted around the $C_{13}-C_{14}$ double bond. Therefore, the effect of the negative charge is largest for this latter isomerization. The energy gap between S_0 and S_1 for RET-H$^+$ 90° twisted around the $C_{13}-C_{14}$ double bond decreases from 34.8 kcal/mol in the absence of a negative charge to 14.9 kcal/mol (see Table 1). Consequently, the counterion near the protonated Schiff base will increase the quantumyield for an isomerization around the $C_{13}-C_{14}$ double bond (as is the case for the photoisomerization of BR_{568} to K_{610}). A much smaller effect is observed for the isomerizations around the C_9-C_{10} and the $C_{11}-C_{12}$ double bonds.

In the original point-charge model of Nakanishi et al.[37], it was assumed that in the case of bacteriorhodopsin there is a second negative charge near the cyclohexene-ring. Such a negative charge will stabilize the *Z*-structures and

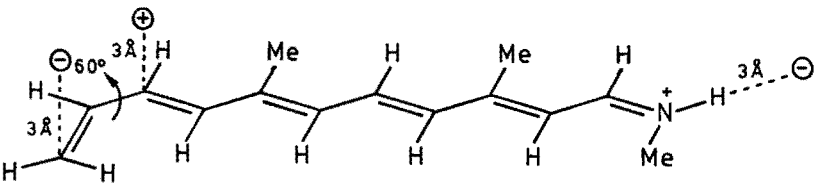

Scheme 5

Table 1. Influence of external point-charges on the energy gap between S_0 and S_1 for RET-H$^+$ (**1**) 90° twisted around the C_9–C_{10}, the C_{11}–C_{12} and the C_{13}–C_{14} bond. RET-H$^+$ with an additional negative charge fixed at 3 Å from the proton at the nitrogen atom in the all-*trans* isomer (**2**), an additional negative charge at 3 Å above C_5 (**3**) and an additional positive charge 3 Å above C_7 (**4**) (see Scheme 5).

	C_9–C_{10}	C_{11}–C_{12}	C_{13}–C_{14}
1	3.1 (*Z*)	13.5 (*D*)	34.8 (*D*)
2	6.1 (*Z*)	8.9 (*D*)	14.9 (*D*)
3	16.8 (*D*)	22.8 (*D*)	37.3 (*D*)
4	16.9 (*Z*)	4.1 (*Z*)	12.3 (*D*)

The energies are in kcal/mol. *D* and *Z* refer to the character of the 90° twisted molecule in the excited state (see text).

destabilize the *D*-structures. Therefore, the energy gap between S_0 and S_1 will increase by this additional negative charge for all twisted conformations where the ground state has *Z*-character. A calculation for RET-H$^+$ with an additional negative charge at 3 Å above C_5 (**3**) shows that this is indeed the case (Table 1). The energy gap for the C_{13}–C_{14} double bond increases from 14.9 kcal/mol to 37.3 kcal/mol, which disagrees with the observed photoisomerization of this double bond in bacteriorhodopsin.

However, Lugtenburg et al.[39] have argued that the negative charge near the C_5 position in the cyclohexene-ring is accompanied by an additional positive charge near C_7. Their conclusions were based on the opsin shift of some dihydro-derivatives of retinal in bacterio opsin and are supported by NMR experiments of the same group[46]. A calculation of the energy gap between S_0 and S_1 for RET-H$^+$ with a negative charge near the protonated nitrogen atom, a negative charge 3 Å above C_5 and a positive charge 3 Å above C_7 (**4**) shows that the isomerization around the C_{13}–C_{14} double bond now becomes favourable again (see Table 1).

Of course, for a more precise evaluation of the effect of external-point charges more information is needed about the structure of the protein and the nature of the counterions. However, the present results clearly show how the electronic interactions which induce the opsin shift of the retynilidene

chromophore also have an important effect on the energy gap between the ground and excited state and the related dynamics of the photoisomerization. The external point-charge model with an ion-pair near the cyclohexene-ring[39,46] is found to be the best model to explain the observed behaviour of bacteriorhodopsin.

3.6 Summary

The aim of this chapter was to demonstrate which intrinsic properties of protonated Schiff bases and which external features account for the highly regioselective and efficient *cis—trans* isomerization observed for the retinylidene chromophore in rhodopsin and bacteriorhodopsin.

MNDO/CI calculations for pentanimine-H^+ revealed that the intrinsic properties can be understood from the bond-densities of the reactant in the excited states and the relative stability of the resonance structures describing the 90° twisted molecule in the ground and excited state. Whereas the light absorption takes place to the first ($^1B_u^+$) excited state, the second ($^1A_g^-$) excited state is found to be particularly photochemical labile. It serves in diminishing (or even removing) the energy barrier on the potential energy curve of the first excited state via an avoided crossing.

The electron deficient nitrogen atom causes a strong stabilization of the polarized structure of the 90° twisted molecule in the excited state, resulting in a decrease of the energy gap between the ground and excited state. When this stabilization is too strong, the polarized *Z*-structure drops below the diradicalar *D*-structure, thereby increasing the energy gap again. This energy gap is found to depend on the distance from the twisted bond to the nitrogen atom, which explains the intrinsic regioselectivity for *cis—trans* isomerization in free protonated Schiff bases.

Dynamical calculations on the isomerization of the double bonds in pentanimine-H^+ by means of semi-classical trajectory calculations made it possible to evaluate explicitely the transition probability of the excited molecule to the ground state. This transition probability depends on the energy gap and the extent of the nonadiabatic coupling between the ground and excited state. The largest transition probability (0.30) was found for the central double bond in pentanimine-H^+. The difference between the *cis* → *trans* and *trans* → *cis* isomerizations arises from the presence of an energy barrier on the potential energy curve for this latter reaction. This causes a number of molecules with low vibrational energies in the excited state not to reach the region of strong coupling. As a result, the quantumyield for this isomerization is smaller than for the reverse reaction.

From an inspection of the bond-densities of pentanimine-H^+ it follows that a simultaneous (bicycle pedal) rotation of the two double bonds should be energetically feasible. A calculation of the transition probability for this concerted

motion shows that a radiationless transition is most likely to occur for a twist angle less than 90° so that the molecule will isomerize back to the initial conformation. However, a calculation of the potential energies and nonadiabatic couplings for the two-dimensional reaction surface of the two double bonds, shows that a rotation around the central double bond can be assisted by a partial rotation of the other double bond. This mechanism may be of importance for the isomerization of the retinylidene chromophore in the confined environment of the protein.

The last part of this chapter describes the influence of external point-charges on the mechanism of *cis–trans* isomerization. Such external point-charge models have been proposed in literature to account for the opsin shift of various intermediates in the photocycles of rhodopsin and bacteriorhodopsin. Calculations on a model for the retinylidene chromophore show that these point-charges also have a very important impact on the stability of the resonance structures of the twisted molecule and, therefore, on the efficiency for photoisomerization. From the present calculations it follows that the primary step in the photoisomerization of bacteriorhodopsin can be best understood from an external point-charge model with a negative charge near the protonated nitrogen atom and an ion-pair near the cyclohexene-ring.

This type of calculations can be very helpful in the elucidating the mechanism of the strikingly efficient *cis–trans* isomerization in the retinylidene chromophore and in developing model systems for an experimental verification of this mechanism.

3.7 References and Notes

1 For some recent reviews see:

M. Ottolenghi in "Advances in Photochemistry", Vol. 12, J.N. Pitts, G.S. Hammond, K. Gollnick, D. Grosjean, Eds., Wiley Interscience, New York, p. 87 (1980)

R.R. Birge, Ann. Rev. Biophys. Bioeng., **10**, 315 (1981)

C. Sandorfy, D. Vocelle, Can. J. Chem., **64**, 2251 (1986)

2 J.B. Hurley, T.G. Ebrey, B. Honig, M. Ottolenghi, Nature, **270**, 540 (1977)

3 A. Cooper, Nature, **282**, 531 (1979)

4 There are strong indications that before the ground state product K_{610} an isomer is formed ("J") directly from BR_{568} within 0.7 psec, which rapidly converts into K_{610} within a few picoseconds. This latter transformation probably involves conformational changes of the protein.

N.C. Nuss, W. Zinth, W. Kaiser, E. Kölling, D.Oesterhelt, Chem. Phys. Lett., **117**, 1 (1985)

H.J. Polland, M.A. Franz, W. Zinth, W. Kaiser, E. Kölling, D. Oesterhelt, Biophys. J., **49**, 651 (1986)

5a S.O. Smith, J.A. Pardoen, J. Lugtenburg, R.A. Mathies, J. Phys. Chem., **91**, 804 (1987)

5b P. Tavan, K. Schulten, Biophys. J., **50**, 81 (1986)

6 C.H. Chang, R. Govindjee, T. Ebrey, K.A. Bagley, G. Dollinger, L. Eisenstein, J. Marque, H. Roder, J. Vittitow, J.-M. Fang, K. Nakanishi, Biophys. J., **47**, 509 (1985)

7 R.R. Birge, T.M. Cooper, Biophys. J., **42**, 62 (1983)

8 K.A. Freedman, R.S. Becker, J. Am. Chem. Soc., **108**, 1245 (1986)

9 R.S. Becker, K.A. Freedman, J. Am. Chem. Soc., **107**, 1477 (1985)

10 K. Schulten, M. Karplus, Chem. Phys. Lett., **14**, 305 (1972)

J. Čížek, J. Paldus, I. Hubač, Int. J. Quant. Chem., **8**, 951 (1974)

11 J. Koutecký, J. Chem. Phys., **47**, 1501 (1967)

12 L.P. Murray, R.R. Birge, Can. J. Chem., **63**, 1967 (1985)

13 W.Th.A.M. van der Lugt, Thesis, Leiden (1968)

14 R.R. Birge, L.M. Hubbard, J. Am. Chem. Soc., **102**, 2195 (1980)

15 M.J.S. Dewar, W.Thiel, J. Am. Chem. Soc., **99**, 4899 (1977)

16 B. Huron, J.-P. Malrieu, P. Rancurel, J. Chem. Phys., **58**, 5745 (1973)

See also chapter 1.

17 C. Galloy, J.C. Lorquet, J. Chem. Phys., **67**, 4672 (1977)

G. Hirsh, P.J. Bruna, R.J. Buenker, S.D. Peyerimhoff, Chem. Phys., **45**, 335 (1980)

R. Cimiraglia, M. Persico, J. Tomasi, Chem. Phys., **53**, 357 (1980)

See also the appendix.

18 W.C.A. van Dorst, Graduation Report, Eindhoven University of Technology (1987)

19 G.J.M. Dormans, G.C. Groenenboom, H.M. Buck, J. Chem. Phys., (1987)

See chapter 2.

20 P. Tavan, K. Schulten, D. Oesterhelt, Biophys. J., **47**, 415 (1985)

21 R.M. Weiss, A. Warshel, J. Am. Chem. Soc., **101**, 6131 (1979)

22 R. Daudel, G. Leroy, D. Peeters, M. Sana in "Quantum Chemistry", J. Wiley & Sons, p. 231 (1983)

B. Roos in "Computational Techniques in Quantum Chemistry and Molecular Physics", Proceedings of the NATO Advanced Study Institute, G.H.F. Diercksen, B.T. Suttcliffe, A. Veillard, Eds., vol. 15, p. 251 (1974)

23 K. Schulten, U. Dinur, B. Honig, J. Chem. Phys., **73**, 3927 (1980)

U. Dinur, B. Honig, K. Schulten, Chem. Phys. Lett., **72**, 493 (1980)

T. Shoda, T. Noro, T. Nomura, K. Ohno, Int. J. Quant. Chem., **30**, 289 (1986)

24 R.R. Birge, Acc. Chem. Res., **19**, 138 (1986)

25 V. Bonačić-Koutecký, P. Bruckmann, P. Hiberty, J. Koutecký, C. Leforestier, L. Salem, Angew. Chem., Int. Ed. Engl., **14**, 575 (1975)

26 See e.g.:

P. Bruckmann, L. Salem, J. Am. Chem. Soc., **98**, 5037 (1976)

I. Baraldi, M.C. Bruni, F. Momicchioli, G. Ponterini, Chem. Phys., **52**, 415 (1980)

G.J.M. Dormans, H.R. Fransen, H.M. Buck, J. Am. Chem. Soc., **106**, 1213 (1984)

L. Pogliani, N. Niccolai, C. Rossi, Chem. Phys. Lett., **108**, 597 (1984)

O. Kikuchi, H. Yoshida, Bull. Chem. Soc. Jpn., **58**, 131 (1985)

B.R. Brooks, H.F. Schaefer III, J. Am. Chem. Soc., **101**, 307 (1979)

I. Nebot-Gil, J.-P. Malrieu, J. Am. Chem. Soc., **104**, 3320 (1982)

P. Karafiloglou, P.C. Hiberty, Chem. Phys. Lett., **70**, 180 (1980)

I.D. Petsalakis, G. Theodorakopoulos, C.A. Nicolaides, R.J. Buenker, S.D. Peyerimhoff, J. Chem. Phys., **81**, 3161 (1984)

27 L. Salem, C. Leforestier, G. Segal, R. Wetmore, J. Am. Chem. Soc., **97**, 479 (1975)

V. Bonačić-Koutecký, J. Köhler, J. Michl, Chem. Phys. Lett., **104**, 440 (1984)

V. Bonačić-Koutecký, J. Koutecký, J. Michl, Angew. Chem., **99**, 216 (1987)

28 R.F. Childs, B.D. Dickie, J. Chem. Soc., Chem. Commun., 1268 (1981)

29 A. Warshel, Nature, **206**, 679 (1976)

30 R.S.H. Liu, A.E. Asato, Proc. Natl. Acad. Sci. USA, **82**, 259 (1985)

R.S.H. Liu, D. Mead, A.E. Asato, J. Am. Chem. Soc., **107**, 6609 (1985)

R.S.H. Liu, H. Matsumoto, A.E. Asato, D. Mead, J. Am. Chem. Soc., **108**, 3796 (1986)

R.S.H. Liu, D. Browne, Acc. Chem. Res., **19**, 42 (1986)

31 A concerted rotation around a double bond and an adjacent single bond seems to be unlikely in the excited state, but it might be feasible for the ground state processes which follow the primary photoisomerization of the retynilidene chromophore.

32 A. Warshel, N. Barboy, J. Am. Chem. Soc., **104**, 1469 (1982)

33 G. Orlandi, K. Schulten, Chem. Phys. Lett., **64**, 370 (1979)

34 M. Desouter-Lecomte, J.C. Leclerc, J.C. Lorquet, Chem. Phys., **9**, 147 (1975)

A. Warshel, M. Karplus, Chem. Phys. Lett., **32**, 11 (1975)

35 The quantumyield for isomerization can be calculated from the expression[21] $\Phi = (1 - f)/(2 - |a_0(t)|^2)$, where f is the fraction of the molecules which do not reach the crossing region.

36 T. Suzuki, R.H. Callender, Biophys. J. **34**, 261 (1981)

37 K. Nakanishi, V. Balogh-Nair, M. Arnaboldi, K. Tsujimoto, B. Honig, J. Am. Chem. Soc., **102**, 7945 (1980)

M.G. Motto, M. Sheves, K. Tsujimoto, V. Balogh-Nair, K. Nakanishi, J. Am. Chem. Soc., **102**, 7947 (1980)

38 F. Derguini, C.G. Caldwell, M.G. Motto, V. Balogh-Nair, K. Nakanishi, J. Am. Chem. Soc., **105**, 646 (1983)

T. Kakitani, H. Kakitani, B. Honig, K. Nakanishi, J. Am. Chem. Soc., **105**, 648 (1983)

J.L. Spudich, D.A.M. McCain, K. Nakanishi, M. Okabe, N. Shimizi, H. Rodman, B. Honig, R.A. Bogomolni, Biophys. J., **49**, 479 (1986)

39 J. Lugtenburg, M. Muradin-Szweykowska, C. Heeremans, J.A. Pardoen, C.S. Harbison, J. Herzfeld, R.G. Griffin, S.O. Smith, R.A. Mathies, J. Am. Chem. Soc., **108**, 3104 (1986)

40 S. Seltzer, J. Am. Chem. Soc., **109**, 1627 (1987)

41 Most crystal structures of retinal-analogues reveal an angle of 40° - 60° between the polyene-chain and the cyclohexene-ring.

C.J. Simmons, A.E. Asato, R.S.H. Liu, Acta Cryst., **C42**, 711 (1986)

One idealised geometry was used for all calculations: $r_{C=C} = 1.40$ Å; $r_{C-C} = 1.42$ Å; $r_{H_3C-C} = 1.50$ Å; $r_{H-C} = 1.10$ Å; $r_{N-C} = 1.35$ Å; $r_{N-H} = 1.00$ Å; $r_{H_3C-N} = 1.46$ Å; $\theta_{H_3C-C-C} = 122°$; $\theta_{H-C-C} = 116°$; $\theta_{H-N-C} = 117°$; $\theta_{H_3C-N-C} = 126°$.

42 R.R. Birge, L.P. Murray, B.M. Pierce, H. Akita, V. Balogh-Nair, L.A. Findsen, K. Nakanishi, Proc. Natl. Acad. Sci. USA, **82**, 4117 (1985)

43 D. Huppert, P.M. Rentzepis, J. Phys. Chem., **90**, 2813 (1986)

44 A separate geometry optimization of both isomers yields an energy difference between the all-*trans* and 11-*cis* isomers of ca 4 kcal/mol. The energy difference with the 9-*cis* and 13-*cis* isomers is ca 1 kcal/mol[20].

45 The effect of external point-charges was introduced by adding so called sparkles to the molecular frame. The sparkles represent pure unpolarizable ionic elements with an integer nuclear charge of +1 or -1. The calculations with sparkles were performed with the AMPAC program package, using the MNDO parametrization[15].

AMPAC (QCPE 506): M.J.S. Dewar, J.J.P. Stewart, Q.C.P.E. Bull., **6**, 24 (1986)

46 G.S. Harbison, S.O. Smith, J.A. Pardoen, J.M.L. Courtin, J. Lugtenburg, J. Herzfeld, R.A. Mathies, R.G. Griffin, Biochemistry, **24**, 6955 (1985)

CHAPTER 4

A Non-Woodward and Hoffmann Reaction Path for Photochemical Sigmatropic Rearrangements

4.1 Introduction

As well as indicating the general importance of the Woodward and Hoffmann concept[1] for the qualitative description of electrocyclic reactions under thermal and photochemical conditions, the determination of potential energy surfaces is of great importance for the description of a chemical reaction.

Concerning thermal reactions, qualitative theoretical treatments based on orbital symmetry considerations[2] are found to be quite successful in interpreting the stereochemical course of electrocyclic reactions[3]. On the whole, this may be attributed to the fact that for thermal reactions the highest occupied molecular orbital contains the two electrons most easily accessible during the reaction.

However, in relation to photochemical reactions, it may be questioned why a photo-induced reaction should be completely governed by the symmetry of a singly occupied molecular orbital. Besides the activation energy, the possibility for a radiationless transition from a well on the potential energy surface dominates the photochemical and photophysical behaviour of a molecule after excitation.

This was nicely demonstrated by van der Lugt and Oosterhoff[4] with a complete π-electron MO and VB calculation for the disrotatory ring opening - ring closure of the cyclobutene - *cis*-butadiene system in the excited state, which is controlled by a favourable symmetric excited state. This state has a well on the potential energy surface at a geometry corresponding with a barrier on the potential energy surface of the ground state, as a result of an avoided crossing between these two states. At this point an internal conversion is possible after which the reaction ends in the ground state.

By means of semi-empirical MNDO calculations with a limited (3x3) CI it was shown[5] that for the photochemical [1,3]-OH shift in 2-propen-1-ol the relaxation of the excited double bond towards a minimum on the excited state surface determines the course of the photochemical process rather than the route controlled by orbital symmetry. The mechanism for this planar sigmatropic shift is depicted in Figure 1.

Upon excitation of 2-propen-1-ol (I) an electron is promoted from a bonding to an antibonding π-MO. In order to diminish the repulsion between the two antibonding p-orbitals, a twisting of the double bond occurs. In an

unsymmetrically substituted alkene like 2-propen-1-ol, this twist will be accompanied by a more or less complete separation of charge in the orthogonal structure. This phenomenon is known as the "sudden polarization" effect, which was first theoretically described by Salem and coworkers[6].

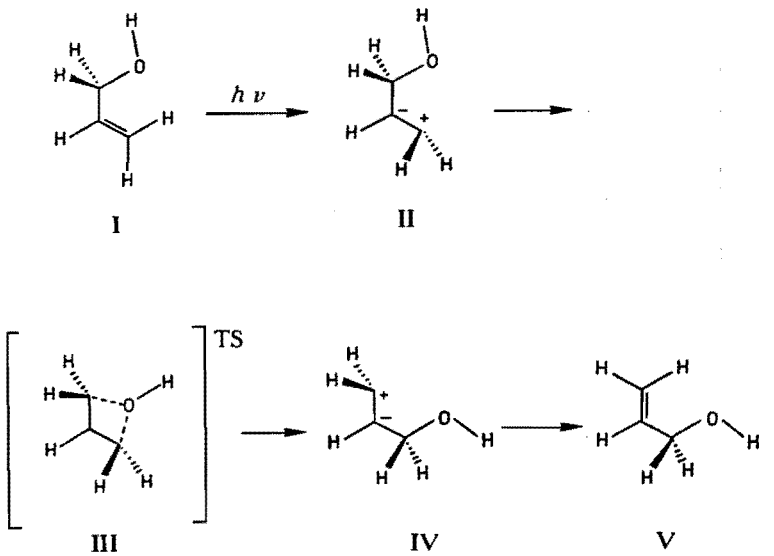

Figure 1. The proposed mechanism for the photochemical planar [1,3]-OH shift in 2-propen-1-ol.

For 2-propen-1-ol this polarization leads to a positive charge on the terminal carbon atom and a negative charge on the central carbon atom (II). The OH-group, which has a partially negative charge, may now shift towards the positively charged terminus *in* the plane of the carbon atoms via a transition state of C_{2v}-symmetry (III). After a radiationless transition from a second twisted conformation (IV) the reaction proceeds on the ground state potential surface towards the shifted product (V).

In this chapter, this mechanism is elaborated for the photochemical [1,3] sigmatropic shifts in propene and 1-butene and the photochemical [1,5] shifts in 1,3-pentadiene and 1,3-hexadiene.

4.2 Method of Calculation

The standard MNDO program package[7a] has been used. The method is described in detail elsewhere[7b]. Only the main features will be repeated here.

The behaviour of an excited alkene is best described by a CI between the configurations Φ_+^2, Φ_-^2 and $\Phi_+\Phi_-$ where Φ_+ and Φ_- are the bonding and antibonding π-orbitals:

$$\Phi_+ = \frac{a + b}{(2 + 2S_{ab})^{1/2}}$$

$$\Phi_- = \frac{a - b}{(2 - 2S_{ab})^{1/2}}$$

Here, a and b represent the localized $2p$-orbitals on the two carbon atoms of the double bond and S_{ab} the overlap integral between them. The configurations $\Phi_\pm^2$ and $\Phi_+\Phi_-$ are best described by a closed and open shell configuration, respectively. The problem which arises is that the best molecular orbitals for a closed and an open shell configuration are eigenfunctions of different operators, leading to nonorthogonality. With a restricted CI, the use of one operator exclusively may lead to an unbalanced description[8]. Therefore, the MNDO program was adapted with the half electron method[9] in which both ground and excited states can be handled by the same closed shell procedure. A minimal (3x3) CI involving the three configurations mentioned before, mimics well the diradicalar model and, therefore, reproduces the essential features of the excited alkene.

In contrast to ab initio CI calculations (see next chapter) it was possible to perform complete geometry optimizations including (3x3) CI within reasonable computer time. Thus, all geometries were fully optimized, within the symmetry constraints, to a minimal energy with the Davidon-Fletcher-Powell algorithm[10].

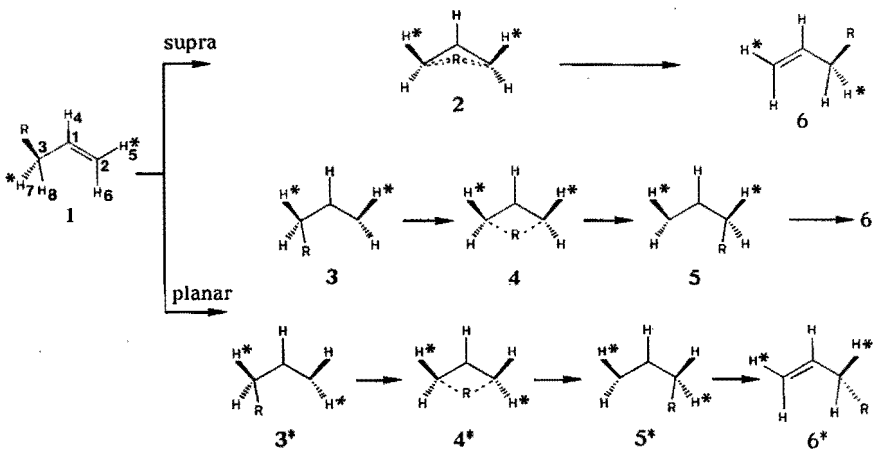

Figure 2. Photochemical suprafacial and planar [1,3]-R shifts in: (a) propene (R = H); (b) 2-propen-1-ol (R=OH) and (c) 1-butene (R=CH_3).

Table 1. Optimized structures and selected atomic charges of the [1,3]-R

	1a	1b	1c	2a	2b	2cR
C2C1	1.432	1.431	1.428	1.416	1.395	1.403
C3C1	1.472	1.482	1.479	1.416	1.395	1.403
C3C2C1	125.0	123.0	130.0	121.8	117.4	126.3
H4C1	1.089	1.090	1.093	1.083	1.099	1.101
H4C1C2	118.0	122.4	116.0	119.1	119.7	116.9
H4C1C2C3	180.0	180.0	180.0	180.0	180.0	159.7
H5C2	1.083	1.088	1.083	1.085	1.087	1.086
H5C2C1	120.0	120.1	122.2	122.6	120.6	121.2
H5C2C1C3	180.0	180.0	180.0	-157.3	-155.2	-173.9
H6C2	1.083	1.084	1.083	1.090	1.090	1.087
H6C2C1	120.0	123.9	122.2	121.7	124.9	124.0
H6C2C1C3	0.0	0.0	0.0	32.6	37.3	16.3
H7C3	1.116	1.132	1.124	1.085	1.087	1.086
H7C3C1	110.9	109.2	107.2	122.6	120.6	121.2
H7C3C1C2	121.0	123.4	124.4	157.3	155.2	173.9
H8C3	1.116	1.132	1.124	1.090	1.090	1.087
H8C3C1	110.9	109.2	107.2	121.7	124.9	124.0
H8C3C1C2	-121.0	-123.4	-124.4	-32.6	-37.3	-16.3
RC3	1.110	1.397	1.533	1.640	2.184	2.283
RC3C1	113.7	113.1	121.0	55.6	77.5	63.3
RC3C1C2	0.0	0.0	0.0	49.6	44.6	68.5
qC1	-0.138	-0.114	-0.123	-0.067	0.020	0.034
qC2	-0.075	-0.069	-0.071	0.045	-0.018	-0.075
qC3	0.070	0.202	0.026	0.045	-0.018	-0.075
qR	-0.003	-0.140	0.018	-0.229	-0.230	-0.112

Distances are in Å, angles and dihedral angles in degrees and atomic charges in eu. The
of configuration, respectively.

4.3 Results and Discussion

For the [1,3] sigmatropic shifts in propene, 2-propen-1-ol, 1-butene (Figure 2 and Table 1) and the [1,5] sigmatropic shifts in 1,3-pentadiene and 1,3-hexadiene (Figure 3 and Table 2) three different reaction routes were investigated, i.e., the suprafacial and antarafacial shifts as considered by Woodward and Hoffmann, and the planar shift (*vide supra*).

The first two reactions were characterized by the energies of the planar excited molecule and the transition states (TSs) of C_s- and C_2-symmetry, respectively. The planar shift was characterized by the excited planar molecule, the 90° twisted structure and the TS of C_{2v}-symmetry.

shifts in: (a) propene (R=H); (b) 2-propen-1-ol (R=OH) and (c) 1-butene ($R=CH_3$)

3a	3b	3c	4a	4b	4cR	4cI
1.356	1.356	1.347	1.427	1.456	1.417	1.448
1.477	1.488	1.486	1.427	1.456	1.417	1.448
128.5	127.8	132.8	89.7	98.2	97.2	111.0
1.095	1.092	1.098	1.059	1.071	1.071	1.081
117.3	117.1	114.8	135.2	130.9	131.4	124.5
180.0	180.0	180.0	180.0	180.0	180.0	180.0
1.102	1.103	1.108	1.105	1.113	1.108	1.104
120.0	125.1	125.7	122.2	121.8	120.8	121.4
-90.0	-90.0	-90.0	-102.4	-108.9	-107.1	-109.8
1.102	1.103	1.108	1.105	1.113	1.108	1.104
120.0	125.1	125.7	122.2	121.8	120.8	121.4
90.0	90.0	90.0	102.4	108.9	107.1	109.8
1.112	1.127	1.117	1.105	1.113	1.108	1.104
111.5	110.2	108.4	122.2	121.8	120.8	121.4
120.1	122.1	123.1	102.4	108.9	107.1	109.8
1.112	1.127	1.117	1.105	1.113	1.108	1.104
111.5	110.2	108.4	122.2	121.8	120.8	121.4
-120.1	-122.1	-123.1	-102.4	-108.9	-107.1	-109.8
1.113	1.404	1.537	1.389	1.508	1.848	1.751
121.4	110.7	117.6	88.7	84.0	76.5	81.5
0.0	0.0	0.0	0.0	0.0	0.0	0.0
-0.984	-0.947	-0.946	-0.988	-0.994	-0.977	-0.986
0.814	0.829	0.808	0.407	0.377	0.348	0.168
0.117	0.249	0.076	0.407	0.377	0.377	0.223
0.006	-0.146	0.015	0.065	0.192	0.065	0.066

numbers refer to Figure 2, R and I to the reactions with retention and inversion

For the [1,3] shifts no antarafacial migrations were calculated. For the suprafacial and planar C-shifts a reaction with retention (R) and a reaction with inversion (I) of configuration on the *p*-orbital of the migrating CH_3 were investigated (Figure 4). The calculated energies are given in Table 3.

In order to get an impression about the activation energy of the photochemical shifts, one-dimensional energy curves were calculated[11]. For the planar shift the energy of the first excited singlet state was calculated as a function of the twist around the double bond. A separation of charge develops along the twist coordinate, resulting in a negative charge on the central carbon atom and a positive charge on the terminal carbon atom for all reactions. The planar shift was calculated starting from the 90° twisted geometry.

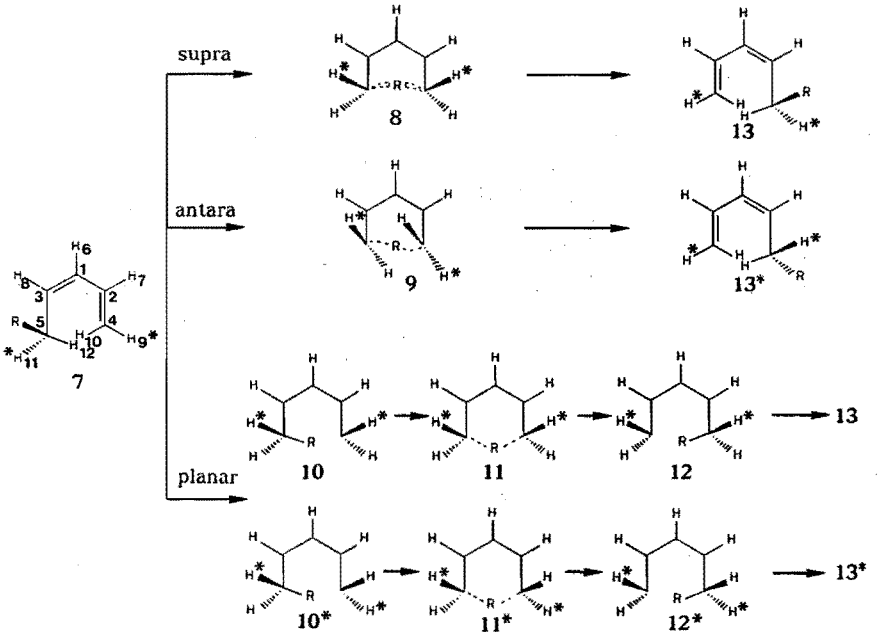

Figure 3. Photochemical suprafacial, antarafacial and planar [1,5]-R shifts in: (a) 1,3-pentadiene (R=H) and (b) 1,3-hexadiene (R=CH_3).

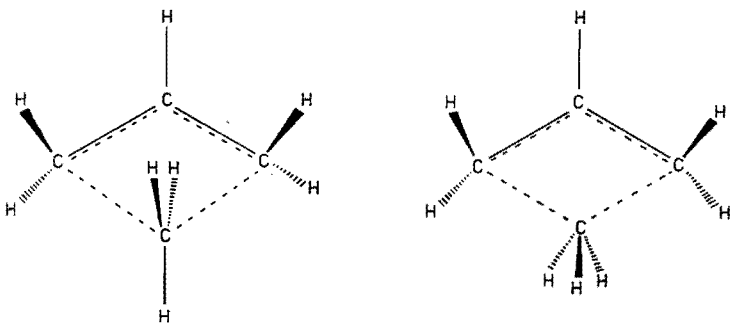

Figure 4. Planar transition states for the photochemical [1,3]-C shifts with inversion (left hand side) and retention (right hand side) of configuration in 1-butene.

Table 2: Optimized structures and selected atomic charges of the [1,5]-R shifts in: (a) 1,3-pentadiene (R=H) and (b) 1,3-hexadiene ($R=CH_3$)

	7a	7b	9a	10a	10b	11a	11bR	11bI
C2C1	1.416	1.416	1.407	1.442	1.437	1.391	1.378	1.392
C3C1	1.406	1.406	1.407	1.350	1.346	1.391	1.378	1.392
C3C1C2	131.7	135.1	125.3	130.1	135.4	121.2	121.6	128.0
C4C2	1.381	1.377	1.405	1.375	1.370	1.444	1.452	1.465
C4C2C1	128.7	130.7	126.7	126.9	130.5	121.8	126.6	126.6
C5C3	1.474	1.481	1.405	1.490	1.495	1.444	1.452	1.465
C5C3C2	134.9	142.2	126.7	131.7	138.8	121.8	126.6	126.6
H6C1	1.098	1.101	1.094	1.097	1.101	1.088	1.088	1.093
H6C1C2	114.2	112.5	117.3	112.6	109.9	119.4	119.2	116.0
H7C2	1.098	1.100	1.100	1.095	1.101	1.087	1.093	1.091
H7C2C1	114.9	113.8	115.8	116.5	115.5	121.1	120.4	119.1
H8C3	1.100	1.105	1.100	1.097	1.103	1.087	1.093	1.091
H8C3C1	113.4	110.6	115.8	116.9	113.5	121.1	120.4	119.1
H9C4	1.085	1.084	1.111	1.101	1.101	1.105	1.113	1.112
H9C4C2	123.4	123.4	125.8	124.2	124.2	119.0	112.9	115.6
H9C4C2C1	180.0	180.0	54.7	90.0	90.0	109.2	117.7	117.3
H10C4	1.085	1.084	1.077	1.101	1.101	1.105	1.113	1.112
H10C4C2	123.4	123.4	120.9	124.2	124.2	119.0	112.9	115.6
H10C4C2C1	0.0	0.0	-125.3	-90.0	-90.0	-109.2	-117.7	-117.3
H11C5	1.112	1.126	1.077	1.112	1.112	1.105	1.113	1.112
H11C5C3	112.2	105.9	120.9	112.1	106.9	119.0	112.9	115.6
H11C5C3C1	-120.6	-124.8	-125.3	-119.9	-123.7	-109.2	-117.7	-117.3
H12C5	1.112	1.126	1.111	1.112	1.119	1.105	1.113	1.112
H12C5C3	112.2	105.9	125.8	112.1	106.9	119.0	112.9	115.6
H12C5C3C1	120.6	124.8	54.7	119.9	123.7	109.2	117.7	117.3
RC5	1.112	1.525	1.527	1.112	1.523	1.330	1.750	1.697
RC5C3	112.0	125.6	95.7	112.1	122.7	104.8	120.0	106.0
qC1	-0.041	-0.034	-0.189	-0.005	-0.004	-0.032	-0.034	-0.043
qC2	-0.062	-0.062	0.268	-0.633	-0.628	-0.552	-0.524	-0.554
qC3	-0.111	-0.097	0.268	-0.450	-0.430	-0.552	-0.524	-0.554
qC4	-0.064	-0.064	-0.446	0.819	0.818	0.417	0.249	0.236
qC5	0.074	0.032	-0.446	0.071	0.026	0.417	0.249	0.236
qR	-0.007	0.023	0.109	-0.006	0.018	0.052	0.407	0.518

Distances are in Å, angles and dihedral angles in degrees and atomic charges in eu. The numbers refer to Figure 3, R and I to the reactions with retention and inversion of configuration, respectively.

4.3.1 Propene

The excitation energy for the relaxed planar geometry was calculated to be 130.9 kcal/mol. The experimental value for the vertical transition energy is 166 kcal/mol[12]. The difference between the calculated and the experimental energy of almost 35 kcal/mol can be attributed to the systematic underestimation of vertical excitation energies by MNDO[13] and to the fact that the excited planar molecule is geometrically optimized.

Relaxation of the torsional angle for the double bond delivers a 33.4 kcal/mol stabilization. The twist results in a negative charge on the central carbon atom

Table 3: Calculated energies[a] of the relaxed planar excited molecules, the 90° twisted conformations and the possible transition states

	1	2	3	4	7	8	9	10	11
Propene	130.9	126.3	97.5	132.9					
2-Propen-1-ol	131.5	142.9	92.5	109.6					
		R 137.4		R 158.0					
1-Butene	135.5		95.5						
		I (b)		I 189.7					
1,3-Pentadiene					111.3	(b)	137.6	89.9	99.3
						R (b)			R 159.8
1,3-Hexadiene					113.0		(c)	89.7	
						I (b)			I 140.6

[a] Energies are in kcal/mol relative to the fully relaxed ground state. R and I refer to the reactions with retention and inversion of configuration, respectively. [b] Geometry optimization gave the corresponding planar transition state. [c] Not calculated.

and a positive charge on the terminal carbon atom. The direction of the polarization is opposite to that calculated by Bonačić-Koutecký et al.[14]. This contradiction might be explained by considering also the second excited singlet state. This state has an opposite polarization (see chapter 2) and it lies close in energy to the first excited state of the twisted molecule. Only a slight change in geometry[15] may cause a crossing between these states leading to a change in the direction of the charge separation.

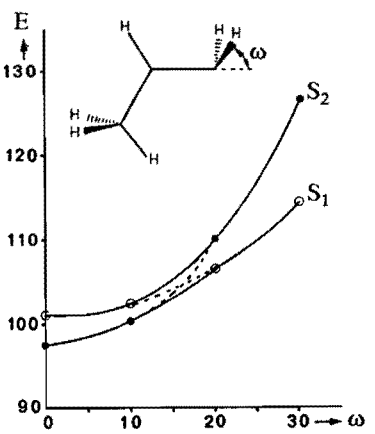

Figure 5. Energy (kcal/mol) of the first two singlet excited states in 90° twisted propene *versus* the pyramidalization angle ω (in degrees).

This is demonstrated by a calculation of the energy of the first two singlet excited states as a function of the pyramidalization angle (ω) of the CH_2-fragment (see Figure 5). The two curves show an avoided crossing near ω = 15°. For larger values of the pyramidalization angle, the negative charge is located on the developing sp_3-orbital of the terminal carbon atom.

As can be seen from Table 3, the suprafacial TS is energetically favoured over the planar TS by 6.6 kcal/mol. However, a calculation of the energy surface showed that the suprafacial shift exhibits an energy barrier somewhere between the initially excited molecule an the supposed TS[16]. The height of this energy barrier could not be calculated exactly, since the SCF calculation showed convergence problems near this maximum. This is caused by the fact that for a suprafacial shift the double bond requires an almost planar conformation, whereas a twisted conformation is energetically favoured in the excited state. The approximated energy barrier amounts to 30 kcal/mol. The activation enthalpy for the planar reaction is 35.4 kcal/mol relative to the 90° twisted structure. In contrast to the former reaction, the planar TS is a real TS since it is a maximum in relation to the reaction coordinate, while all other coordinates are geometrically relaxed.

4.3.2 2-Propen-1-ol

For the [1,3]-OH shift in 2-propen-1-ol the planar shift is strongly favoured over the suprafacial shift. The activation enthalpy for the latter reaction was estimated by calculating the energy as a function of a number of geometries obtained by a linear interpolation between the geometries of the vertically excited molecule and the "TS"[5,16], The calculated energy barrier was 56.8 kcal/mol.

The planar shift is initiated by the relaxation of the molecule towards a twisted conformation which delivers 39.0 kcal/mol. The partially negatively charged hydroxyl group now shifts towards the postively charged terminus. The activation enthalpy for this planar shift is only 17.1 kcal/mol.

4.3.3 1-Butene

For both the suprafacial and planar [1,3]-C shifts, the two TSs which show retention and inversion of configuration were considered (Figure 4). It was not possible to find a TS for the suprafacial shift with inversion of configuration. Optimization of the geometry led to the planar TS which indicates that the suprafacial TS is energetically unfavourable compared to the

planar one.

For the reaction with retention of configuration, the suprafacial "TS" is more stabilized than the planar TS (137.4 kcal/mol *versus* 158.0 kcal/mol). Again the suprafacial shift exhibits a maximum located at another geometry than the supposed TS (*vide supra*).

Concerning the two possibilities for the configuration of the migrating CH_3-group, it was found that the reaction with retention of configuration has a lower activation enthalpy than the reaction with inversion of configuration (158.0 kcal/mol *versus* 189.7 kcal/mol). This is in agreement with experimental findings[17].

4.3.4 1,3-Pentadiene

Going from the 2π-electron system to the 4π-electron system, the gain in energy due to relaxation of the molecule towards the twisted geometry is reduced from 35-40 kcal/mol to 20-25 kcal/mol (Table 3). This difference is caused by a reduction of the vertical excitation energy[18] ($\approx$ 21 kcal/mol) while the extra stabilization due to the delocalization of the negative charge in the larger π-fragment is much smaller ($\approx$ 6.5 kcal/mol)[19].

The deviation of the concept of Woodward and Hoffmann is most striking for the [1,5]-H shift in 1,3-pentadiene. Orbital symmetry considerations predict an antarafacial shift in which the migrating hydrogen atom passes through the plane of the carbon skeleton. For reasons of sterical hindrance this shift is expected to have a high activation energy and is, therefore, unlikely to occur. However, this is in contradiction with the experiments which show that photochemical [1,5]-H shifts, of so far unknown stereochemistry, occur frequently in open, but not in cyclic systems[1].

These findings may be explained by considering a planar shift. The calculations show that the antarafacial TS is located at 26.3 kcal/mol above the relaxed planar excited molecule. Relaxation of the terminal double bond delivers 21.4 kcal/mol. From the twisted geometry a photochemical [1,5]-H shift is possible which only demands a 9.4 kcal/mol activation enthalpy, while the energy of the TS is still considerably lower (12 kcal/mol) than the energy of the initially excited molecule.

4.3.5 1,3-Hexadiene

As for the [1,3]-C shift in 1-butene, the reactions with retention and inversion of configuration were compared for the [1,5]-C shift in 1,3-hexadiene.

For both reactions in the suprafacial way, geometry optimization led to the planar TS. This indicates that for the [1,5]-C shift both reactions appear to proceed in a planar fashion after relaxation of the terminal double bond.

In contrast to the [1,3]-C shift, the [1,5]-C migration with inversion of configuration is lower in energy than the corresponding one with retention of configuration (140.6 kcal/mol *versus* 159.8 kcal/mol). Again, this is in agreement with experimental findings[17].

4.4 Summary

After excitation of the molecule a suprafacial (or antarafacial) shift may take place as shown in Figure 6. Contrary to expectations, the TS of this reaction is located somewhere between the initially excited molecule and the supposed symmetric TS. After the energy barrier has been passed, an internal conversion may occur for the symmetric conformation. The reaction then ends in the ground state.

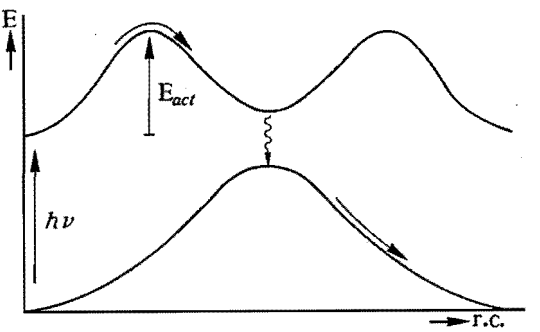

Figure 6. Potential energy curve of the ground and first excited singlet state for a photochemical suprafacial shift.

Strongly competitive with this mechanism is the relaxation of the double bond towards a twisted geometry. As can be seen from Figure 7, this twisted conformation is an intermediate from which a radiationless transition may occur resulting in the formation of the (isomerized) reactant.

Alternatively, the molecule may undergo a photochemical rearrangement. In contrast to the former reaction, the symmetric conformation now is a real TS. To get the product, the internal conversion must take place from a second twisted conformation, after the TS has been passed (Figure 7). The activation enthalpy for this type of reaction is considerably smaller than for the corresponding suprafacial reaction.

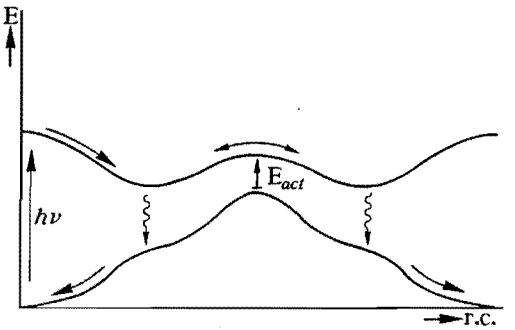

Figure 7. Potential energy curve of the ground and first singlet excited state for a photochemical planar shift.

The stereochemical outcome of the photochemical reaction is essentially different for the planar shift. As can be seen from Figures 2 and 3, the suprafacial and antarafacial shift result in a transfer of chirality. However, so far efforts have failed to find this transfer in acyclic systems[20]. This was explained by assuming that *cis-trans* isomerization is faster than the photochemical shift. The *cis-trans* isomerization is known to proceed via a twisted conformation from which a planar shift may take place. Leaving out possible steric restrictions, the twisting motion may take place in two opposite directions, thus accounting for the scrambling of the chirality at the terminal carbon atoms (see Figures 2 and 3).

The stereochemical fate of the migrating CH_3-group was found to be in agreement with the experiments[20]. For photochemical rearrangements in cyclic systems, the planar shift may become less favourable due to the constraints within the ring system which prevent a twist around the double bond.

4.5 Conclusions

For the photochemical rearrangements in acyclic conjugated alkenes the planar mechanism described in this chapter offers an interesting alternative to the Woodward and Hoffmann mechanism. Activation enthalpies for this type of reactions are calculated to be smaller than the corresponding activation enthalpies for the reactions as considered by the conservation of orbital symmetry. The known experimental results are in agreement with this.

4.6 References and Notes

1 R.B. Woodward, R. Hoffmann, J. Am. Chem. Soc., **87**, 395, 2046 (1965)

2 K. Fukui, Acc. Chem. Res., **4**, 57 (1971)

H.E. Zimmermann, Acc. Chem. Res., **5**, 393 (1975)

M.J.S. Dewar, Angew. Chem., Int. Ed. Engl., **10**, 761 (1971)

3 G.G. Gill, Q. Rev. (London), **22**, 338 (1968)

T.L. Gilchrist, R.C. Storr in "Organic Reactions and Orbital Symmetry", Cambridge University Press, Cambridge (1972)

4 W.Th.A.M. Van der Lugt, L.J. Oosterhoff, J. Am. Chem. Soc., **91**, 6042 (1969)

5 H.R. Fransen, Thesis, Eindhoven (1983)

G.J.M. Dormans, H.R. Fransen, H.M. Buck, J. Am. Chem. Soc., **106**, 1213 (1984)

6 V. Bonačić-Koutecký, P. Bruckmann, P. Hiberty, J. Koutecký, C. Leforestier, L. Salem, Angew. Chem., Int. Ed. Engl., **14**, 575 (1975)

L. Salem, Acc. Chem. Res., **12**, 87 (1979)

7a MNDO: W. Thiel, Q.C.P.E., **11**, 353 (1978)

7b M.J.S. Dewar, W. Thiel, J. Am. Chem. Soc., **99**, 4899 (1977)

8 L. Salem, C. Leforestier, G. Segal, R. Wetmore, J. Am. Chem. Soc., **97**, 479 (1975)

9 M.J.S. Dewar, J.A. Hashmall, C.G. Venier, J. Am. Chem. Soc., **90**, 1953 (1968)

10 W.C. Davidon, Comput. J., **10**, 406 (1968)

R. Fletcher, Comput. J., **8**, 33 (1965)

R. Fletcher, M.J.D. Powell, Comput. J., **6**, 163 (1963)

11 To describe a reaction path, the central carbon atom was placed on the x-axis and the outside carbon atoms on the y-axis. The y-coordinate of the migrating atom (group) was chosen as the reaction coordinate (r.c.) whereas its x- and z-coordinate were optimized.

12 M.B. Robin in "Higher Excited States of Polyatomic Molecules", Academic Press, New York (1974)

13 A. Schweig, W. Thiel, J. Am. Chem. Soc., **103**, 1425 (1981)

14 V. Bonačić-Koutecký, L. Pogliani, M. Persico, J. Koutecký, Tetrahedron, **38**, 741 (1982)

15 The optimized bond length for the twisted double bond is 1.356 Å, whereas Bonačić-Koutecký et al.[14] used a value of 1.416 Å.

16 In fact this supposed TS is an intermediate, but for convenience this kind of geometries are indicated as "TSs" throughout this chapter.

17 J.A. Berson in "Rearrangements in Ground and Excited States", Vol. 1, P. De Mayo (Ed.), Academic Press, New York (1980)

N.D. Epiotis, S.S. Shaik, W. Zander in "Rearrangements in Ground and Excited States", Vol. 2, P. De Mayo (Ed.), Academic Press, New York (1980)

18 An empirical expression for the size dependence of the vertical excitation energy is: $\Delta E = A + B/2n$ where n is the number of conjugated double bonds.

B. Hudson, B. Kohler, Ann. Rev. Phys. Chem., **25**, 437 (1974)

19 This value may be compared with the results of Nebot-Gil and Malrieu who calculated this stabilization to be 4 kcal/mol.

I. Nebot-Gil, J.-P. Malrieu, J. Am. Chem. Soc., **104**, 3320 (1982)

20 R.F.C. Brown, R.C. Cookson, J. Hudec, Tetrahedron, **24**, 3955 (1968)
R.C. Cookson, J. Hudec, M. Sharma, J. Chem. Soc., Chem. Commun., 107,108 (1971)
M. Sharma, J. Am. Chem. Soc., **97**, 1153 (1975)

CHAPTER 5

An Ab Initio CI Study on the Role of C_{2v}-Transition States in Thermal and Photochemical Sigmatropic Shifts

5.1 Introduction

Sigmatropic shifts are an example of the general class of pericyclic reactions, which can be qualitatively described with orbital symmetry considerations[1]. They are assumed to proceed along a suprafacial or antarafacial reaction path depending on the symmetry of the HOMO. When the migrating group (atom) is bonded to the π-system with a p-orbital, the reaction may take place either with retention or inversion of configuration of the migrating group. For reactions in which the product and the reactant are identical, the suprafacial and antarafacial reactions pass through a transition state (TS) of C_s- or C_2-symmetry, respectively.

However, Kwart et al.[2a] proposed a TS of C_{2v}-symmetry for the thermal [1,5]-H shift in 1,3-pentadiene, based on the experimental work of Roth and König[3]. In the preceding chapter, such C_{2v}-structures were proposed as possible TSs for photochemical sigmatropic rearrangements[4,5] on the basis of semiempirical calculations (MNDO with (3x3) CI). This idea originated from the observation that the primary photoprocess for an alkene is the relaxation of the excited double bond towards a twisted structure. From this geometry a planar shift may take place through a TS of C_{2v}-symmetry.

In this chapter, calculations are presented at the ab initio level with inclusion of CI among the leading configurations while treating the other configurations through a second order perturbation. The importance of CI is stressed on the basis of qualitative MO diagrams, after which the results of the calculations are presented and discussed.

5.2 MO Considerations

The MOs for the [1,3]-H shift in propene and the [1,5]-H shift in *cis*-1,3-pentadiene can be constructed from the interaction of the 1*s* AO of the hydrogen atom and the MOs of the allyl and pentadienyl radicals. For the suprafacial and antarafacial shifts in propene this leads to the MO diagrams shown in Scheme 1.

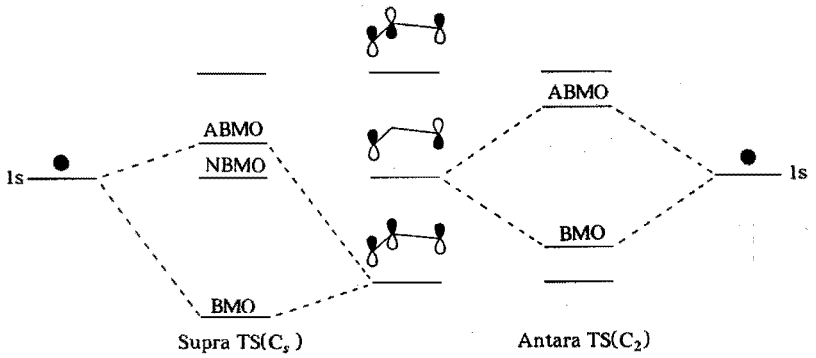

Scheme 1

As can be seen from this scheme, the thermal antarafacial TS is strongly stabilized since the HOMO is a bonding MO (BMO). For the excited state an electron is promoted from a BMO to an antibonding MO (ABMO) which is highly unfavourable. In the case of a suprafacial TS there are two MOs close in energy. Thus, a proper description of this TS should at least involve a CI between the three singlet configurations which can be built up from these two MOs. As these MOs are of the nonbonding MO (NBMO) and ABMO type, a suprafacial TS should be unfavourable for both the thermal and photochemical process.

This is an agreement with the quantumchemical calculations of Bouma et al.[6] and Bernardi et al.[7]. In their calculations, geometry optimization of a suprafacial structure in C_s-symmetry led to a trimethylene-like structure in which the migrating hydrogen atom is bound to the central carbon atom. In fact this structure turns out to be a TS for the disrotation of the two methylene groups and a local minimum for a [1,2]-H shift along the C-C bond.

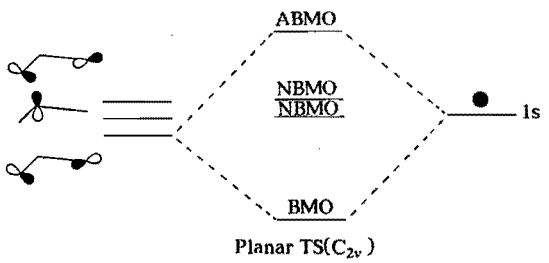

Scheme 2

In summary, a thermal [1,3]-H shift is expected to proceed through an antarafacial TS, which is photochemically "forbidden". The suprafacial TS is

unfavourable in both the thermal and photochemical process.

In the case of a C_{2v}-TS the MO diagram can be constructed from the 1*s* AO of the hydrogen atom and the MOs of a distorted allyl radical in which both methylene groups are twisted around 90° (Scheme 2).

As in the case of a suprafacial TS, CI should be very important in describing the electronic states of this TS. When compared with the thermal antarafacial TS it is seen that the planar TS is less favourable since the electrons are now placed in two nearly degenerate NBMOs. A comparison of the MO diagrams of the suprafacial TS (where the electrons are placed in a NBMO and an ABMO that are nearly degenerate) with the planar TS turns out to be in favour of the latter one in both the thermal and photochemical process. Therefore, a thermal [1,3]-H shift is expected to proceed through an antarafacial TS and the photochemical reaction through a planar TS.

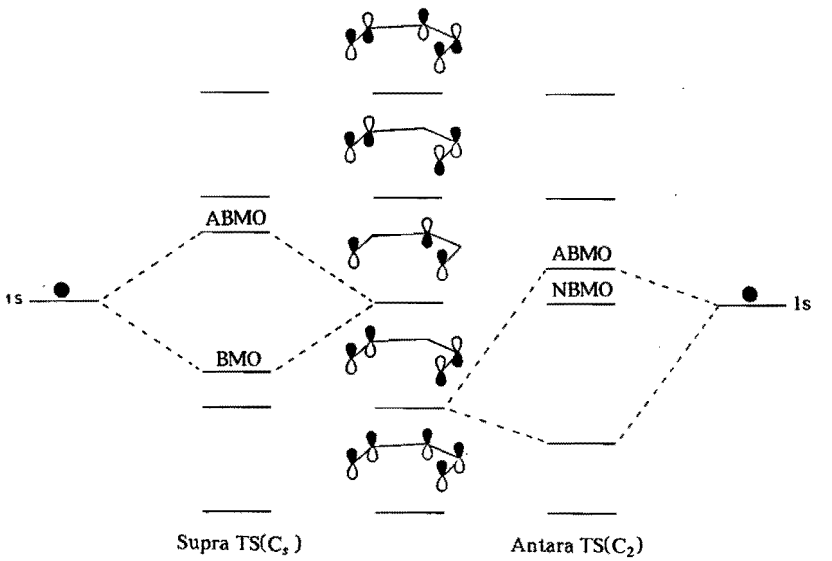

Scheme 3

For the [1,5]-H shift in *cis*-1,3-pentadiene the MO diagrams of the suprafacial and antarafacial TSs are given in Scheme 3 and that of the planar TS in Scheme 4. From the same arguments as for the [1,3]-H shift in propene, it is expected that CI will be important in the description of the electronic states of the antarafacial and planar TSs. Therefore, the calculations of Hess and co-workers[2b], who did not include CI, are misleading (*vide infra*).

A comparison of the three MO diagrams for the considered TSs shows that the thermal process will proceed via a suprafacial TS whereas the photochemical process will be controlled by a planar TS.

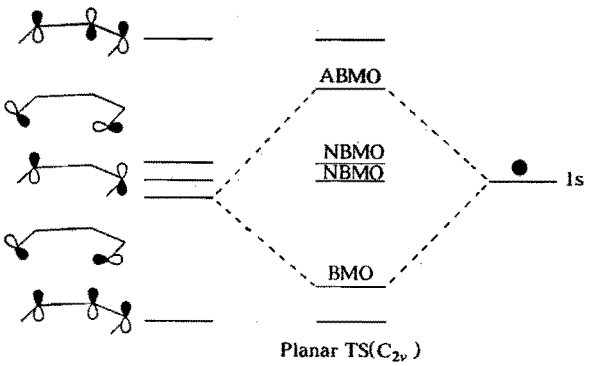

Scheme 4

5.3 Calculational Method

Calculations were performed with the GAUSSIAN 80 program system[8]. Energy optimizations were performed with the 3-21G basis set[9] using the Restricted Hartree-Fock (RHF) Hamiltonian. For open shell states, the Unrestricted Hartree-Fock (UHF) Hamiltonian was used. Structures were fully optimized within the symmetry constraints.

Each optimized structure was characterized by calculating the eigenvalues and eigenvectors of the complete matrix of second derivatives of the energy, which were calculated by finite differences (0.005 au) from analytical first derivatives. Vibrational frequencies and the corresponding normal modes were calculated using the conventional **FG** method[10].

CI calculations were performed from the RHF-MOs for closed shell systems. For open shell systems, the "half-electron" effective Hamiltonian was used[11]. Throughout the calculations the core MOs were kept doubly occupied whereas those virtual MOs with an eigenvalue larger than 1.0 au were excluded. This led to a set of 22 MOs for propene and 32 MOs for pentadiene.

The CI calculations were performed with the SPINCIP program[12], which is a symmetry adapted generalization of the CIPSI (Configuration Interaction by Perturbation of a multiconfigurational wavefunction Selected Iteratively) algorithm[13]. In a first stage, a zeroth order wavefunction was constructed for the three lowest lying singlet states, by a CI between four configurations of the appropriate symmetry, which were selected from a preliminary CI (4M/3R treatment). In a second stage, configurations were selected through a perturbational calculation of all possible configurations with a maximum of six unpaired electrons. Those configurations with a coefficient[14] of $\eta > 0.10$ were used in a second CI. This yielded CI subspaces with a maximum of 50

calculated through a second-order Möller-Plesset (MP2) perturbational approach[15], including up to 5×10^5 determinants for propene and 2×10^6 determinants for pentadiene.

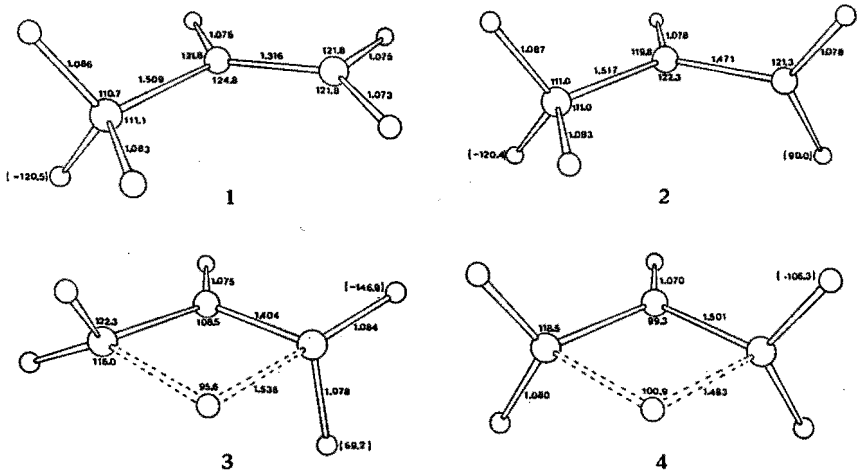

Figure 1. Optimized 3-21G geometries of the starting conformation (**1**, C_s), the twisted structure (**2**, C_s), the antarafacial TS (**3**, C_2) and the planar TS (**4**, C_{2v}) for propene. Dihedral angles (HCCC) are given in parentheses.

Table 1. Energies (au) of the ground state for the characteristic structures of the [1,3]-H shift in propene

	$1(A')^a$	$2(A'')$	$3(A)$	$4(A_2)$
3-21G	-116.424009	-116.358157	-116.252535	-116.264464
6-31G**//3-21G	-117.079943	-117.015931	-116.914644	-116.923074
3-21G/CI-MP2	-116.530101	-116.434483	-116.381575	-116.362452
6-31G**//3-21G/CI-MP2	-117.244206	-117.144277	-117.102676	-117.076099

[a] The symmetry used in the SCF calculation

5.4 Results and Discussion

5.4.1 Thermal [1,3]-H Shift in Propene

For the [1,3]-H shift in propene the geometries were calculated for the reactant (**1**) in C_s-symmetry, a twisted structure (**2**) in C_s-symmetry and two

possible TSs of C_2- (3) and C_{2v}-symmetry (4) (Figure 1). To study the effect of larger basis sets, single point 6-31G** calculations[16] were performed at the 3-21G optimized geometries (see Tables 1 and 2).

Table 2. Relative energies (kcal/mol) of the lowest lying singlet states for the characteristic structures of the [1,3]-H shift in propene.

Structure	State	3-21G/CI-MP2	6-31G**//3-21G/CI-MP2
1	$1A'$	0.0	0.0
	$2A'$	218.6	181.2
	$3A'$	220.9	206.2
2	$1A''$	60.0	62.7
	$1A'$	136.8	128.2
	$2A'$	147.2	140.4
3	$1A$	93.2	88.8
	$1B$	211.7	201.4
	$2A$	236.2	218.2
4	$1A_2$	105.2	105.5
	$1A_1$	169.9	161.6
	$2A_1$	174.8	169.2

Both Hess and co-workers[2b] and Bouma et al.[6] located two TSs for the thermal [1,3]-H shift in propene. The one of C_s-symmetry represents a "forbidden" suprafacial TS and the one of C_2-symmetry an "allowed" antarafacial TS. It was found that both TSs lie close in energy at all levels of computation (see Table 3).

Table 3. Activation energies for the three possible thermal [1,3]-H shifts in propene (energies are in kcal/mol relative to structure **1**).

	Via TS		
	C_s	C_2(3)	C_{2v}(4)
3-21G[a]	-	107.6	100.1
3-21G[b]	119	108	155
4-31G[c]	123.9	111.7	-
6-31G[b]	117	107	154
6-31G*[b]	111	106	143
DZP//4-31G[c]	105.3	103.5	-
6-31G**//3-21G[a]	-	103.7	98.4
3-21G//CI-MP2[a]	-	93.2	105.2
6-31G*/MP2[b]	93	90	137
DZP//4-31G/CEPA[c]	95.6	92.9	-
6-31G**//3-21G/CI-MP2[a]	-	88.8	105.5

[a] This work. [b] Hess et al.[2b]. [c] Bouma et al.[6].

MCSCF calculations by Bernardi et al.[7] showed that at this level of computation the C_2-structure indeed represents a real TS, which can readily be described with only one closed shell RHF configuration. Conversely, the C_s-

structure can not be described with a single configuration. This TS even turns out to be an intermediate for a [1,2]-H shift instead of a TS for a [1,3]-H shift.

Hess has also calculated a structure of C_{2v}-symmetry which he found considerably higher in energy than the C_s-TS (see Table 3). However, Bernardi showed that in this region a diradicalar configuration is lower in energy than the closed shell configuration.

A CI-MP2 analysis of Hess' C_{2v}-structure indeed shows that there is a diradicalar state of A_2-symmetry which is considerably lower in energy than the lowest A_1-state. Therefore, an open shell UHF calculation was performed for this A_2-configuration (structure **4**). The optimized structure is found to be a true TS as it is characterized by a single imaginary frequency (2546i cm^{-1}). A coefficient of 0.96 of the leading configuration in the CI expansion of the wavefunction for this state indicates that the authenticity of this state will remain unchanged at a higher level of computation.

The energy of this state is 98.4 kcal/mol above that of the reactant (**1**) at the 6-31G**//3-21G SCF level which is 5.3 kcal/mol lower than the antarafacial TS. After CI and MP2 this energy ordening is reversed (see Table 3). The imaginary frequency corresponds to a movement of the migrating hydrogen atom in the plane of the carbon skeleton (planar shift) towards one of the terminal carbon atoms. This yields a twisted structure (**2**) for which the lowest energy state is described by an open shell configuration of A''-symmetry (see Table 2). From numerous theoretical studies this conformation is known to be a TS for the thermal *cis-trans* isomerization in propene (which is confirmed by a single imaginary frequency of 779i cm^{-1} which corresponds to a rotation of the twisted methylene group).

A vibrational analysis of Hess' C_{2v}-structure reveals three negative eigenvalues. Therefore, this structure does not represent a TS. When the C_{2v}-constraint is released, this structure is found to optimize towards a structure of C_s-symmetry in which the hybridization of the central carbon atom is changed from sp^2 to sp^3 (see Figure 2). The hydrogen atom bound to this atom is twisted out of the plane of the carbon skeleton by 69.5° whereas this angle for the migrating hydrogen atom is 6.7°.

This structure is characterized by a single imaginary frequency (1102i cm^{-1}) which corresponds with an almost horizontal movement of the migrating hydrogen atom in the direction of one of the terminal carbon atoms. The energy of this TS is 133.7 kcal/mol above that of propene (**1**) at the SCF level and 132.6 kcal/mol after CI and MP2, which is still considerably higher than the energies found for the former two TSs and far above the dissociation limit of propene. The true authenticity of this structure should be confirmed at a higher level of computation.

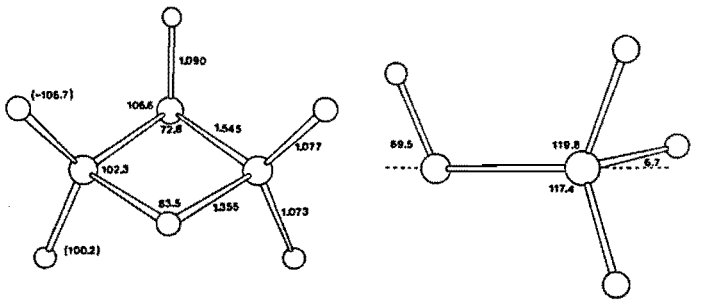

5

Figure 2. Optimized 3-21G geometry of the C_s-structure of propene. Dihedral angles (HCCC) are given in parentheses.

5.4.2 Photochemical [1,3]-H Shift in Propene

In the preceding chapter[4], it was demonstrated by means of semi-empirical calculations that for this excited state process a TS of C_{2v}-symmetry is preferred. From Table 2 it can be seen that the ab initio CI calculations yield a comparable picture, i.e. the energy of the lowest excited state of the planar TS (**4**) is lower than that of the vertically excited propene (**1**). Therefore, this state can easily be reached in the photochemical process. This is not the case for the C_2-structure (**3**) and the C_s-structure (**5**).

It should be mentioned here that Rydberg orbitals were not included in the basis set used in this work. These orbitals are known to play an important role in the description of the vertically excited states in propene. However, Bonačić-Koutecký and co-workers[17] have shown that both the energies and the properties of the lowest excited states of twisted propene (**2**) are not sensitive to the choice of the basis set. No Rydberg states are found in the neighbourhood of the lowest excited states as twisting is highly unfavourable for any excited state containing Rydberg orbitals. As the changes in geometry are small going from structure 2 to structure **4**, it is not expected that the inclusion of Rydberg orbitals for this latter geometry will influence the results significantly.

From Table 2 it is seen that for the planar structure there are two A_1-states which are close in energy. The energy difference with the next excited state is more than 35 kcal/mol. With both basis sets it is found that the $1A_1$-state is mainly described by the doubly excited configuration $(...(6a_1)^2(3b_2)^2)$ in the CI expansion. The $2A_1$-state is mainly described by the closed shell $(...(6a_1)^2(2b_1)^2)$ configuration. Scheme 5 shows the orbital and state

correlation diagram between the structures 2 and 4.

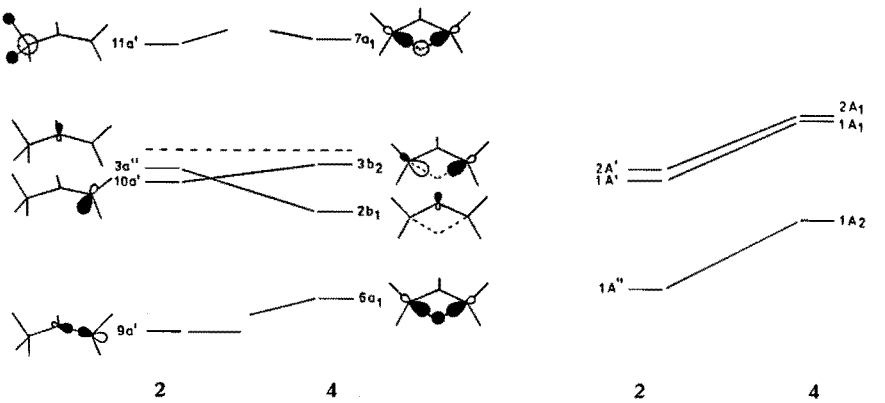

Scheme 5

It is seen that the two excited states mentioned correlate with the two A'-excited states of the twisted propene. These states are known to be ionic. The lowest one has an expansion coefficient of 0.97 for the $(...(9a')^2(10a')^2)$ configuration. This state is thus strongly polarized and bears the negative charge on the twisted methylene group. The polarization in the second excited state is opposite. The energy difference between these two states is 10.4 kcal/mol calculated with the minimal basis set and 12.2 kcal/mol with the extended basis set. The energy gap between the neutral ground state and the first ionic excited state is 76.8 kcal/mol for the smaller basis set and 65.5 kcal/mol for the extended basis set. In their turn the two twisted excited states correlate with the vertical $(\pi-\pi^*)$ and $(\pi-\pi^*)^2$ states of propene via a twist of the double bond.

The photochemical [1,3]-H shift in propene can now be described as follows (see Figure 3). After excitation, the double bond twists in order to avoid the antibonding interaction of the two p-orbitals which form the π-bond. This results in a twisted structure (2) which, in its lowest excited state, bears the negative charge on the twisted methylene group. From Figure 3 it is seen that this structure is an intermediate on the excited state potential energy surface. If the nonadiabatic coupling with the ground state is large enough, a radiationless transition will occur which results in the backformation of the (isomerized) reactant.

Alternatively a photochemical [1,3]-H shift may take place. The energy barrier for this planar shift is 33.4 kcal/mol (extended basis set). This shift leads to a second twisted intermediate from which, through a radiationless transition, the shifted product is formed in its ground state.

All along the planar shift the point group of the reacting molecule is C_s. The ground state has A''-symmetry and the two excited states A'-symmetry (see Table 2). The reaction coordinate Q is described by the motion of the migrating hydrogen atom in the symmetry plane. Therefore, Q and the operator $\partial/\partial Q$

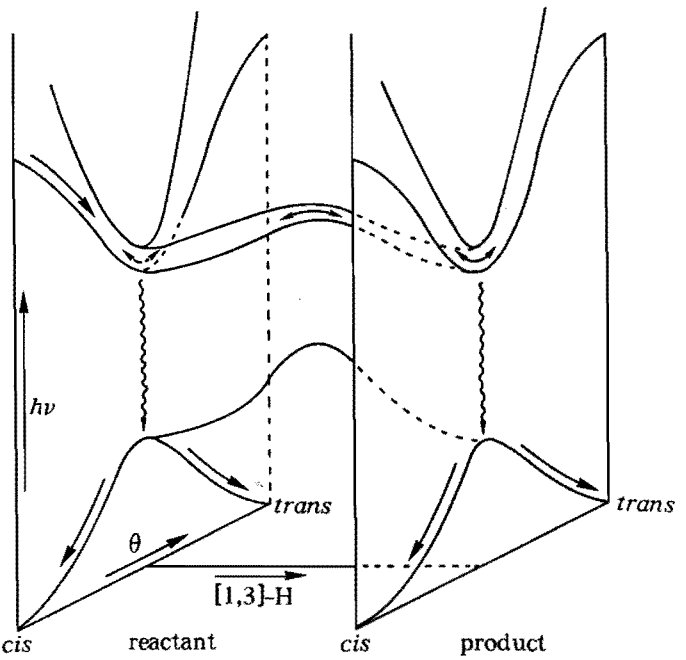

Figure 3. Energy profiles of the three lowest lying singlet states for the [1,3]-H shift in propene.

which couples the potential energy surfaces nonadiabatically (see chapter 1), belong to the A' -representation.

From these symmetry considerations it can be concluded that the coupling $<\psi_K \mid \partial/\partial Q \mid \psi_L>$ between the ground state and the two excited states must equal zero everywhere along the planar shift. No internal conversion can take place during this shift. Of course, a slight change in geometry will destroy these symmetry restrictions and will cause the coupling to be non-zero but, as Galloy and Lorquet [18] have pointed out, this coupling will be small.

During the twist, the operator which couples the potential energy surfaces is $\partial/\partial\theta$, where θ represents the twist angle (see e.g. reference 17 and chapter 2). For the twisted structure (2) this operator belongs to the A'' -representation and, therefore, may induce the radiationless transition from the A' -excited states to the A'' -ground state.

In summary, it is concluded that the photochemical [1,3]-H shift in an acyclic alkene will proceed through a planar shift. This shift will always be accompanied by a *cis-trans* isomerization of the excited double bond.

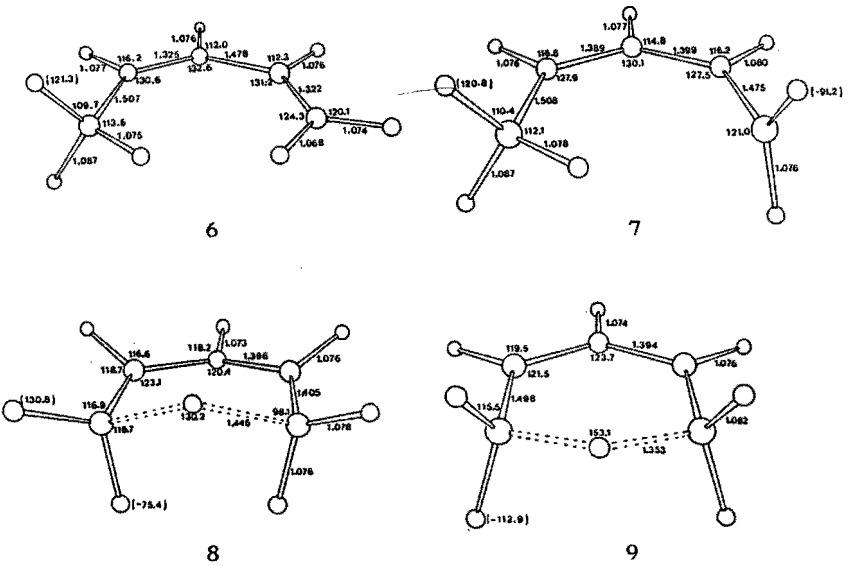

Figure 4. Optimized 3-21G geometries of the starting conformation (**6**, C_s), the twisted structure (**7**, C_s), the suprafacial TS (**8**, C_s) and the planar TS (**9**, C_{2v}) for *cis*-1,3-pentadiene. Dihedral angles (HCCC) are given in parentheses.

5.4.3 Thermal [1,5]-H Shift in *cis*-1,3-Pentadiene

For the [1,5]-H shift in *cis*-1,3-pentadiene the reactant (**6**) in C_s-symmetry, a twisted structure (**7**) in C_s-symmetry and two possible TSs of C_s- (**8**) and C_{2v}-symmetry (**9**) were calculated (see Figure 4 and Tables 4 and 5). Structure **8** is identical with the one found by Hess and co-workers[2b] and Rondan and Houk[2c].

According to orbital symmetry considerations, the thermal [1,5]-H shift in pentadiene is expected to proceed via a suprafacial TS of C_s-symmetry. Kwart et al.[2a] proposed a thermal TS of C_{2v}-symmetry. This structure has been calculated by Hess and Schaad[2b] and found to be of considerably higher energy than the suprafacial TS **8** (see Table 6).

A vibrational analysis for the C_{2v}-structure of Hess, yielded two negative eigenvalues of the force constant matrix. Therefore, this structure cannot represent a real TS. When this structure is released from its C_{2v}-constraints to C_s-constraints, it is found to optimize towards structure **8**. This structure has only one imaginary frequency (1925i cm^{-1}) and, therefore, is a saddle point on the potential energy surface. The corresponding normal mode indeed represents

Table 4. Energies (au) of the ground state for the characteristic structures of the [1,5]-H shift in *cis*-1,3-pentadiene.

	$6(A')^a$	$7(A'')$	$8(A')$	$9(B_1)$
3-21G	-192.869668	-192.833877	-192.792533	-192.793295
3-21G/CI-MP2	-193.064049	-192.990694	-192.983571	-192.962402

[a] The symmetry used in the SCF calculation

Table 5. Relative energies (kcal/mol) of the lowest lying singlet states for the characteristic structures of the [1,5]-H shift in *cis*-1,3-pentadiene.

Structure	State	3-21G/CI-MP2	Structure	State	3-21G/CI-MP2
6	$1A'$	0.0	**8**	$1A'$	50.5
	$2A'$	163.5		$1A''$	160.4
	$3A'$	191.9		$2A'$	190.8
7	$1A''$	46.0	**9**	$1B_1$	63.8
	$2A''$	121.1		$1A_1$	124.3
	$1A'$	121.2		$2A_1$	125.1
	$2A'$	131.7		$1A_2$	142.1

Table 6. Activation energies for the two possible thermal [1,5]-H shifts in 1,3-pentadiene (energies are in kcal/mol relative to structure **6**)

	Via TS	
	C_s (**8**)	C_{2v} (**9**)
3-21G[a]	48.4	47.9
3-21G//CI-MP2[a]	50.5	63.8
3-21G[b]	48.4	116.1
6-31G*//3-21G[b]	52.5	117.5

[a] This work. [b] Hess et al.[2b].

a suprafacial shift. These findings prompted Hess to conclude that the thermal [1,5]-H shift in pentadiene proceeds via a suprafacial TS, despite the findings of Kwart.

However, a CI-MP2 treatment for this C_{2v}-structure showed that the lowest energy singlet state has B_1-symmetry and thus cannot be described properly by a RHF calculation. Therefore, an UHF/3-21G optimization of the B_1-configuration in C_{2v}-symmetry was performed. The SCF energy of this optimized structure (**9**) was found to be lower than the energy of the suprafacial structure (**8**) by 0.5 kcal/mol (see Table 6). This energy ordening is reversed after inclusion of CI and MP2. However, the energy difference is not so large that this structure can be ruled out as a possible TS for the thermal [1,5]-H shift in pentadiene.

The optimized CHC-angle at the migrating hydrogen atom of the C_{2v}-structure is 153.1°, which is still far from the collinear arrangement supposed

by Kwart to explain the temperature dependence of the kinetic isotope effect for this reaction. The vibrational analysis for 9 gave only one imaginary frequency (2206i cm^{-1}) which supports the idea that this structure might be a true TS for the reaction under consideration. The normal mode corresponding to this imaginary frequency shows a planar shift of the migrating hydrogen atom in the plane of the carbon skeleton towards one of the terminal carbon atoms, while leaving the other methylene group twisted.

These findings closely agree with a recent suggestion of Dewar et al.[19] that the thermal [1,5]-H shift in pentadiene might take place via tunneling. However, the difference in geometry between the reactant and the product is too large for tunneling. He suggested that this is not the case for a vibrationally excited form of the reactant in which the terminal double bond is twisted. In the next chapter this suggestion will be elaborated by a calculation of the classical reaction rates, kinetic isotope effects and vibrationally assisted tunneling rates for the reactions via the TSs of C_s- and C_{2v}-symmetry.

5.4.4 Photochemical [1,5]-H Shift in *cis*-1,3-Pentadiene

On the basis of orbital symmetry considerations an antarafacial TS is expected for the photochemical [1,5]-H shift in pentadiene. However, a geometry optimization of such a structure in C_2-symmetry for both the A- and B-configurations with the 3-21G basis set yields a structure of C_{2v}-symmetry. This supports the idea that a photochemical sigmatropic shift in an acyclic alkene proceeds through a TS of C_{2v}-symmetry via a planar shift.

Table 5 shows that the energies of the three lowest lying singlet states of the C_{2v}-structure (9) are considerably lower than the vertically excited states of the reactant (6). As the SCF geometry optimization was performed for the ground state, these energies must be seen as an upper bound for these excited states. This structure is thus easily accessible after excitation of the molecule.

Scheme 6 shows the orbital and state correlation diagrams between the planar TS (9) and the twisted structure (7), which is found to be a TS for the thermal *cis-trans* isomerization of pentadiene. For 9, the lowest excited states have A_1-symmetry. In the CI expansion the $1A_1$-state is mainly described by the closed shell $(...(2b_1)^2(7b_2)^2)$ configuration and correlates with the lowest excited $1A'$-state $(...(3a'')^2(16a')^2)$ of the twisted molecule. The $2A_1$-state is principally built up from the doubly excited $(...(2b_1)^2(2a_2)^2)$ configuration and correlates with the $2A'$-state $(...(3a'')^2(4a'')^2)$ of 7.

Until now there has been a close resemblance with the situation for the photochemical [1,3]-H shift in propene. The first difference is that the barrier on the excited state potential energy surface has almost vanished. A second difference is that there is a third excited state close in energy to the former two excited states. This state may play an important role in the photochemical process as it has the same symmetry as the ground state (*vide infra*).

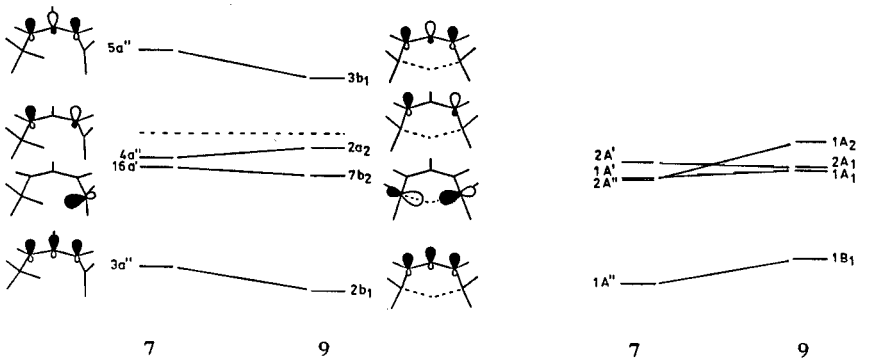

Scheme 6

The CI expansion of the A_2-state of structure 9 is dominated by two configurations with almost equal weights $(0.76(...(2b_1)^2(7b_2)^1(3b_1)^1) + 0.62(...(2b_1)^1(7b_2)^1(2a_2)^2))$. The orbital correlation diagram (Scheme 6) shows that this state is directly correlated with the $2A"$ excited state of the twisted structure. This state is also mainly built up from two configurations $(0.66(...(3a")^2(16a')^1(5a")^1) + 0.52(...(3a")^1(16a')^1(4a")^2))$. Unlike the two ionic states, this latter state is a covalent one. A large amount of theoretical work has been performed to find the energy ordening of these three excited states for the closely related twisted butadiene[20]. This molecule has the same chromophore as 1,3-pentadiene, with the only difference that one hydrogen atom is replaced by a methyl group. It was found that the energy ordening depends on the geometry and calculational details.

The present calculations give the covalent $2A"$-state as the lowest excited state. However, the energy difference with the lowest A'-state is only 0.1 kcal/mol. The energy gap between the two ionic states is larger (10.5 kcal/mol) and in favour of the one with the negative charge on the twisted methylene group. Similar to the case of propene, the two ionic states of twisted pentadiene correlate with the $(\pi-\pi^*)$ and $(\pi-\pi^*)^2$ configurations of the reactant. The covalent $2A"$-state correlates with the $2A'$-state of structure 6 which is predominantly built up from three configurations with almost equal weights. It is closely related to the nonabsorbing $^1A_g^-$-state of linear polyenes, whereas the $3A'$-state is related to the $^1B_u^+$-state of linear polyenes (see chapters 2 and 3). The overall scheme for the planar [1,5]-H shift in *cis*-1,3-pentadiene is given in Figure 6.

After excitation of the diene chromophore, a twist of the terminal double bond is energetically favourable for all three excited states. During the twist there is no symmetry element left in the molecule. Therefore, all three excited states will mix with each other and several avoided crossings may be present (see chapter 2). Moreover, all three excited states may couple nonadiabatically with the ground state.

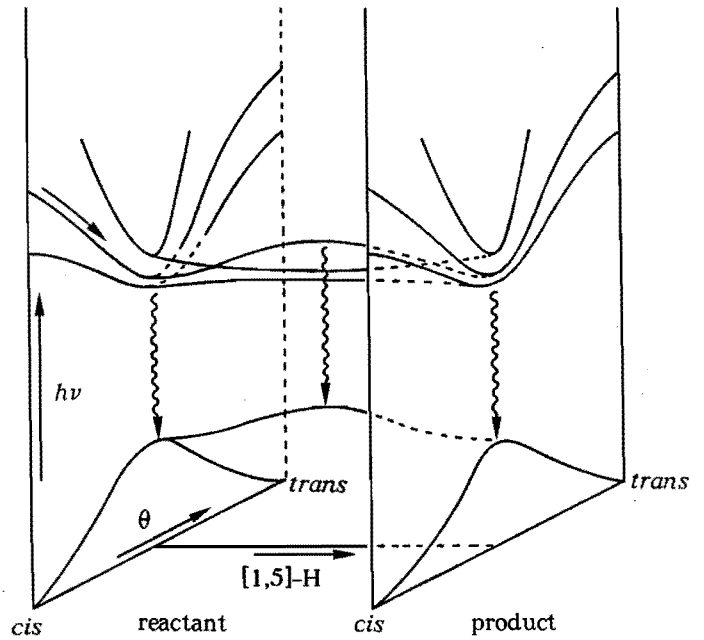

Figure 6. Energy profiles of the four lowest lying singlet states for the [1,5]-H shift in *cis*-1,3-pentadiene

For a twist angle of exactly 90°, the symmetry group of the molecule is C_s. The operator $\partial/\partial\theta$ has A''-symmetry and couples the ground state (A'') with the two ionic A'-states. The coupling $<\psi_K|\partial/\partial\theta|\psi_L>$ equals zero at this point on the reaction coordinate for the two covalent states. Therefore, this twisted structure can only act as a funnel through which a radiationless transition to the ground state may occur for the two ionic states. This would lead to the backformation of the (*cis-trans* isomerized) reactant.

During the planar shift, the ground state and the two ionic states belong to different representations of the molecular point group. The coupling operator $\partial/\partial Q$ has A'-symmetry (see section 5.4.2). Therefore, no internal conversion to the ground state is possible for these excited states. The energy barrier for the planar photochemical [1,5]-H shift is only 3.1 kcal/mol in the first excited state, whereas it is absent for the second symmetric excited state. As seen previously, the transition to the ground state must occur from a twisted structure (before or after the shift) so that the photochemical [1,5]-H shift will always be accompanied by a *cis-trans* isomerization of the double bond, provided that the reaction proceeds via an ionic excited state.

For the covalent excited state the picture is different. The calculated activation energy for a reaction via this state is 21.0 kcal/mol. As the ground state has

the same symmetry, the coupling is non-zero everywhere along the planar shift. Therefore, a radiationless transition from this state is possible anywhere between the two twisted structures. It will depend on the extent of the nonadiabatic coupling where the possibility for an internal conversion is maximal.

5.5 Conclusions

For the thermal [1,3]-H shift in propene and the thermal [1,5]-H shift in *cis*-1,3-pentadiene a TS is found as expected from orbital symmetry considerations, i.e. an antarafacial TS for propene and a suprafacial TS for pentadiene. In both cases there is a second TS of C_{2v}-symmetry which is close in energy. In contrast to the former two TSs, these TSs are described by an open shell configuration.

For the photochemical shifts it is found that the C_{2v}-structure can act as a TS for a planar shift of the hydrogen atom, from one twisted structure to another twisted structure in the plane of the carbon skeleton. On the basis of symmetry considerations for the nonadiabatic coupling of the potential energy surfaces, it is concluded that the photochemical shifts will always be accompanied by a *cis-trans* isomerization of the double bond

For the photochemical [1,5]-H shift in *cis*-1,3-pentadiene the situation is more complicated as there is an excited state of the same symmetry as the ground state, for which an internal conversion is possible during the planar shift of the hydrogen atom.

It is to be expected that this mechanism, which is initiated by a twist of the excited double bond, plays an important role in the photochemistry of acyclic alkenes.

5.6 References and Notes

1 R.B. Woodward, R. Hoffmann, J. Am. Chem. Soc., **87**, 395, 2046 (1965)

2a H. Kwart, M.W. Brechbiel, R.M. Acheson, D.C. Ward, J. Am. Chem. Soc., **104**, 4671 (1982)

2b B.A. Hess, L.J. Schaad, J. Am. Chem. Soc., **105**, 7185 (1983)
B.A. Hess, L.J. Schaad, J. Pančir, J. Am. Chem Soc., **107**, 149 (1985)

2c N.G. Rondan, K.N. Houk, Tetrahedron Lett., **25**, 2519 (1984)

3 W.R. Roth, J. König, Liebigs Ann. Chem., **699**, 24 (1966)

4 G.J.M. Dormans, H.R. Fransen, H.M. Buck, J. Am. Chem. Soc., **106**, 1213 (1984)

G.J.M. Dormans, W.J.G.M. Peijnenburg, H.M. Buck, J. Mol. Struct. (Theochem), **20**, 367 (1985)

5 A similar TS has been proposed by Hoppilliard and Bouchoux for the [1,3] sigmatropic shifts in odd electron ions:

Y. Hoppilliard, G. Bouchoux, Org. Mass. Spectrom., **17**, 534 (1982)

6 W.J. Bouma, M.A. Vincent, L. Radom, Int. J. Quantum Chem., **14**, 767 (1978)

W.R. Rodwell, W.J. Bouma, L. Radom, Int. J. Quantum Chem., **18**, 107 (1980)

7 F. Bernardi, M.A. Rob, H.B. Schlegel, G. Tonachini, J. Am. Chem. Soc., **106**, 1198 (1984)

8 J.S. Binkley, R.A. Whiteside, R. Krishnan, R. Seeger, D.J. DeFrees, H.B. Schlegel, S. Topiol, L.R. Kahn, J.A. Pople, GAUSSIAN 80, Department of Chemistry, Carnegie-Mellon University, Pittsburgh, PA (1980)

9 J.S. Binkley, J.A. Pople, W.J. Hehre, J. Am. Chem. Soc., **102**, 939 (1980)

10 E.B. Wilson, J.C. Decius, P.C. Cross in "Molecular Vibrations", McGraw-Hill, New York (1955)

11 N.C. Baird, R.F. Barr, Theor. Chim. Acta, **36**, 125 (1975)

12 J.F. Gouyet, M.T. Prat, B. Huron, Q.C.P.E., **13**, 376 (1981)

For corrections to this program (SPINCIP) see:

G.J.M. Dormans, M.C.A. Donkersloot, H.M. Buck, Q.C.P.E. Bull., **5**, 14 (1985)

13 B. Huron, J.-P. Malrieu, P. Rancurel, J. Chem. Phys., **58**, 5745 (1973)

14 See chapter 1

15 C. Möller, M.S. Plesset, Phys. Rev., **46**, 618 (1934)

16 P.C. Hariharan, J.A. Pople, Theor. Chim. Acta, **28**, 213 (1973)

17 V. Bonačić-Koutecký, L. Pogliani, M. Persico, J. Koutecký, Tetrahedron, **38**, 741 (1982)

M. Persico, V. Bonačić-Koutecký, J. Chem. Phys., **76**, 6018 (1982)

M. Persico, J. Am. Chem. Soc., **102**, 7839 (1980)

18 C. Galloy, J.C. Lorquet, J. Chem. Phys., **67**, 4672 (1977)

19 M.J.S. Dewar, K.M. Merz Jr., J.J.P. Stewart, J. Chem. Soc., Chem. Commun., 166 (1985)

20 See e.g.:

V. Bonačić-Koutecký, M. Persico, J. Döhnert, A. Sevin, J. Am. Chem. Soc., **104**, 6900 (1982)

I. Nebot-Gil, J.-P. Malrieu, J. Am. Chem. Soc., **104**, 3320 (1984)

J.-P. Malrieu, I. Nebot-Gil, J. Sánchez-Marín, Pure Appl. Chem., **56**, 1241 (1984)

CHAPTER 6

Mechanism of the Thermal [1,5]-H Shift in *cis*-1,3-Pentadiene. Kinetic Isotope Effect and Vibrationally Assisted Tunneling

6.1 Introduction

The thermal [1,5]-H shift in *cis*-1,3-pentadiene is an example of the general class of sigmatropic reactions (see Scheme 1). In 1966, Roth and König[1] studied this reaction in the temperature range of 185-210 °C. They established an activation enthalpy of 35.4 kcal/mol and a kinetic isotope effect (KIE) for $k_H/k_D = 5.1$. The temperature dependence of the KIE was found to be $k_H/k_D = 1.15 \exp(1.4(\text{kcal/mol})/RT)$. From these observations they concluded that the reaction is a concerted process which proceeds through a symmetric pericyclic transition state (TS), thus confirming the predictions based on orbital symmetry considerations.

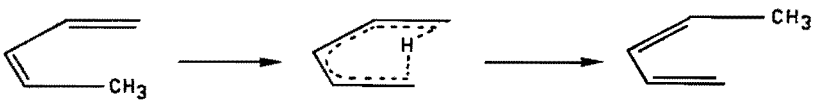

1 2 1'

Scheme 1

Kwart[2] used this temperature dependence of the KIE as a criterion for the geometry of the TS involved. In particular, a temperature independent KIE should be associated with a bent TS. In view of these facts, Kwart et al.[3] concluded that the TS for the [1,5]-H shift in *cis*-1,3-pentadiene must have a collinear arrangement of the migrating hydrogen atom and the two terminal carbon atoms (see Scheme 2).

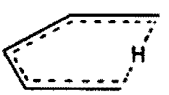

Scheme 2

However, the use of the temperature dependence of the KIE as a mechanistic criterion has been questioned recently[4–6]. It was found[6] that both a linear and a bent TS have a temperature dependent KIE, the latter being somewhat smaller due to the greater sensitivity of the bending vibrations to isotopic substitution. Further indications for a nonlinear TS were given by quatumchemical calculations at the semi-empirical[7,8] and various ab initio[9–11] levels of computation. In all cases, a TS was found with an acute angle at the migrating hydrogen atom.

Hess and Schaad[10] noticed that the collinear TS has C_{2v}-symmetry. They optimized this structure at the RHF/3-21G level and compared it with a bent TS of C_s-symmetry. It was found that the former TS is considerably higher in energy (67.7 kcal/mol). Moreover, the optimized C_{2v}-TS had a distinct angle of 151.9° at the migrating hydrogen atom. A TS with a collinear arrangement would even be higher in energy.

In the preceding chapter it was shown that the lowest energy configuration (ground state) of the C_{2v}-TS has B_1-symmetry and, therefore, cannot be described by a closed shell RHF calculation[12]. In contrast, the ground state of the C_s-TS does have A'-symmetry. So a comparison of these two TSs is incorrect.

All calculated reaction enthalpies [7–12] and KIEs[8,10b] show a large discrepancy with the observed parameters[1]. From these facts, Dewar[8] concluded that quantumchemical tunneling might play an important role in this reaction. However, the geometries of the reactant (**1**) and the product (**1'**) differ too much to make direct tunneling likely (Scheme 3). Therefore, he proposed a mechanism (vibrationally assisted tunneling: VAT) in which tunneling takes place from a twisted form of the reactant (**3**) to a twisted form of the product (**3'**) via a TS of C_s-symmetry. The only geometrical change involved then is the position of the migrating hydrogen atom. Dewar's MINDO/3 calculations showed that the [1,5]-H shift should proceed dominantly via VAT in the temperature range of 185-210 °C.

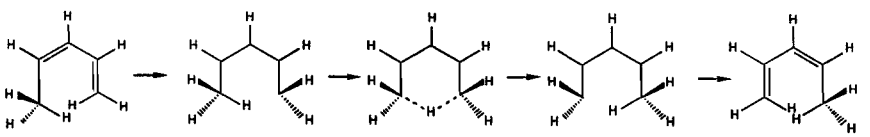

Scheme 3

In this chapter both TSs of C_{2v}- and C_s-symmetry are compared by an appropriate SCF geometry optimization with the 3-21G basis set. A complete vibrational analysis is presented from which the KIE and VAT tunneling rates are calculated. The difference between the two TSs is best accentuated for the tunneling mechanism, which is most likely to proceed via the TS of C_{2v}-symmetry.

6.2 Calculational Method and Results

Calculations were performed with the GAUSSIAN 80 program system[13]. The relevant structures **1**, **2a**, **2b**, and **3** were fully optimized with the 3-21G basis set[14], using the RHF Hamiltonian for the closed shell structures **1** and **2a** and the UHF Hamiltonian for the open shell structures **2b** (B_1-symmetry) and **3** (A''-symmetry). The resulting geometries and energies are given in Figure 1. Hess and Schaad[10] found that the geometries for similar sigmatropic shifts are almost unaffected by the size of the basis set used. So the 3-21G structures were not reoptimized with a larger basis set.

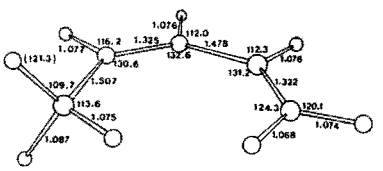

E = -192.869668 au

1

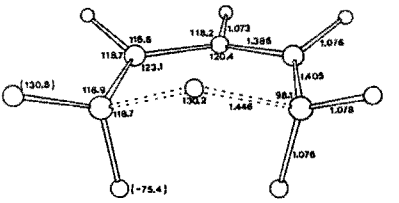

E = -192.793295 au

2a

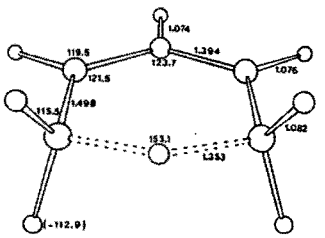

E = -192.792533 au

2b

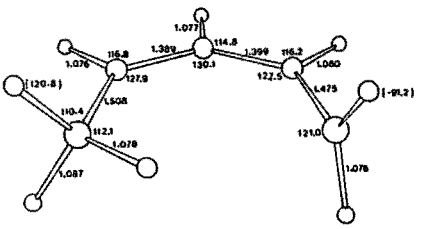

E = -192.833877 au

3

Figure 1. 3-21G optimized structures and energies of the reactant (**1**), the transition states of C_s-symmetry (**2a**) and C_{2v}-symmetry (**2b**), and the twisted reactant (**3**).

The bare potential energy barriers for the reactions via **2a** and **2b** are 48.4 and 47.9 kcal/mol, respectively. This difference might be affected by larger basis sets and calculations at a higher level of theory (configuration interaction and perturbation treatment[12]). However, as the vibrational analysis was performed at the 3-21G geometries, it was consistent to use the corresponding energies in the rest of the calculation.

It is seen that both structures **2a** and **2b** show a distinct angle at the migrating hydrogen atom. These CHC angles are 130.2° (**2a**) and 153.1° (**2b**), respectively. This confirms earlier suggestions that the TS for the [1,5]-H shift in *cis*-1,3-pentadiene does not have a collinear arrangement as supposed by Kwart et al.[3].

For each structure the force constant matrix was calculated by finite differences (0.005 au) from analytical first derivatives of the energy. Vibrational frequencies and corresponding normal modes were calculated by using the conventional **FG** method[15]. The vibrational frequencies of the deuterated molecules were calculated using the same force constant matrix. The results are given in Table 1.

Table 1. Calculated (3-21G) harmonic vibrational frequencies for structures **1-3**[a-c]

1		2a		2b		3	
a'	3317(3315)	a'	3247(3247)	a_1	3424(3242)	a'	3310*(2420*)
	3247(2369)		3320(3219)		3216(3213)		3230(3230)
	3234(3234)		3176(3176)		3160(3160)		3218(3219)
	3225(3225)		1715(1690)		1731(1189)		3201(3201)
	3218(3217)		1632(1209)		1527(1462)		3170(3170)
	3214(3214)		1625(1608)		1457(1455)		3119(3119)
	3120(3114)		1584(1555)		1380(1369)		1673(1317)
	1876(1876)		1540(1492)		950(931)		1488(1475)
	1785(1785)		1468(1383)		780(776)		1425(1425)
	1674(1625)		1338(1328)		671(666)		1395(1395)
	1670(1477)		1218(1215)		224(219)		1331(1331)
	1494(1494)		1124(1052)	a_2	3268(3268)		1273(1269)
	1419(1411)		1053(1025)		1067(1048)		1262(1252)
	1332(1323)		852(816)		974(969)		1181(1175)
	1280(1277)		726(699)		279(278)		1069(1047)
	1271(1258)		610(601)		229(229)		973(973)
	1249(1212)		529(522)	b_1	3248(3247)		863(861)
	1211(1190)		452(447)		1575(1561)		758(718)
	1162(1006)	a''	3274(3274)		1293(1261)		462(458)
	764(723)		3261(3261)		956(951)		340(327)
	354(340)		3226(3226)		832(830)		263(242)
	168(158)		3172(3172)		587(573)	a''	3300(3300)
a''	3206(3206)		1679(1661)		434(409)		3197(3197)
	1217(1212)		1606(1589)	b_2	3225(3225)		1786(1785)
	1172(1141)		1526(1471)		3149(3149)		1677(1620)
	1135(1127)		1489(1461)		2022(1834)		1638(1638)
	1059(1059)		1360(1351)		1566(1537)		1454(1442)
	919(919)		1277(1277)		1358(1345)		1307(1306)
	880(878)		1232(1226)		1346(1340)		1254(1248)
	650(635)		1139(1136)		1257(1231)		1080(992)
	374(364)		1009(995)		1194(1194)		393(387)
	323(308)		311(311)		1122(1096)		238(232)
	144(143)		1925i(1521i)		2206i(1830i)		565i(565i)

[a] Units are in cm^{-1}. [b] The frequencies of the structures where the migrating hydrogen atom is substituted by a deuterium atom are given in parentheses. [c] The reaction coordinate mode for the twisted structure **3** is marked with an asterisk.

It is seen that the structures **2a**, **2b**, and **3** are characterized by a single imaginary frequency, which means that these three structures represent real TSs. For **2a** and **2b**, the corresponding normal modes show a horizontal movement of the migrating hydrogen atom toward one of the terminal carbon atoms, thus representing a real hydrogen shift.

For structure **3**, the imaginary frequency corresponds to a twist of the terminal double bond. Therefore, this structure is a TS for the *cis-trans* isomerization of this bond[16]. A comparison of the vibrational frequencies of **1** with the experimental ones of 1,3-pentadiene[17], shows that the 3-21G frequencies are systematically overestimated by ca. 10%, which is customary for this type of calculations[18].

6.3 Classical Reaction Rates and Kinetic Isotope Effect

The activation parameters for the [1,5]-H shift via the structures **2a** and **2b** are given in Table 2. These parameters have been calculated from the frequencies in Table 1 using the rigid-rotor-harmonic oscillator approximation. The activation enthalpies corrected for zero-point energies for the [1,5]-H shift via **2a** and **2b** are 48.8 and 43.6 kcal/mol, respectively. The enthalpy difference of 5.2 kcal/mol comes mainly (4.7 kcal/mol) from the differences in the zero-point energies of the two TSs. This is caused by the shift of the skeletal vibrations of the bent TS **2a** toward higher wavenumbers (see Table 1). This effect is also reflected in a more negative entropy of activation for this reaction.

Table 2. Calculated (3-21G) and experimental activation parameters and reaction rates for the [1,5]-shift in *cis*-1,3-pentadiene at 473 K

	reaction via					
	2a		**2b**		obsd[a]	
	H	D	H	D	H	D
$\Delta H^{\ddagger}$[b]	48.8	49.6	43.6	44.2	35.4	36.8
$\Delta S^{\ddagger}$[c]	-8.3	-8.6	-3.8	-4.0	-7.1	-7.4
k[d]	1.1×10^{-11}	4.3×10^{-12}	3.0×10^{-8}	1.3×10^{-8}	4.5×10^{-6}	0.9×10^{-6}

[a] Reference 1. [b] Activation enthalpies ($\Delta H^{\ddagger}$) in kcal/mol corrected for zero-point energies relative to **1**. The bare potential energy barriers are 48.4 kcal/mol (**2a**) and 47.9 (**2b**). [c] Activation entropies ($\Delta S^{\ddagger}$ in cal/mol K). [d] Reaction rates in s^{-1} as calculated from the parameters in this table.

The classical reaction rates (neglecting tunneling) were calculated from the activation parameters within transition state theory. These rates are also given in Table 2. It is seen that the calculated rates are considerably smaller than the observed ones, which is hardly astonishing in view of the calculated activation enthalpies.

Within transition state theory, it is also possible to calculate the KIE. According to this theory, the KIE arises from differential changes in the entropies and enthalpies of the reactant and the TS due to isotopic substitution. It depends on both the geometries (moments of inertia) and the vibrational frequencies of the TS involved. Therefore, it is expected that the KIE should give detailed information about the structure of the TS.

The KIE was calculated from Bigeleisen's equation[19] (1) (which is a rigid-rotor-harmonic oscillator approximation).

$$k_H / k_D = \nu_H^{\ddagger} / \nu_D^{\ddagger} \cdot EXC \cdot ZPE \cdot VP \qquad 1$$

In this equation, $\nu_H^{\ddagger} / \nu_D^{\ddagger}$ is the isotopic ratio of the imaginary frequencies along the reaction coordinate in the TS. In Bigeleisen's formulation it represents the KIE at an infinite temperature and it equals the result obtained from classical theory. All other terms are pure quantummechanical in origin. The *VP* is a vibrational frequency product, *EXC* a vibrational excitation term, and *ZPE* the contribution due to differences in the vibrational zero-point energies. The

equation originates from the assumption that isomeric substitution does not influence the geometries and the potential energy surfaces.

Table 3. Calculated (3-21G) and observed kinetic isotope effects (k_H/k_D) for the [1,5]-shift in *cis*-1,3-pentadiene as a function of temperature. Results have been obtained from eq. 1 (see text).

	reaction via		
T[a], K	**2a**	**2b**	obsd[b]
460	2.52	2.18	5.32
470	2.48	2.15	5.15
480	2.44	2.12	4.99
490	2.40	2.09	4.84

[a] Absolute temperatures. [b] Results for the observed KIE: $k_H/k_D = 1.15 \exp(1.4(\text{kcal/mol})/RT)$; see reference 1.

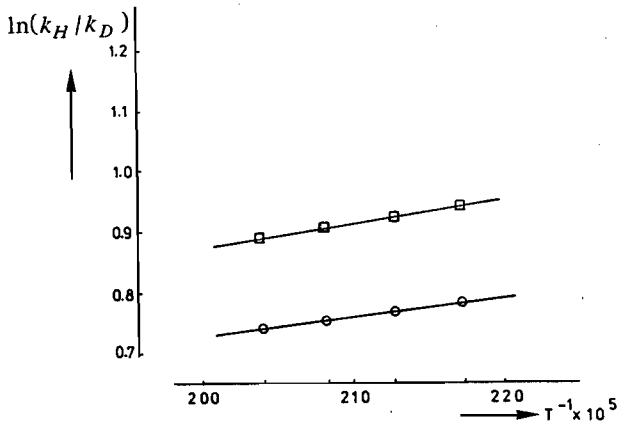

Figure 2. Temperature dependence of $\ln(k_H/k_D)$ for the thermal [1,5]-shift in *cis*-1,3-pentadiene. (□) Reaction via TS **2a**. (○) Reaction via TS **2b**.

The results for the KIE as a function of temperature are given in Table 3 and Figure 2. From these values, the temperature dependence of the KIE was calculated for the reactions via **2a** and **2b** (see Table 4). Both reactions show a temperature dependent KIE, in contrast to Kwart's suggestion[2] that a bent TS should be associated with a temperature independent KIE.

The calculated ΔE_D^H values are considerably smaller than the observed one[1]. This is reflected in the value of the KIE at room temperature. For the reactions via **2a** and **2b**, k_H/k_D equals 3.9 and 3.2, respectively. The extrapolated value of the experimental KIE at this temperature is 12.2, which is anomalously large. On the other hand, the calculated frequency factor ratio A_H/A_D is of comparable size and in line with other theoretical predictions[6,20].

When the KIEs for the two reactions are compared, it is seen that the TS with the larger angle at the migrating hydrogen atom (**2b**, 153.1°) shows the smaller KIE. The same relation holds for the temperature dependence (ΔE_D^H) of the

Table 4. Temperature dependence of the kinetic isotope effect

	reaction via		
	2a	2b	obsd[a]
ΔE_D^H [b]	0.73	0.63	1.40
A_H/A_D [c]	1.14	1.09	1.15
k_H/k_D (473 K)	2.5	2.1	5.1
k_H/k_D (298 K)	3.9	3.2	12.2

[a] See reference 1. [b] Activation energy difference for H and D transfer in kcal/mol. [c] Preexponential frequency factor ratio.

KIE. Thus, where it is frequently assumed that a larger angle should be associated with a larger temperature dependence of the KIE[21], these calculations show that this criterion should not be used.

Both the calculated reaction rates and the KIEs are considerably smaller than the observed ones. This may be caused by the deficiencies in the calculational method. It is clear that the reaction rates are sensitive to the activation parameters, which depend on the calculated bare potential energy barriers and the harmonic vibrational frequencies. However, it is not expected that the differences between calculated and observed activation energies will be completely cancelled by using larger basis sets[10b] or configuration interaction and a perturbational treatment[12]. The calculated vibrational frequencies deviate by 10% from the observed ones (*vide infra*). Therefore, the corresponding errors in the enthalpies and entropies are expected to be relatively small.

The calculations have been performed within transition state theory which implies the simplifying feature that the geometries and force constant matrices are independent of isotopic substitution. However, especially for a reaction where a light atom is transferred between two heavy atom fragments via a symmetric or nearly symmetric TS, this approximation breaks down[22]. In such a case, the TSs should be variationally optimized seperately for the hydrogen and deuterium substituted structures[23], which generally leads to lower reaction rates. This effect is larger for the reaction in which a hydrogen atom is transferred than for a deuterium exchange[24]. Therefore, such an optimization would lead to even lower reaction rates and smaller KIEs in the present case.

6.4 Vibrationally Assisted Tunneling

A complete description of the tunneling mechanism for the [1,5]-H shift in *cis*-1,3-pentadiene would involve the calculation of the tunneling rate going directly from the reactant (1) to the product (1'). Such an approach requires the detailed knowledge of the (3N-6) dimensional potential energy surface, which is out of the question.

An approximate solution to this practical problem would be the use of the reaction path Hamiltonian[25]. The only data needed then, are the potential energy and all force constants along a reaction path, which is choosen as the steepest descent path in mass-weighted coordinates through the TS. However, even this one-dimensional approach runs into difficulties in regions where the reaction path has a large curvature.

It was pointed out by Carrington and Miller[22b] that a more accurate description of such a situation requires at least two reaction-like degrees of freedom. However, a calculation based on this reaction surface Hamiltonian is still a very time consuming matter for a molecular system of the dimensions of pentadiene.

In the VAT-model of Dewar[8], tunneling takes place from a twisted form of the reactant (**3**) to a twisted form of the product (**3'**). The geometrical changes involved then, are restricted to the motion of the migrating hydrogen atom between the two terminal carbon atoms. This suggestion is elaborated through a geometry optimization of the twisted structure (see Figure 1). The energy needed to distort the reactant to the twisted form is 22.41 kcal/mol (corrected for zero-point energies). In the preceding chapter it was shown that this structure directly correlates with the TS of C_{2v}-symmetry, which makes this TS to be especially suited for VAT. Tunneling via the TS of C_s-symmetry asks for more drastic geometrical changes.

The tunneling rates were calculated going from the twisted reactant (**3**) to the twisted product (**3'**) via the TSs of C_s- and C_{2v}-symmetry following the procedure described by Bicerano et al.[26]. They obtained encouraging results with a one-dimensional approximation of the tunneling dynamics for proton transfer in malonaldehyde. The present model for tunneling between the two twisted structures in *cis*-1,3-pentadiene is very similar to this system.

The calculation is based on the method of periodic orbits for one-dimensional tunneling in a symmetric double well potential[27]. In this model, the tunneling rate ω_n is given by eq. 2 in which ΔE_n is the splitting of the energy levels in the two potential energy wells due to tunneling.

$$\omega_n = 2\Delta E_n / h \qquad 2$$

For small splittings, ΔE_n can be calculated within the WKB approximation[28] by eq. 3.

$$\Delta E_n = \hbar \frac{\nu_f}{\pi} e^{-\Theta_n} \qquad 3$$

Here, ν_f is the (harmonic) vibrational frequency of the normal mode F which leads to reaction. It is obvious to choose for this mode the C-H stretching vibration of the hydrogen atom that tunnels (see Table 1).

When the potential energy barrier is approximated by an Eckart function[29], the penetration integral Θ_n is given by eq. 4.

$$\Theta_n = 2\frac{\pi}{\hbar \nu_i}[V_{eff} - (E_n V_{eff})^{1/2}] \qquad 4$$

In this expression, ν_i is the imaginary frequency which corresponds to the

reaction coordinate motion in the TS. V_{eff} is the effective energy difference between the lowest vibrational state in one of the potential energy wells and the first vibrational level at the top of the potential energy barrier[26]. In the harmonic approximation, E_n is given by eq. 5.

$$E_n = \tfrac{1}{2}(n+1)\hbar\nu_f \qquad n = 0,1,2,... \qquad 5$$

In the VAT-model it is necessary to include tunneling from all bound vibrational states of the normal mode F. The overall tunneling rate is then given by eq. 6.

$$k_t = e^{-\Delta E_a/RT} \sum_{n=0}^{N-1} f_n \omega_n \qquad 6$$

In this equation, ΔE_a is the energy needed to distort the reactant (**1**) to the twisted structure (**3**), f_n the fraction of the molecules in the vibrational state with energy E_n, and ω_n the tunneling rate as calculated from eqs. 2-5. The summation is carried out for all N states below the barrier maximum.

For both reactions via **2a** and **2b**, there are three bound vibrational states for the hydrogen shift and four bound vibrational states for the deuterium shift. The vibrational frequencies used are those of Table 1. As indicated before, these values are overestimated by ca. 10% so that all frequencies (including the imaginary) were scaled down in the calculation by this factor.

Table 5. Calculated (3-21G) VAT rates (k_t) for the [1,5]-shift in *cis*-1,3-pentadiene[a]

	reaction via			
	2a		**2b**	
T[b], K	H	D	H	D
460	1.7×10^{-7}	2.6×10^{-9}	7.8×10^{-5}	3.0×10^{-6}
470	3.4×10^{-7}	6.0×10^{-9}	1.4×10^{-4}	6.1×10^{-6}
480	5.9×10^{-7}	1.4×10^{-8}	2.4×10^{-4}	1.2×10^{-5}
490	1.3×10^{-6}	3.0×10^{-8}	4.4×10^{-4}	2.3×10^{-5}

[a] Tunneling rates (in s^{-1}) have been calcutated from eqs. 2-6 using the frequencies given in Table 1 (scaled down by 10%; see text). [b] Absolute temperatures.

In Table 5, the calculated overall tunneling rates k_t are given for the two reactions via **2a** and **2b** in the temperature range in which the [1,5]-H shift in 1,3-pentadiene has been studied. From a comparison of Tables 2 and 5, it is seen that the calculated tunneling rates are larger than the calculated classical reaction rates by several powers of ten. This indicates that the proposed mechanism of VAT should indeed play an important role for this sigmatropic shift.

Tunneling is found to be more efficient for the reaction via the TS of C_{2v}-symmetry than for the reaction via the TS of C_s-symmetry. This is partly caused by the lower activation energy of the former reaction. More decisive is the larger imaginary frequency of the reaction coordinate mode for this TS which is a measure for the width of the barrier between the two potential energy wells[30].

The VAT-model introduces a strong temperature dependence of the tunneling rates (see Table 5) which is markedly different for hydrogen and deuterium transfer. For example, an Arrhenius plot of the tunneling rates for the reaction via **2b** yields an activation enthalpy of 25.8 kcal/mol for the H shift and 30.7 kcal/mol for the D shift. This difference comes from the fact that for the deuterium shift the tunneling from higher vibrational states is more important.

At this point it is worth making some reservations about the reliability of these results. First it can be seen that the calculated tunneling rates are relatively sensitive to the calculated barrier heights for the twist of the double bond (eq. 6) and the barrier height for the actual shift (eq. 4). However, the same proviso has to be made for the classical reaction rates.

Additionally it was assumed that the vibrational mode F behaves harmonically. For the lowest bound state, this approximation is fairly reasonable, but for the higher bound states deviations will become more important. Generally, the anharmonicity will lead to lower tunneling rates ω_n. This will be partly cancelled by an increasing population f_n of the upper vibrational levels so that the overall effect upon the VAT-rate k_t is indistinct. As the classical reaction rates and the KIE were calculated within the harmonic oscillator approximation, it is merely a matter of self-consistency to use this approximation also to calculate the tunneling rates.

A further remark must be made about the validity of the one-dimensional approach. In the derivation of the equations, it was assumed that all vibrations (except ν_f) attribute adiabatically to the tunneling rate. As discussed earlier, this approximation becomes less reliable for a large reaction path curvature[22a]. It is to be expected that a more realistic multi-dimensional model will lead to lower tunneling rates[31].

In view of these facts, it is clear that the absolute values should be interpreted with care. However, it was only the intention to calculate within a consistent model whether the tunneling mechanism might play a role in the [1,5] shift in *cis*-1,3-pentadiene and if so, via which TS the reaction is most likely to proceed.

6.5 Conclusions

The 3-21G calculations strongly support Dewar's suggestion[8] that tunneling from a twisted form of the reactant should play an important role in the mechanism of the thermal [1,5]-H shift in *cis*-1,3-pentadiene. The reaction is most likely to proceed via a TS of C_{2v}-symmetry. Both optimized TSs have an acute angle at the migrating hydrogen atom, which contradicts the suggestion of Kwart et al.[3] that the TS should have a collinear geometry.

The calculated KIEs are found to be temperature dependent, thus confirming recent model studies where it was found that not only a linear but also a bent

TS should exhibit a temperature dependent KIE.

The mechanism of VAT also shows a temperature dependence which arises from an essentially different origin than the one for the classical reaction kinetics. Therefore, an Arrhenius extrapolation of the results of Roth and König to room temperature and conclusion based thereupon are not justified.

6.6 References and Notes

1 W.R. Roth, J. König, Liebigs Ann. Chem., **699**, 24 (1966)

2 H. Kwart, Acc. Chem. Res., **15**, 401 (1982)

3 H. Kwart, M.W. Brechbiel, R.M. Acheson, D.C. Ward, J. Am. Chem. Soc., **104**, 4671 (1982)

4 A.A. Vitale, J. San Filippo, J. Am. Chem. Soc., **104**, 7341 (1982)

5 B. Anhede, N.-Å. Bergman, J. Am. Chem. Soc., **106**, 7634 (1984)

6 D.J. McLennan, P.M.W. Gill, J. Am. Chem. Soc., **107**, 2971 (1985)

7 W.A.M. Castenmiller, H.M. Buck, Tetrahedron, **35**, 397 (1979)

8 M.J.S. Dewar, K.M. Merz Jr., J.J.P. Stewart, J. Chem. Soc., Chem. Commun., 166 (1985)

9 W.J. Bouma, M.A. Vincent, L. Radom, Int. J. Quant. Chem., **14**, 767 (1978)

10a B.A. Hess, L.J. Schaad, J. Am. Chem. Soc., **105**, 7185 (1983)

10b B.A. Hess, L.J. Schaad, J. Pančir, J. Am. Chem. Soc., **107**, 149 (1985)

11 N.G. Rondan, K.N. Houk, Tetrahedron Lett., **25**, 2519 (1984)

12 G.J.M. Dormans, H.M. Buck, J. Mol. Struct. (Theochem), **29**, 121 (1986)

13 J.S. Binkley, R.A. Whiteside, R. Krishnan, R. Seeger, D.J. DeFrees, H.B. Schlegel, S. Topiol, L.R. Kahn, J.A. Pople, GAUSSIAN 80, Department of Chemistry, Carnegie-Mellon University, Pittsburgh, PA (1980)

14 J.S. Binkley, J.A. Pople, W.J. Hehre, J. Am. Chem. Soc., **102**, 939 (1980)

15 E.B. Wilson, J.C. Decius, P.C. Cross in "Molecular Vibrations", McGraw-Hill, New York (1955)

16 A further pyramidalization of the twisted methylene group so that it adopts a similar geometry as the methyl group is energetically unfavourable for the ground state. See e.g.:

I. Nebot-Gil, J.-P. Malrieu, J. Am. Chem. Soc., **104**, 3320 (1982)

17 D.A.C. Compton, W.O. George, W.F. Maddams, J. Chem. Soc., Perkin. Trans. 2, 1311 (1977)

18 Y. Yamaguchi, H.F. Schaefer III, J. Chem. Phys., **73**, 2310 (1980)

19 J. Bigeleisen, M. Wolfsberg, Adv. Chem. Phys., **1**, 15 (1958)

W.A. van Hook in "Isotope Effects in Chemical Reactions", C.J. Collins, N.S. Bowman, Eds., Van Nostrand, New York (1970)

20 M.J. Stern, R.E. Weston Jr., J. Chem. Phys., **60**, 2808 (1974)

21 When the calculated values for (the temperature dependence of) the KIE are fitted to the values from the model study of McLennan and Gill[6], the calculations fit with their model B for TS **2a** and their model C for TS **2b**.

22a Such a reaction is characterized by a small skew angle between the reaction paths at the reactant and product sides of the potential energy surface in mass-weighted coordinates. See e.g.:

V.K. Babamov, R.A. Marcus, J. Chem. Phys., **74**, 1790 (1981)

B.C. Garrett, D.G. Truhlar, A.F. Wagner, T.H. Dunning, J. Chem. Phys., **78**, 4400 (1983)

22b T. Carrington Jr., W.H. Miller, J. Chem. Phys., **81**, 3942 (1984)

23 See e.g.:

D.G. Truhlar, B.C. Garrett, Ann. Rev. Phys. Chem., **35**, 159 (1984)

24 B.C. Garrett, D.G. Truhlar, J. Am. Chem. Soc., **102**, 2559 (1980)

25 W.H. Miller, N.C. Handy, J.E. Adams, J. Chem. Phys., **72**, 99 (1980)

26 J. Bicerano, H.F. Schaefer III, W.H. Miller, J. Am. Chem. Soc., **105**, 2550 (1983)

27 W.H. Miller, J. Phys. Chem., **83**, 960 (1979)

28 See e.g.:

M.D. Harmony, Chem. Soc. Rev., **1**, 211 (1972)

29 R.P. Bell in "The Tunnel Effect in Chemistry", Chapman and Hall, London (1980)

30 Notice that the C-H distance for the migrating hydrogen atom is considerably smaller for the TS of C_{2v}-symmetry (1.353 Å) than for the TS of C_s-symmetry (1.446 Å).

31 See e.g.:

P. Bopp, D.R. McLaughlin, M.Z. Wolfsberg, Z. Naturforsch. A., **37A**, 398 (1982)

APPENDIX

The Calculation of Nonadiabatic Coupling Elements

The nonadiabatic coupling element $g_{KL} = <\Psi_K \mid \partial/\partial Q \mid \Psi_L>$ can be evaluated numerically by writing the wavefunction $\mid \Psi_K>$ in its CI expansion:

$$\mid \Psi_K> = \sum_{i=1}^{N} c_{Ki} \mid \Phi_i> \qquad 1$$

$$<\Psi_K \mid \partial/\partial Q \mid \Psi_L> = <\sum_{i=1}^{N} c_{Ki}\Phi_i \mid \partial/\partial Q \mid \sum_{j=1}^{N} c_{Lj}\Phi_j> \qquad 2$$

$$= <\sum_{i=1}^{N} c_{Ki}\Phi_i \mid \sum_{j=1}^{N} \frac{\partial c_{Lj}}{\partial Q}\Phi_j> + <\sum_{i=1}^{N} c_{Ki}\Phi_i \mid \sum_{j=1}^{N} c_{Lj}\frac{\partial \Phi_j}{\partial Q}>$$

$$= \sum_{i=1}^{N} c_{Ki} \sum_{j=1}^{N} \frac{\partial c_{Lj}}{\partial Q} <\Phi_i \mid \Phi_j> + \sum_{i=1}^{N}\sum_{j=1}^{N} c_{Ki}c_{Lj} <\Phi_i \mid \partial/\partial Q \mid \Phi_j>$$

The first term is called the CI-term, because it involves the differentiation of the CI coefficients. It can be simplified using the orthonormality condition for configurations : $<\Phi_i \mid \Phi_j> = \delta_{ij}$.

$$g_{KL}^{CI} = \sum_{i=1}^{N} c_{Ki} \frac{\partial c_{Li}}{\partial Q} \qquad 3$$

The second term is called the MO-term because it can be reduced to a differentiation of MOs. The term $<\Phi_i \mid \partial/\partial Q \mid \Phi_j>$ equals zero if i=j (because of the antisymmetry condition $<\Phi_i \mid \partial/\partial Q \mid \Phi_j> = -<\Phi_j \mid \partial/\partial Q \mid \Phi_i>$) and if the configurations $\mid \Phi_i>$ and $\mid \Phi_j>$ differ by two or more MOs. Only in the case that $\mid \Phi_i>$ and $\mid \Phi_j>$ differ by exactly one MO (say $\phi_{p(i)}$ for $\mid \Phi_i>$ and $\phi_{q(j)}$ for $\mid \Phi_j>$) a contribution to g_{KL}^{MO} is found:

$$g_{KL}^{MO} = \sum_{i=1}^{N}\sum_{j\neq i}^{N} c_{Ki}c_{Lj}M_{ij} <\phi_{p(i)} \mid \partial/\partial Q \mid \phi_{q(j)}> \qquad 4$$

In this equation, M_{ij} is a constant determined by the type and sign of the configurations $\mid \Phi_i>$ and $\mid \Phi_j>$. Both g_{KL}^{CI} and g_{KL}^{MO} can now be evaluated numerically by performing two separate SCF/CI calculations for $Q = Q$ and for $Q = Q+\Delta Q$. For values of Q where the wavefunctions change rapidly, the numerical accuracy can be increased by a calculation at more points on the reaction coordinate. In practice, care should be taken that the wavefunctions (both their MOs and their CI expansion) have the same phase.

$$g_{KL}^{CI} = \frac{1}{\Delta Q}\sum_{i=1}^{N} c_{Ki}(Q)[c_{Li}(Q+\Delta Q) - c_{Li}(Q)] \qquad 5$$

$$g_{KL}^{MO} = \frac{1}{\Delta Q} \sum_{i=1}^{N} \sum_{j \neq i}^{N} c_{Ki} c_{Lj} M_{ij} [\langle \phi_{p(i)}(Q) | \phi_{q(j)}(Q+\Delta Q) \rangle - \langle \phi_{p(i)}(Q) | \phi_{q(j)}(Q) \rangle] \quad 6$$

At this point a difference arises between ab initio and semi-empirical (MNDO) calculations. For ab initio wavefunctions, the MOs are orthonormal so that the last term in eq. 6 equals zero. For MNDO wavefunctions, the MOs are not orthogonal but fulfill the condition that the sum of the squares of the MO-coefficients in the AO-expansion equals 1. Eq. 6 can now be simplified by expanding the MOs in the AO-basis (σ_k):

$$\phi_{p(i)} = \sum_{k=1}^{M} a_{pk} \sigma_k \quad 7$$

Ab initio:

$$g_{KL}^{MO} = \frac{1}{\Delta Q} \sum_{i=1}^{N} \sum_{j \neq i}^{N} c_{Ki} c_{Lj} M_{ij} \sum_{k=1}^{M} \sum_{l=1}^{M} a_{pk} a_{ql} \langle \sigma_k(Q) | \sigma_l(Q+\Delta Q) \rangle \quad 8$$

MNDO:

$$g_{KL}^{MO} = \frac{1}{\Delta Q} \sum_{i=1}^{N} \sum_{j \neq i}^{N} c_{Ki} c_{Lj} M_{ij} \sum_{k=1}^{M} \sum_{l=1}^{M} [a_{pk} a_{ql} \langle \sigma_k(Q) | \sigma_l(Q+\Delta Q) - \langle \sigma_k(Q) | \sigma_l(Q) \rangle] \quad 9$$

The element $\langle \sigma_k(Q) | \sigma_l(Q) \rangle$ is the overlap between the AOs σ_k and σ_l and is calculated in most quantumchemical programs. The element $\langle \sigma_k(Q) | \sigma_l(Q+\Delta Q) \rangle$ represents the overlap between two AOs located on two molecules with a slightly different geometry. In practice it is evaluated by performing a separate calculation for a fictitious "double" molecule. For example, in the case that Q stands for the twist (θ) around the double bond in ethylene, the "double" molecule would be (in a Newman-projection).

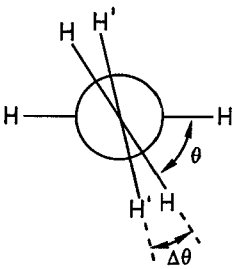

A calculation of the overlap matrix for this molecule then provides the necessary overlap elements between the AOs at a different geometry.

Theoretically, the total coupling element $g_{KL} = g_{KL}^{CI} + g_{KL}^{MO}$ fulfills the antisymmetry condition $g_{KL} = -g_{LK}$. In practice, both g_{KL} and g_{LK} are evaluated so that an estimate can be made for the numerical accuracy of the calculation.

SUMMARY

This thesis describes a theoretical study on two types of organic photochemical reactions: *cis-trans* isomerizations and sigmatropic shifts. By means of quantumchemical calculations the mechanism of these reactions has been studied in detail. Both reactions have in common that they are initiated by an energetically favourable rotation of an excited double bond towards a 90° twisted structure, representing a local minimum on the excited state potential energy surface. The difference between the *cis-trans* isomerizations and sigmatropic shifts arises from the nonadiabatic interactions between the ground and excited state for the twisted geometry. For *cis-trans* isomerizations a large nonadiabatic interaction is a requisite for the occurence of an efficient radiationless transition to the ground state. On the contrary, a small nonadiabatic interaction provides a situation where the excited molecule has a certain lifetime in the twisted conformation during which a photochemical shift may take place.

In chapter 2 a quantummechanical treatment is presented for the description of the dynamics of *cis-trans* isomerization. The potential energy curves, transition dipole moments and nonadiabatic couplings for the double bond isomerizations of ethylene, butadiene and the outside double bond of hexatriene have been calculated at the ab initio CI level. The vibrational wavefunctions for the rotation around the double bond have been calculated explicitely via the inclusion of the moment of inertia for this nuclear motion in the model Hamiltonian. The total time dependent wavefunction is constructed then from the electronic and vibrational wavefunctions with inclusion of the nonadiabatic interactions. It is shown that this one-dimensional treatment gives an adequate description of the photoisomerization of double bonds. Both the appearance of the UV absorption spectra of these molecules and their photodynamical behaviour can be related to the shape of the potential energy curve of the excited state. Going from ethylene to hexatriene the molecules show an increasing tendency to be planar in the excited state.

Chapter 3 describes the photoisomerization of retinal in the systems rhodopsin and bacteriorhodopsin. The protonated Schiff base of retinal acts as the chromophore which converts the absorbed light energy into a nerve signal (rhodopsin) or an electrochemical gradient across a cell membrane (bacteriorhodopsin). The initial photochemical step in both systems is a highly selective and efficient photoisomerization of one of the conjugated double bonds of the chromophore. This highly efficient isomerization seems to contradict with the increasing tendency of longer polyenes to be planar in the excited state. MNDO/CI calculations for protonated 1-imino-2,4-pentadiene show that this difference arises from a strong stabilization of the 90° twisted structure in the excited state by the electron deficient protonated nitrogen atom. The transition probability to the ground state has been evaluated from semi-classical trajectory calculations. The regioselectivity of the photoisomerization in these type of molecules can be explained from the extent of the stabilization of the 90° twisted

structures in the excited state and the related transition probability to the ground state. These features depend on the distance from the twisted bond to the nitrogen atom. Calculations on a model compound of the protonated Schiff base of retinal show that the extent of the stability of the twisted molecule can be directed by providing external point-charges around the molecule. In nature, these point-charges are provided by the protein opsin. From the calculations it follows that the primary step in the photoisomerization of bacteriorhodopsin can be best explained with a negatively charged counterion near the protonated nitrogen atom and an ion-pair near the cyclohexene-ring of retinal.

The last three chapters of this thesis deal with sigmatropic shifts. Classically, the mechanism of this type of reactions is described by the rules of Woodward and Hoffmann, which are based on the symmetry of the highest occupied MO. In chapter 4 a new mechanism is presented for photochemical sigmatropic shifts. This mechanism is initiated by the energetically favourable rotation of an excited double bond towards a 90° twisted structure. From this local minimum on the potential energy surface, the shift then proceeds in the plane of the carbon skeleton (planar shift) via a highly symmetric transition state. MNDO calculations for various photochemical shifts show that the activation energy for this type of mechanism is considerably smaller than for the mechanism based on the Woodward and Hoffmann rules.

Extensive ab initio CI calculations followed by a second order perturbation as presented in chapter 5 for the [1,3]-H shift in propene and the [1,5]-H shift in 1,3-pentadiene, confirm the model of the planar shift for photochemical sigmatropic reactions. For the thermal reactions, a shift is found according to the Woodward and Hoffmann rules, i.e. an antarafacial [1,3]-H shift in propene and a suprafacial [1,5]-H shift in 1,3-pentadiene. However, in both cases the activation energy for the planar shift is only slightly larger.

Finally, in chapter 6 it is shown that for the thermal [1,5]-H shift in 1,3-pentadiene the observed reaction kinetics can not be explained from a classical mechanism. The reaction rates and temperature dependence of the kinetic isotope effect have been evaluated from an ab initio vibrational analysis of the reactant and the transition states of C_s- and C_{2v}-symmetry. The calculated parameters are considerably smaller than the observed ones. Therefore, a mechanism is suggested in which the shift occurs via quantummechanical tunneling between two high-vibrational states of the reactant and the product. It is shown that this mechanism is most likely to proceed via the transition state of C_{2v}-symmetry. The calculated tunneling rates indicate that the [1,5]-H shift in 1,3-pentadiene mainly takes place via this mechanism.

SAMENVATTING

Dit proefschrift beschrijft een theoretische studie naar twee soorten organische fotochemische reakties: *cis-trans* isomerisaties en sigmatrope shifts. Het mechanisme van deze reakties is bestudeerd met behulp van kwantumchemische berekeningen. Voor beide reakties geldt dat ze beginnen met een energetisch gunstige draaiing van de dubbele binding naar een 90° gedraaide struktuur die een lokaal minimum beschrijft op het potentiaaloppervlak van de aangeslagen toestand. Het verschil tussen de *cis-trans* isomerisaties en de sigmatrope shifts wordt veroorzaakt door de grootte van de niet-adiabatische koppeling tussen de grond- en aangeslagen toestand van het gedraaide molekuul. Voor de *cis-trans* isomerisatie is een sterke niet-adiabatische koppeling een vereiste voor een efficiënte stralingsloze terugval naar de grondtoestand. Daarentegen veroorzaakt een kleine niet-adiabatische koppeling een situatie waarin het molekuul een bepaalde levensduur heeft waarbinnen een fotochemische shift kan optreden.

In hoofdstuk 2 wordt een kwantummechanische beschrijving gegeven van de dynamika van *cis-trans* isomerisatie. De potentiaalcurven, overgangsdipoolmomenten en niet-adiabatische koppelingen voor de isomerisatie van de dubbele binding in etheen, butadieen en de buitenste dubbele binding van hexatrieen zijn bepaald met behulp van ab initio CI berekeningen. De vibrationele golffunkties behorende bij de draaiing rond de dubbele binding zijn expliciet berekend door het meenemen van het traagheidsmoments behorende bij deze kernbeweging in de model-Hamiltoniaan. De tijdsafhankelijke golffunktie kan dan worden opgebouwd uit een kombinatie van de elektronische en vibrationele golffunkties na meename van de niet-adiabatische interakties. Dit ééndimensionale model blijkt een adequate beschrijving te geven van de fotoisomerisatie van dubbele bindingen. Zowel de vorm van het UV-absorptiespektrum van deze molekulen als hun fotodynamisch gedrag kunnen gerelateerd worden aan de vorm van de potentiaalcurve van de aangeslagen toestand. Gaande van etheen naar hexatrieen vertonen deze molekulen een toenemende neiging om vlak te blijven in de aangeslagen toestand.

Hoofdstuk 3 beschrijft de fotoisomerisatie van retinal in de systemen rhodopsine en bacteriorhodopsine. De geprotoneerde Schiffse base van retinal funktioneert als een chromofoor dat de geabsorbeerde lichtenergie omzet in een zenuwsignaal (rhodopsine) of een elektrochemische gradiënt over een celmembraan (bacteriorhodopsine). In beide systemen is de primaire fotochemische stap een zeer selektieve en efficiënte isomerisatie van één van de gekonjugeerde dubbele bindingen van retinal. Dit zeer efficiënte mechanisme lijkt in tegenspraak met de neiging van langere polyenen om vlak te blijven in de aangeslagen toestand. MNDO/CI berekeningen voor geprotoneerd 1-imino-2,4-pentadieen laten zien dat dit verschil veroorzaakt wordt door een sterke stabilisatie van de 90° gedraaide struktuur in de aangeslagen toestand door het elektrondeficiënte stikstofatoom. De overgangswaarschijnlijkheid naar de

grondtoestand werd bepaald met behulp van semi-klassieke baanberekeningen. De regioselektiviteit van de fotoisomerisatie kan verklaard worden uit de mate van stabilisatie van het 90° gedraaide molekuul en de daaraan gerelateerde overgangswaarschijnlijkheid naar de grondtoestand. Deze eigenschappen blijken onder andere af te hangen van de afstand van de gedraaide dubbele binding tot het stikstofatoom. Berekeningen aan een modelstof voor geprotoneerd retinal laten zien dat de mate van deze stabilisatie gemoduleerd kan worden door het aanbrengen van externe puntladingen in de buurt van het molekuul. In de natuur worden deze puntladingen geleverd door het omringende eiwit opsine. Uit de berekeningen volgt dat de primaire stap in de fotoisomerisatie van bacteriorhodopsine het best verklaard kan worden met een negatief geladen tegenion in de buurt van het geprotoneerde stikstofatoom en een ionenpaar nabij de cyclohexeenring van retinal.

De laatste drie hoofdstukken van dit proefschrift behandelen sigmatrope shifts. Klassiek gezien, wordt het mechanisme hiervan beschreven door de regels van Woodward en Hoffmann, die berusten op de symmetrie van de hoogste bezette MO. In hoofdstuk 4 wordt een nieuw mechanisme voorgesteld voor fotochemische sigmatrope shifts. Dit mechanisme begint met een energetisch gunstige draaiing van de dubbele binding in de aangeslagen toestand naar een 90° gedraaide struktuur. Vanuit dit lokale minimum op het potentiaaloppervlak vindt dan de shift plaats in het vlak van het koolstofskelet via een hoogsymmetrische overgangstoestand (planaire shift). MNDO berekeningen voor verschillende fotochemische shifts laten zien dat de aktiveringsenergie voor dit mechanisme aanzienlijk lager is dan voor het mechanisme gebaseerd op de regels van Woodward en Hoffmann.

De ab initio CI berekeningen gevolgd door een tweede orde storingsrekening zoals beschreven in hoofdstuk 5 voor de [1,3]-H shift in propeen en de [1,5]-H shift in 1,3-pentadieen, bevestigen het model van de planaire shift voor fotochemische sigmatrope reakties. Voor de thermische reakties wordt, conform de regels van Woodward en Hoffmann, een antarafaciale [1,3]-H shift in propeen en een suprafaciale [1,5]-H shift in 1,3-pentadieen gevonden. Echter, in beide gevallen blijkt dat de planaire shift nagenoeg eenzelfde aktiveringsenergie heeft.

Tenslotte wordt in hoofdstuk 6 de reaktiekinetiek van de thermische [1,5]-H shift in 1,3-pentadieen bestudeerd. De reaktiesnelheden en de temperatuursafhankelijkheid van het kinetisch isotoopeffekt werden berekend uit een ab initio vibratieanalyse van de reaktant en de overgangstoestanden van C_s- en C_{2v}-symmetrie. De berekende waarden hiervoor blijken aanzienlijk kleiner dan de experimenteel waargenomen parameters. Daarom wordt een mechanisme voorgesteld waarbij de shift optreedt via tunneling tussen twee hoogvibrationele toestanden van de reaktant en het produkt. Het blijkt dat dit mechanisme het meest waarschijnlijk is voor de reaktie via de overgangstoestand van C_{2v}-symmetrie. De berekende snelheden voor tunneling wijzen er op dat de [1,5]-H shift in 1,3-pentadieen voornamelijk via dit mechanisme zal plaatsvinden.

LEVENSLOOP

De schrijver van dit proefschrift werd geboren op 23 december 1958 te Geleen. Na het behalen van het diploma atheneum B aan het Sint Michiellyceum te Geleen in 1977, werd in datzelfde jaar begonnen met de studie chemische technologie aan de afdeling der Scheikundige Technologie van de Technische Hogeschool te Eindhoven. In 1981 werd hem de Chevron Chemie-prijs toegekend. Het afstudeerwerk werd verricht bij de vakroep Organische Chemie onder leiding van prof. dr. H.M. Buck en dr. ir. H.R. Fransen. In april 1983 werd het ingenieursexamen met lof afgelegd.

Vanaf 1 mei 1983 tot 1 oktober 1983 was hij werkzaam als wetenschappelijk assistent in dienst van de Technische Hogeschool Eindhoven. Daarna kwam hij in dienst als wetenschappelijk assistent van de Nederlandse Stichting voor Zuiver Wetenschappelijk Onderzoek. Het in dit proefschrift beschreven werk werd uitgevoerd onder leiding van prof. dr. H.M. Buck.

Na zijn promotie zal hij in dienst treden als wetenschappelijk medewerker bij het Philips Natuurkundig Laboratorium te Eindhoven.

NAWOORD

Graag wil ik allen, die op enigerlei wijze hebben bijgedragen aan de totstandkoming van dit proefschrift, bedanken.

Van zeer groot belang is het werk geweest van ir. Willie J.G.M. Peijnenburg, ir. Gerrit C. Groenenboom en ir. Wim C.A. van Dorst, dat zij met veel inzet en enthousiasme tijdens en na hun afstudeerperiode voor mij hebben verricht.

Verder ben ik dr. ir. Maarten C.A. Donkersloot en dr. ir. René A.J. Janssen dank verschuldigd voor de voortdurende steun die zij mij gegeven hebben tijdens mijn promotieonderzoek.

Tenslotte wil ik Henk Eding bedanken voor de voortvarende wijze waarop hij de vele tekeningen en de lay-out van dit proefschrift heeft verzorgd.

The work described in this thesis was supported by the Netherlands Foundation for Chemical Research (S.O.N.) with financial aid from the Netherlands Organization for the Advancement of Pure Research (Z.W.O.).

Stellingen

1. De polariteit van het oplosmiddel dient als extra parameter te worden meegenomen in het theoretisch model dat de dynamika beschrijft van de, niet door een potentiaalbarriere gehinderde, fotoisomerisatie van cyanine kleurstoffen in oplossing.

   E. Åkesson, H. Bergström, V. Sundström, T. Gillbro, Chem. Phys. Lett., 126, 385 (1986)

2. De suggestie van Tordo et al. dat in diarylfosforanylradikalen een belangrijk gedeelte van de spindichtheid gelokaliseerd is op zuurstof en niet op fosfor, berust op een onvolledige weergave van zowel de kwantumchemische berekeningen als de ESR analyse van deze radikalen.

   N.J. Winter, B. Beccard, Y. Berchadsky, F. Vila, L. Werbelow, P. Tordo, J. Phys. Chem., 90, 6749 (1986)
   M. Geoffrey, E.A.C. Lucken, Mol. Phys., 22, 257 (1971)

3. De fotochemie van β-t-butylstyrenen kan goed verklaard worden met het door Ohmine voorgestelde mechanisme voor niet-adiabatische overgangen via (partiele) waterstofshifts.

   O. Kikuchi, H. Yoshida, Bull. Chem. Soc. Jpn., 58, 131 (1985)
   I. Ohmine, J. Chem. Phys., 83, 2348 (1985)

4. Het verdient aanbeveling onderzoek te verrichten naar de base-base stacking interakties in het vertakte nucleotide $A^{2'\text{-}5'G}_{3'\text{-}5'U}$, teneinde inzicht te krijgen in het mechanisme van niet-enzymatische splicing van pre-*m*RNA.

   G. Remaud, J.-M. Vial, A. Nyilas, N. Balgobin, J. Chattopadhyaya, Tetrahedron, 43, 947 (1987)
   T.R. Cech, Scientific American, 255, 76 (1986)

5. Het lijkt zeer onwaarschijnlijk dat het waargenomen isotoopeffekt voor de $E-Z$ isomerisatie van t-butylhexatrienen verklaard kan worden uit een koppeling van de torsie van de centrale dubbele binding met de out-of-plane beweging van de waterstofatomen.

A.M. Brouwer, proefschrift Leiden (1987)

6. De door Cooper et al. uitgevoerde spingekoppelde berekeningen aan benzeen zijn veeleer een demonstratie van het al lang bekende gegeven dat een MO-beschrijving met volledige configuratie interaktie hetzelfde resultaat oplevert als een VB-beschrijving met alle ionogene strukturen, dan een aanwijzing dat benzeen beter beschreven wordt door een Kekulé struktuur dan door een gedelokaliseerde struktuur.

D.L. Cooper, J. Gerrat, M. Raimondi, Nature, 323, 699 (1986)

7. De organische chemie wordt in Nederland ondergewaardeerd als belangrijk toepassingsgebied van de kwantumchemie.

8. Het fotochemisch onderzoek waarbij metingen verricht worden op femtoseconde tijdschaal, verdient omschreven te worden als experimentele kwantumchemie.

9. De bewering van Alexander et al. dat de g-waarde verschuiving in de nitroxide radikalen, gevormd in 3-hydroxideguanine, niet verklaard kan worden door een spindelokalisatie op zwavel, duidt op een schromelijke onderschatting van de intelligentie van de lezers van dit artikel.

C. Alexander jr., A.N.M. Shahidain, M.S. Jahan, J. Magn. Res., 67, 531 (1986)

10. Het in werking treden van de nieuwe Wet en Besluit op de Ruimtelijke Ordening, die het opnemen van sociale bepalingen in bestemmingsplannen juridisch mogelijk maakt, op een moment dat de stadsvernieuwing in de oude wijken van de grote steden haar voltooiing nadert, toont eens te meer aan dat de nederlandse wetgeving onvoldoende in staat is om op beleidsontwikkelingen in te spelen.

Staatsblad, 626, 627 (1985)

11. Dat zowel voor voetbalspelers als voor schilderijen tegenwoordig exorbitant hoge "transfersommen" betaald worden betekent nog niet dat voetbal een kunst, dan wel schilderen oorlog zou zijn.

G.J.M. Dormans

Eindhoven, 16 juni 1987